WIND TUNNEL MODEL DISPERSION TESTS OF KODAK PARK PROCESS EMISSIONS

by

R. L. Petersen[1] and J. E. Cermak[2]

Prepared for

Eastman Kodak Company
Rochester, New York 14650

Fluid Mechanics and Wind Engineering Program
Fluid Dynamics and Diffusion Laboratory
Department of Civil Engineering
Colorado State University
Fort Collins, Colorado 80523

November 1979 CER79-80RLP-JEC64

[1]Research Assistant Professor, Department of Civil Engineering, Colorado State University, Fort Collins, Colorado.

[2]Professor-in-Charge, Fluid Mechanics and Wind Engineering Program, Department of Civil Engineering, Colorado State University, Fort Collins, Colorado.

TABLE OF CONTENTS

ABSTRACT

Kodak Park, Rochester, New York is a major manufacturing complex consisting of 190 buildings located on a 100-acre tract approximately 5.6 km Northwest of Rochester's central business district. To evaluate the air quality and aid in developing atmospheric dispersion models for the Kodak Park Area, wind tunnel modeling was performed. A scale model of buildings 301, 302, 303, and 304 along with models of the buildings up and downwind of the plant for six wind directions was constructed and positioned in the Colorado State University Environmental Wind Tunnel for each wind condition simulated. A tracer gas was released from each of the four stacks on buildings 301, 302, 303 and 304 and the resulting ground level and aerial concentration distributions measured. A total of six wind directions and at least four wind speeds for each direction were studied. To document the flow for each direction a series of velocity and turbulance intensity profiles were taken.

Prior to conducting the scale model tests, dispersion and boundary layer measurements were conducted in the tunnel with a uniform surface roughness. These tests showed that the flow and dispersion characteristics of the wind tunnel are similar to the atmosphere.

Included in this report are a discussion on similarity criteria, the experimental methods, and results of concentration and boundary layer measurements.

ACKNOWLEDGMENTS

The authors wish to recognize the following individuals for their contribution to this research effort: Bob Beazley for supervising the collection of concentration data; Paul Worley for collecting the velocity data; Eric Hoppe for calibrating flowrators and concentration data collection; Evan Twombly for writing the data analysis programs; Peggy Kramer for assisting in the report preparation and data processing; Kenneth Streebe and B. A. Hoffman for drafting the figures and Linda Jensen for typing the report.

We also want to thank Dr. Jim Halitsky for his comments and review of the report.

LIST OF SYMBOLS

Symbol	Definition	Units
A	Hot-film calibration constant	(-)
B	Hot-film calibration constant	(-)
C_p	Specific heat at constant pressure	$(m^2 s^{-2} {}^oK^{-1})$
CF	Calibration factor	(ppm/mv-s)
d	Diameter of hot film or displacement height	(m)
D_i	Stack diameter	(m)
D	Dilution ratio	(-)
e	rms error	(varies)
E	Hot-film voltage	(V)
Ec	Eckert number $\left[u_o^2/(C_{p_o} \ \Delta T_o)\right]$	(-)
F_L	Lagrangian spectral function	(s)
Fr	Stack Froude number $\left[\dfrac{u_s}{\sqrt{g\gamma D_i}}\right]$	(-)
F(n)	Frequency spectrum of velocity	$(m^2 s^{-1})$
g	Acceleration due to gravity	(ms^{-2})
Gr	Grashof number $\left[\dfrac{gd^3(T_w - T_g)}{\nu_g^2 T_g}\right]$	(-)
H	Height of plume	(m)
h	Height of stack	(m)
$i_{x,y,z}$	Turbulence intensity in x, y or z direction [u'/u, v'/u, w'/u]	(-)
I	Current through wire or integrated value	(varies)
k	Thermal conductivity	$(Wm^{-1} {}^oK^{-1})$
k_s	Uniform sand grain height	(m)
K	Dimensionless concentration $\left[\dfrac{\chi u_h H_b^2}{\chi_o Q}\right]$ or $\left[\dfrac{\chi u H_b^2}{q}\right]$	(-)

Symbol	Definition	Units
L	Length scale	(m)
M_o	Momentum ratio $\left[\dfrac{\rho_s u_s^2}{\rho_a u_a^2}\right]$	(-)
m	Molecular weight	(g)
P	Pressure	$(gm^{-1}s^{-2})$
Pr	Prandtl number $\left[\dfrac{\nu_o \rho_o C_{p_o}}{k_o}\right]$	(-)
q	Mass flow rate	(g/s)
Q	Volume flow rate	(m^3/s)
Q'	Zero order moment of nondimensional concentration	(m)
R	Velocity ratio $[u_s/u_r]$	(-)
R_c	Hot resistance at calibration conditions	(Ω)
Re	Reynolds number $\left[\dfrac{L_o u_o}{\nu_o}\right]$	(-)
R_H	Film hot resistance	(Ω)
Ri	Richardson number $\left[\dfrac{\Delta T_o g L_o}{T_o u_o^2}\right]$	(-)
R_m	Universal gas constant	$(m^2/s^2 {}^oK)$
Ro	Rossby number $\left[\dfrac{u_o}{L_o \Omega_o}\right]$	(-)
$R(\tau)$	Autocorrelation	(-)
t,τ,ξ	Time or time scales	(s)
ΔT	Temperature difference	$({}^oK)$
T,θ	Temperature or potential temperature	$({}^oK)$
t_1	Center of gravity of autocorrelation curve	(s)
t_o	Integral time scale	(s)
u,v,w	Velocities in x, y and z direction respectively	(m/s)

Symbol	Definition	Units
u', v', w'	Root-mean-square velocity in x, y or z direction	(m/s)
u^*	Friction velocity $\sqrt{(\overline{-u'w'})}$	(m/s)
V	Volume	(m^3)
x, y, z	Cartesian coordinates	(m)
$\overline{z}$	Center of mass	(m)
z_o	Surface roughness factor	(m)

Greek Symbols

Symbol	Definition	Units
δ	Kronecker delta tensor	(-)
ε	Tensor permutation tensor	(-)
χ	Concentration	(ppm)
χ_o	Source strength	(ppm)
γ	Density ratio $\left[\frac{\rho_a-\rho_s}{\rho_a}\right]$	(-)
Λ	Length scale	(m)
μ	Dynamic viscosity	$(gs^{-1}m^{-1})$
ν	Kinematic viscosity	(m^2s^{-1})
Ω	Angular velocity	(s^{-1})
ϕ^*	Dissipation term	(-)
ρ	Density	(gm^{-3})
σ_z,σ_y	Vertical and horizontal standard deviation of concentration distribution	(m)

Subscripts

Symbol	Definition
a	Pertaining to ambient conditions
BG	Pertaining to background data
c	Pertaining to calibration temperature
g	Pertaining to gas
h	Pertaining to reference height h
i,j,k	Tensor or summation indices
i	Pertaining to tracer i
m	Model
o	General reference quantity or initial condition
p	Prototype
r	Reference quantity
s	Pertaining to stack exit conditions
SO_2	Pertaining to SO_2 concentrations
w	Pertaining to hot wire
z_o	Pertaining to logarithmic law
∞	Free stream

Superscripts

'	Root-mean-square of quantity
*	Dimensionless parameter

LIST OF TABLES

LIST OF FIGURES

LIST OF FIGURES

LIST OF FIGURES

1.0 INTRODUCTION

Kodak Park is a major photographic manufacturing complex of the Eastman Kodak Company. This industrial complex consists of 190 buildings located on a 100-acre tract approximately 5.6 kilometers northwest of Rochester's central business district. Air quality in the Kodak Park area is evaluated routinely using a mathematical dispersion model to predict the impact of emissions from approximately 800 process sources. The dispersion model is based on criteria developed by the Environmental Protection Agency and published in the "Workbook of Atmospheric Dispersion Estimates" by D. B. Turner (1970). With this particular model Kodak Park has had the capability to evaluate the short-term impact of emissions from more common types of sources and from single or multiple sources.

Field tests conducted at Kodak Park have shown that the dispersion model lacks the performance desired. This is due to the fact that the emissions are discharged to the atmosphere through flush vents in building walls or roofs or through short stacks into regions of disturbed flow created by contiguous or closely spaced buildings. Calculation of gas dispersion under such circumstances is difficult because intuitive assumptions must be made as to the nature of the wake dispersion. As a result, a program was initiated to develop an improved mathematical dispersion model based upon wind-tunnel studies of selected sources at the industrial complex.

Wind-tunnel modeling with a neutrally stratified airstream can provide reliable dispersion data for low-level releases in an industrial complex under neutral and near neutral atmospheric stability conditions. The model tests then form an adequate data base for estimating short-term concentrations directly; also, long-term concentrations may be calculated by employing short-term concentration estimates and on-site wind frequency data. The wind-tunnel data not only serves to give reliable estimates of the expected concentrations but also will provide data from which an improved mathematical model could be developed and validated. This model can then be used to predict concentrations for conditions which were not modeled in the wind tunnel as long as the stratification of the atmosphere is near neutral.

Specifications for the wind-tunnel study were provided in the Request for Proposal dated October 17, 1978. The specifications at that time included a three-phase program. This study was concerned with Phase I. The Phase I program basically includes two parts: part I will be referred to as an "atmospheric dispersion comparability test," (ADCT) and part II will be referred to as "routine concentration measurement tests" (RCMT).

The atmospheric dispersion comparability test (ADCT) was conducted to validate the performance of the wind tunnel. For the ADCT a flat tunnel with appropriate roughness was used to generate the desired boundary layer, and the resulting concentration patterns were measured. These data were collected to show that the wind-tunnel performance compared with that expected for the atmosphere both with respect to dispersion processes and the structure of the atmospheric boundary layer.

Once the adequacy of the wind tunnel was established the RCMT were performed. For these tests a scale model of the Kodak Park facility was placed in the wind tunnel for six wind directions (southwest, west, northwest, northeast, east and south). Mean velocity profiles and turbulence intensity profiles were obtained over the center of the test section and at one elevation lateral to the test section for each direction studied. Subsequently, gases with tracers mixed were released from four stacks on buildings 301, 302, 303 and 304 and a detailed set of concentration measurements were obtained. Concentrations were obtained on the building, the ground and in two vertical arrays. Two test series were run for the southwest wind direction. The first was the present building configuration at Kodak Park and the second the configuration after new construction. The future configuration includes additional buildings 337B and 337C. For this set of data, five ambient conditions were run for the future and the present building configuration. After an analysis of this set of data with Kodak Park representatives and James Halitsky, consultant to Kodak Park, it was decided to rerun this set of data with only four velocity ratios to check the repeatability of the tests and also to supplement the data in the two-dimensional arrays. Thereafter the remaining five wind directions were studied using four ambient flow conditions and the present building configuration.

Included in this report are a discussion on the similarity requirements for wind-tunnel modeling, the details on the experimental methods used to conduct the wind-tunnel simulation, a summary of the velocity measurement results both single-wire measurements and split-film measurements, a discussion of the concentration measurement results, and a summary and conclusions. Appended to this report are a complete set of black and white photographs, color slides, and a 16 mm motion picture.

2.0 WIND-TUNNEL SIMILARITY REQUIREMENTS

2.1 Basic Equations

The basic equations governing atmospheric and plume motion (conservation of mass, momentum and energy) may be expressed in the following dimensionless form (Cermak, 1974; Snyder, 1979):

$$\frac{\partial \rho^*}{\partial t} + \frac{\partial (\rho^* u_i^*)}{\partial x_i^*} = 0, \tag{2.1}$$

$$\frac{\partial u_i^*}{\partial t^*} + u_j^* \frac{\partial u_i^*}{\partial x_j^*} + \left[\frac{L_o \Omega_o}{u_o}\right] 2\varepsilon_{ijk} u_j^* \Omega_k^* =$$

$$- \frac{\partial p^*}{\partial x_i^*} - \left[\frac{\Delta T_o L_o g_o}{T_o u_o^2}\right] \Delta T^* g^* \delta_{i3} \tag{2.2}$$

$$+ \left[\frac{\nu_o}{u_o L_o}\right] \frac{\partial^2 u_i^*}{\partial x_k^* \partial x_k^*} + \frac{\partial}{\partial x_j^*} (-\overline{u'^*_i u'^*_j})$$

and

$$\frac{\partial T^*}{\partial t^*} + u_i^* \frac{\partial T^*}{\partial x_i^*} = \left[\frac{k_o}{\rho_o C_{p_o} \nu_o}\right] \left[\frac{\nu_o}{L_o u_o}\right] \frac{\partial^2 T^*}{\partial x_k^* \partial x_k^*} \tag{2.3}$$

$$+ \frac{\partial}{\partial x_i^*}(-\overline{\theta'^* u_i'^*}) + \left[\frac{\nu_o}{u_o L_o}\right] \left[\frac{u_o^2}{C_{p_o} (\Delta T)_o}\right] \phi^*$$

The dependent and independent variables have been made dimensionless (indicated by an asterisk) by choosing appropriate reference values.

For exact similarity, the bracketed quantities and boundary conditions must be the same in the wind tunnel and in the plume as they are in the corresponding full-scale case. The complete set of requirements for similarity is:

1) Undistorted geometry

2) Equal Rossby number: $Ro = u_o/(L_o\Omega_o)$

3) Equal gross Richardson number: $Ri = \dfrac{\Delta T_o g\ L_o}{T_o u_o^2}$

4) Equal Reynolds numbers: $Re = u_o L_o/\nu_o$

5) Equal Prandtl number: $Pr = (\nu_o \rho_o C_{p_o})/k_o$

6) Equal Eckert number: $Ec = u_o^2/[C_{p_o}(\Delta T)_o]$

7) Similar surface-boundary conditions

8) Similar approach-flow characteristics.

For exact similarity, each of the above parameters must be matched in model and prototype for the stack gas flow and ambient flow separately. Naturally, the reference quantities will change depending on which flow is being considered. To insure that the stack gas rise and dispersion are similar relative to the air motion, three additional similarity parameters are required (Snyder, 1979):

9) Momentum ratio: $M_o = \dfrac{\rho_s u_s^2}{\rho_a u_a^2}$

10) Froude number : $Fr = \dfrac{u_s}{\sqrt{g\gamma D_i}}$

11) Density ratio : $\gamma = \dfrac{\rho_a - \rho_s}{\rho_a}$

All of the above requirements cannot be simultaneously satisfied in the model and prototype. However, some of the quantities are not important for the simulation of many flow conditions. The parameters which can be neglected and those which are important will be discussed in the following subsections.

2.2 Neglected Scaling Parameters

For plume rise and dispersion studies equal Reynolds number for model and prototype is not possible since the length scaling is 1:120 and unreasonably high model velocities would result. However, this inequality is not a serious limitation.

The Reynolds number related to the stack exit is defined by

$$Re_s = \frac{u_s D_i}{\nu_s} .$$

Hoult and Weil (1972) reported that plumes appear to be fully turbulent for exit Reynolds numbers greater than 300. Their experimental data show that the plume trajectories are similar for Reynolds numbers above this critical value. In fact the trajectories appear similar down to $Re_s = 28$ if only the buoyancy dominated portion of the plume trajectory is considered. Hoult and Weil's study was in a laminar cross flow (water tank) with low ambient turbulence levels, and hence the rise and dispersion of the plume would be predominantly dominated by the plume's own self-generated turbulence. For this study, a minimum u_s is 1.1 m/s, $D_i = 0.0114$ m and $\nu = 0.15 \times 10^{-4}$ m^2/s giving $(Re_s)_{min} = 836$, well above the recommended minimum value. These arguments for Reynolds number independence only apply to plumes in low ambient turbulence or to the initial stage of plume rise where the plume's self-generated turbulence dominates.

When wind velocities are sufficiently high, the stack effluent will descend into the stack wake. The character of the wake is defined by the stack $Re_{D_i} = u_a D_i/\nu$ Using a $D_i = 0.0114$ and a u_a of 1.5 m/s (representative of scale model tests) $Re_{D_i} = 1140$. According to Goldstein (1965) pp. 431-433, the transition from laminar to turbulent wake flow occurs in the range $50,000 < Re_D < 200,000$, even with augmented airstream turbulence and boundary layer tripping devices. Therefore, the model stack wake will probably remain laminar within the range of wind-tunnel velocities used for testing. Since the prototype Re_{D_i} are large enough to insure a turbulent wake, diffusion in the stack wake cannot be accurately reproduced in the model. Fortunately, the stack wake region is small compared to the building wakes and distance to maximum concentration. Hence, inaccuracies in the stack wake simulation will produce little effect on concentrations once the plume is engulfed in a building wake or when the plume rise is sufficient to avoid the stack wake.

Buildings in an airstream create local disturbed patterns with internal flow zones that are sensitive to Re. Halitsky, in Slade (1963) page 42, described experiments by Golden with sharp-edged buildings wherein concentration distributions were found to change when $R_H = u_H H/\nu$ falls below 11,000. Applying this criterion to an average building in the model with $H = 0.0762$ m, the critical velocity is $u_H = 2.2$ m/s. Extropolated to the reference height of 38 cm gives $(u_r)_{crit} = 3.2$ m/s. Lower values of u_r were used here for wind-tunnel testing after experimentally validating the invariability of the results with wind speed or Reynolds number.

For similarity in the region dominated by ambient turbulence consider Taylor's (1921) relation for diffusion in a stationary homogeneous turbulence

$$\sigma_z^2(t) = \overline{2w'^2} \int_o^\xi \int_o^t R(\xi) d\xi t \qquad (2.4)$$

which can be simplified to (see Csanady, 1973)

$$\sigma_z^2(t) \cong \overline{w'^2} t^2 \cong i_z^2 \, x^2 \qquad (2.5)$$

for short travel times; or,

$$\sigma_z^2(t) = 2\overline{w'^2} t_o(t-t_1) \; ; \tag{2.6}$$

for long travel times where

$$t_o = \int_o^\infty R(\tau)d\tau \tag{2.7}$$

is an integral time scale and

$$t_1 = \frac{1}{t_o} \int_o^\infty \tau R(\tau)d\tau \tag{2.8}$$

is the center of gravity of the autocorrelations curve. Hence, for geometric similarity at short travel times,

$$\frac{[\sigma_z^2]_m}{[\sigma_z^2]_p} = \frac{[L^2]_m}{[L^2]_p} = \frac{[i_z^2 \; x^2]_m}{[i_z^2 \; x^2]_p}$$

or,

$$[i_z]_m = [i_z]_p \; . \tag{2.9}$$

For similarity at long travel times

$$\frac{L_m^2}{L_p^2} = \frac{[\sigma_z^2]_m}{[\sigma_z^2]_p} = \frac{[\overline{w'^2} \; t_o(t-t_1)]_m}{[\overline{w'^2} \; t_o(t-t_1)]_p}$$

$$= \frac{[i_z^2]_m}{[i_z^2]_p} \; \frac{[t_o(t-t_1)/u^2]_m}{[t_o(t-t_1)/u^2]_p} = \frac{[Li_z^2 \; \Lambda]_m}{[Li_z^2 \; \Lambda]_p} \; ,$$

if it is assumed $t_1 < < t$, $t_o/u = \Lambda$ and $t/u = L$. Thus, the turbulence length scales must scale as the ratio of the model to prototype length scaling if $(i_z)_m = (i_z)_p$ or,

$$\frac{L_m}{L_p} = \frac{\Lambda_m}{\Lambda_p} \; . \tag{2.10}$$

An alternate way of evaluating the similarity requirement is by putting 2.4 in spectral form or (Snyder, 1972),

$$\sigma_z^2 = \overline{w'^2} t^2 \int_0^\infty F_L(n) \left[\frac{\sin \pi nt}{\pi nt}\right]^2 dn \tag{2.11}$$

$$= \overline{w'^2} t^2 \, I$$

where

$$I = \int_0^\infty F_L(n) \left[\frac{\sin \pi nt}{\pi nt}\right]^2 dn$$

F_L = Langrangian Spectral function.

The quantity in brackets is a filter function the form of which can be seen in Pasquill (1974). In brief for $n > 1/t$ the filter function is very small and for $n < 1/10t$ virtually unity.

For geometric similarity of the plume the following must be true:

$$\frac{L_m^2}{L_p^2} = \frac{[\sigma_z^2]_m}{[\sigma_z^2]_p} = \frac{[w'^2 t^2 I]_m}{[w'^2 t^2 I]_p} = \frac{[L^2 i_z^2 I]_m}{[L^2 i_z^2 I]_p}$$

or,

$$\frac{[i_z^2 I]_m}{[i_z^2 I]_p} = 1 \tag{2.12}$$

If $[i_z]_m = [i_z]_p$ the requirement is $I_m = I_p$. For short travel times, the filter function is essentially equal to one; hence, $I_m = I_p = 1$ and the same similarity requirement as previously deduced for short travel times is obtained (Equation 2.9).

For long travel times the larger scales (smaller frequencies) of turbulence progressively dominate the dispersion process. If the spectra in the model and prototype are of a similar shape, then similarity would be achieved. However, for a given turbulent flow a decrease in Reynolds number (hence, wind velocity) decreases the range (or energy) of the high frequency end of the spectrum. Fortunately, due to the nature of the filter function, the high frequency (small wave length) components do not contribute significantly to the dispersion. There would be, however, some critical Reynolds number below which too much of the high frequency turbulence is lost. If a study is run with a Reynolds number in this range, similarity may be impaired. Tests were conducted to insure wind speeds above the critical value were used for wind-tunnel testing.

The ambient flow field also affects the plume trajectories and consequently similarity between model and prototype is required. The mean flow field will become Reynolds number independent if the flow is fully turbulent (Schlichting, 1968; Sutton, 1953). The critical Reynolds number for this criteria to be met is based on the work of Nikuradse as summarized by Schlichting (1968) and is given by

$$(Re)_{k_s} = \frac{k_s u_*}{\nu} > 70.$$

In this relation k_s is a uniform sand grain height. If the scaled down roughness gives a $(Re)_{k_s}$ less than 70, then exaggerated roughness would be required. In the tunnel k_s may be approximated as the average height of buildings or 0.0762 m. With $\nu = 0.15\ cm^3/s$ that means u^* must be greater than 1.38 cm/s or assuming $u^*/u_r \sim 0.08$, u_r must be greater than 0.17 m/s. All tests were run well above this speed.

The Rossby number, Ro, is a quantity which indicates the effect of the earth's rotation on the flow field. In the wind tunnel, equal

Rossby numbers between model and prototype cannot be achieved. The effect of the earth's rotation becomes significant if the distance scale is large. Snyder (1978) puts a conservative cutoff point at 5 km for diffusion studies. For this particular study, the maximum range over which the plume is transported is less than 0.3 km in the horizontal and 0.15 km in the vertical.

When equal Richardson numbers are achieved, equality of the Eckert number between model and prototype cannot be attained. This is not a serious compromise since the Eckert number is equivalent to a Mach number squared. Consequently, the Eckert number is small compared to unity for laboratory and atmospheric flows.

2.3 Relevant Scaling Parameters

Since air is a transport medium in the wind tunnel and the atmosphere, near equality of the Prandtl number is assured.

The remaining relevant parameter is the momentum ratio,

$$M_o = \frac{\rho_s u_s^2}{\rho_a u_a^2}$$

Since $\rho_s \sim \rho_a$ this ratio reduces to a velocity ratio squared, or

$$M_o = \frac{u_s^2}{u_a^2} = R^2.$$

Henceforth, the velocity ratio R will be considered the relevant parameter and will be equal in model and prototype. To summarise, the following scaling criteria are applicable for the Kodak Park neutral boundary layer simulation:

1) $Fr = \frac{u_s}{\sqrt{g \gamma D}}$; $(Fr)_m = (Fr)_p = \infty$

2) $R = \frac{u_s}{u_a}$; $R_m = R_p =$ variable

3) $\gamma = \frac{\rho_a - \rho_s}{\rho_s}$; $\gamma_m = \gamma_p = 0$

4) $Ri = \frac{g\left(\frac{\Delta\theta}{\Delta z}\right)}{T\left(\frac{\Delta u}{\Delta z}\right)^2}$; $(Ri)_m = (Ri)_p = 0$

5) Similar geometric dimensions and dimensionless boundary conditions (i.e., velocity and turbulence profiles)

6) Sufficiently high Reynolds number to insure Reynolds number independence.

3.0 EXPERIMENTAL METHODS

3.1 Summary

The objective of this study is to obtain quantitative information on the dispersion characteristics around Kodak Park, specifically on effluent released from stacks on Buildings 301, 302, 303 and 304. These data are to be used to predict maximum expected ground-level concentrations resulting from process emissions and also for developing and validating a numerical model. To meet these objectives a two phase experimental program was undertaken. The two parts will hereafter be referred to as 1) atmospheric dispersion comparability test (ADCT), and 2) routine concentration measurements tests (RCMT).

For the ADCT a neutral boundary layer was developed over a 2.54 cm uniform roughness in the CSU Environmental Wind Tunnel. Measurements of velocity and concentration distributions from a point source were obtained to verify that the wind-tunnel characteristics match those expected for the atmosphere. The test conditions for these runs are enumerated in Table 3.1.

For the RCMT a 1:120 scale model of the Kodak Park facility for six wind directions (southwest, west, northwest, northeast, east and south) centered on Buildings 301, 302, 303 and 304 was constructed and placed in the CSU Environmental Wind Tunnel. A neutral boundary layer was developed naturally over the model surface and tracer gas releases were made through four stacks. These stacks are designated 301, 302, 303 and 304-7. The model operating conditions are given in Table 3.2 and for reference the full-scale conditions are enumerated in Table 3.3. A total of 38 test conditions were simulated in the wind tunnel. The run number, wind direction, reference velocity and wind speed for each test are given in Table 3.4.

All tests were conducted in a similar manner. A neutral boundary layer characteristic of the Kodak Park vicinity was established and measurements of velocity were made above Building 303. Profiles were taken to 1) document the wind characteristics over the buildings, 2) verify that the boundary layer was representative of the site, and 3) determine the velocity settings for the subsequent concentration tests.

After completing the velocity measurements, a metered quantity of neutrally buoyant gas was allowed to flow from the model stacks and the wind speed was adjusted to simulate the desired ambient value. Concentration measurements were made on the building at ground level and in a vertical array at two downwind locations.

To qualitatively document the flow pattern, the plumes were made visible by passing a gas mixture through titanium tetrachloride prior to emission from the stacks. Stills (color and black and white) and motion pictures of the tests in Table 3.4 were obtained. For the photographic portion of the study, only visualization of the smoke from Buildings 301 and 304-7 were obtained.

A more detailed description of every facet of the study will now be given.

3.2 Scale Models and Wind Tunnel

A 1:120 scale model of Buildings 301, 302, 303, 304, 337A, 337B, 337C and 339, as well as the adjacent buildings or structures with equal vertical and horizontal scales was designed and constructed for study in the CSU Environmental Wind Tunnel. The model was constructed by Kodak Park personnel according to the specifications of James Halitsky in his guidance document dated October 31, 1978. The model was constructed so that six wind directions could be studied in the tunnel. The overall length of the model for each wind direction was 5.88 m or 705.6 m in the full-scale. For each wind direction, buildings and structures were constructed with sufficient detail to reproduce the turbulence generated by each building. The main features of the prototype buildings were reproduced retaining the maximum external dimensions but omitting projections and depressions whose characteristic measurements were less than 60 cm in the prototype. Freestanding structures and equipment with characteristic dimensions greater than 15 cm in the prototype were included. Banks of piping with supporting steel work were simulated by wire screen. A picture of portions of the model is given in Figure 3.2-1.

Buildings 301-304 were positioned near the center of the test section and were designed to have a total of nine stacks discharging upward. These stacks were produced accurately as to inside diameter as given in Table 3.2 but the wall thicknesses were approximated. The coordinates of each stack are given in Table 3.5 and the location shown in Figure 3.2-2.

During concentration measurements, four of the stacks, designated 301, 302, 303 and 304-7, were supplied with a mixture of air and tracer gas. The tracers used were methane, ethane, propane and butane. The other five stacks (304-4, 304-5, 304-6, 304-8 and 304-9) were supplied with an air mixture. All nine stacks were then operated simultaneously during the concentration measurement tests. For the visualization phase of the project only the stack plume made visible was operating. The volume flow rate from each stack was controlled by a Flowrator. The Flowrators which were used are given in Table 3.16. A single Flowrator followed by a flow proportioner was used for stacks 304-4, 304-5, 304-6, 304-8 and 304-9. The respective proportion of the total flow going to each stack was 25.6, 26.4, 24.8, 11.6 and 11.6 percent. A single Flowrator was used to control the volume flow for the remaining stacks. It should be noted that stacks 301, 302 and 303 consisted of two flues. The total flow was divided equally between each flue. A schematic of the flow setup is shown in Figure 3.2-3.

Two wind-tunnel test configurations were employed. The first referred to as the atmospheric dispersion comparability test (ADCT) was a test with a uniform 2.54 cm roughness placed in the tunnel along with a 23.18 cm trip and spires. The configuration of the tunnel for this test is shown in Figures 3.2-4 and 3.2-5. A gas was released horizontally and isokinetically at 10.5 cm above the surface to document the dispersion characteristics of the tunnel for comparison with full-scale atmospheric values. Also a series of velocity measurements were obtained to document the characteristics of the flow in the tunnel without large roughness such as buildings present. The second test configuration involved placing the Kodak Park model in the tunnel for the different wind directions and releasing gases from the model stacks and measuring velocities above Building 303. This test series is referred to as the routine concentration measurements test (RCMT).

3.3 Flow Visualization

The purpose of this part of the study is to visually assess the transport of the plumes released from the Kodak Park stacks numbered 301 and 304-7. Data collected consisted of a series of photographs with the smoke emitted from the stacks for the different tests enumerated in Table 3.4. As documentation, a series of black and white and color slides were also taken of various equipment and test setups. Table 3.6 gives a description of the information portrayed on the color slides, while Table 3.7 gives a description of the information portrayed on the black and white photographs. These photographs and slides include information on the atmospheric dispersion comparability test, the Kodak Park building model sections, equipment setup, installation of southwest wind directions, the tunnel configuration during testing, the Flowrators which were used, the gas chromatograph and the gas sampling system, and finally the runs showing the smoke released from Buildings 301 and 304-7. A complete set of slides and photographs are appended to this report.

For the visualization phase, the smoke was produced by passing compressed air through a container of titanium tetrachloride located outside the tunnel and transported through the tunnel wall by means of Tygon tubing terminating at the stack inlets. The plume was illuminated with high-intensity lamps and a visible record was obtained by means of black and white photographs taken with a Graflex supergraphic camera (lens focal length 127 mm) and color slides taken with a Cannon F1 camera (focal length 40 mm). The shutter speed for the black and white photographs ranged from 1/5 to 1/50 of a second and for the color slides ranged from 1/4 to 1/30 of a second. The longer shutter speed was used for some runs to obtain an average plume trajectory. For these pictures the turbulent motions within the plume are not evident. For the fast shutter speed runs, five pictures were taken consecutively and superimposed on one negative. This procedure was performed to obtain an average plume trajectory and not lose the details of the turbulent motion as happens at the longer shutter speeds. Black and white photographs were taken from the side so that the distribution of smoke from 301 and 304-7 could be assessed in the vertical and also from an overhead window so that the horizontal movement of plumes could be assessed. Color slides were taken from the side only.

A series of 16 mm motion pictures was taken of all tests. A Bolex movie camera was used with a speed of 24 frames per second. The movies consisted of taking an initial closeup of the smoke release after which the camera was panned from the model stack to approximately 300 m downwind in the prototype.

3.4 Gas Tracer Technique

- General

The purpose of this phase of the experimental study is to provide quantitative information on the transport and dispersion of the plumes emitted from the stacks numbered 301, 302, 303 and 304-7. Specifically, this phase is to provide information that can be used to assess maximum concentration levels for Kodak Park process emissions and also provide information for developing and validating a numerical model. The model can then be used to predict concentration levels for meteorological conditions and locations not considered in the wind-tunnel test. To meet this goal a comprehensive set of concentration measurements was taken for the range of ambient wind conditions shown in Table 3.4. The data obtained included ground-level samples, an array of samples elevated above the ground and an array of samples on Buildings 301, 302, 303, 337A, 337B, 337C and 339. For the atmospheric dispersion comparability test, samples were obtained in a horizontal and vertical array at three downwind locations.

- Sample Locations

An array of 32 sampling tubes was run into the tunnel under the model terrain and fastened to 0.16 cm ID brass tubes having outlets at different locations on the building surface. These locations are given in Table 3.8 and shown visually in Figure 3.2-2. Ground level samples were obtained using from 16 to 18 0.32 cm tygon tubes which were run into the tunnel and taped in position on the model surface for each wind direction. The coordinates of the sampling points for each wind direction are given in Table 3.9 for each wind direction. A two-dimensional distribution of concentration was obtained approximately 1.22 m (146 m in prototype) and 2.74 m (39.9 m) downwind of Buildings 301-304. The rake used to obtain these samples is shown in Figure 3.4-1. At each distance (designated near and far) and for each wind direction, 70 samples were obtained at the locations specified in Tables 3.10 and 3.11. Since the sampling device was capable of obtaining 50 samples, four tests (five for one test series) labelled A, B, C and D (or E) using the same tunnel setting were required to complete one run. The key giving the sampling points included for each draw of tracer from the tunnel is given in Table 3.12. For the atmospheric dispersion comparability tests concentrations were measured in a horizontal and vertical array at three downwind locations. The sampling rake used for obtaining these data is shown in Figure 3.4-2 and coordinates given with the data tabulations as discussed in Section 5.1.

- Test Procedure

The test procedure consisted of: 1) setting the proper tunnel wind speed, 2) releasing a metered mixture of source gas of the required density (that of air) from the release stacks, 3) withdraw samples of air from the tunnel at the locations designated, and 4) analyze the samples with a flame ionization gas chromatograph (FIGC). Photographs of the sampling system and gas chromatograph are shown in Figure 3.4-3. The samples were drawn into each syringe over a 60 s (approximate) time and consecutively injected into the FIGC.

The procedure for analyzing air samples from the tunnel was as follows: 1) a 2 cc sample volume drawn from the wind tunnel is introduced into the flame ionization detector (FID), 2) the output from the electrometer (in microvolts) is sent to the Hewlett Packard 3380 Integrator, 3) the output signal is analyzed by the HP3380 to obtain the proportional amount of hydrocarbons present in the sample, 4) the record is integrated and the methane, ethane, propane or butane concentration determined by multiplying the integrated signal (μvs) times a calibration factor (ppm/μvs), 5) a summary of the integrator analysis (gas retention time and integrated area (μv-s)) is printed out on the integrator at the wind tunnel, 6) the integrated values and associated run information are tabulated on a form such as given in Figure 3.4-6, 7) the integrated values for each tracer are key punched into a computer along with pertinent run information (the format is given in Figure 3.4-5), and 8) the computer program converts the raw data to a dilution ratio and all values are stored on a file for subsequent analysis. The integrated values are converted to a dilution ratio as follows:

$$D = \frac{\chi}{\chi_o} \qquad (3.1)$$

where

D = Dilution ratio

χ = $[(I - I_{BG})\ CF]_i$

χ_o = Tracer gas source strength in ppm

I = Integrated value of sample for tracer i

I_{BG} = Integrated value of background sample

CF_i = Calibration factor for tracer i

The calibration factor was obtained by introducing a known quantity, χ_s, of propane in the HPGC and recording the integrated value, I_s, in μv-s.

The CF_i value for propane is then

$$CF_p = \frac{\chi_s(\text{ppm})}{I_s(\mu\text{v-s})} \tag{3.2}$$

For the other tracers, the calibration factor was obtained by multiplying by the ratio of molecular weights as follows

$$CF_i = CF_p * \frac{m_p}{m_i}, \tag{3.3}$$

where

m_p = molecular weight of propane - 44 g

m_i = molecular weight of i = 1, methane (16 g); i = 2, ethane (30 g); i = 3, butane (58 g).

Calibrations were obtained at the beginning and end of each measurement period.

The tracer gas mixtures were supplied by Scientific Gas Products who also certified the mixture for select bottles as shown in Table 3.13. Those gas mixtures which were not certified by Scientific Gas Products were analyzed using the HPGC. The integrated response from the HPGC for these mixtures was based on the ratio of integrated values between the uncertified and certified mixtures.

Table 3.14 gives for each stack the: 1) run number, 2) tracer gas, 3) flow rator type and setting, 4) source strength (rated/certified or corrected), 5) propane calibration factor (CF_p), 6) gas mixture bottle number, 7) background concentration-integrated value, 8) ambient temperature during the run, 9) ambient pressure, and 10) the volume flow rate through the stacks corrected for ambient conditions and back pressure.

- Gas Chromatograph

The FID operates on the principle that the electrical conductivity of a gas is directly proportional to the concentration of charged particles within the gas. The ions in this case are formed by the effluent gas being mixed in the FID with hydrogen and then burned in air. The ions and electrons formed enter an electrode gap and decrease the gap resistance. The resulting voltage drop is amplified by an electrometer and fed to the HP3380 integrator. When no effluent gas is flowing, a carrier gas (nitrogen) flows through the FID. Due to certain impurities in the carrier some ions and electrons are formed creating a background voltage or zero shift. When the effluent gas enters the FID, the voltage increases above this zero shift in proportion to the degree of ionization or correspondingly the amount of tracer gas present. Since the chromatograph[2] used in this study features a temperature control on the flame and electrometer, there is very low zero drift. In case of any zero drift, the HP3380A which integrates the effluent peak also subtracts out the zero drift.

The lower limit of measurement is imposed by the instrument sensitivity and the background concentration of tracer within the air in the wind tunnel. Background concentrations were measured and subtracted from all data quoted herein.

[2] A Hewlett Packard 5700 gas chromatograph was used in this study (shown in Figure 3.4-3).

- Sampling System

The tracer gas sampling system shown in Figure 3.4-3 consists of a series of fifty 30 cc syringes mounted between two circular aluminum plates. A variable-speed motor raises a third plate which in turn raises all 50 syringes simultaneously. A set of check valves and tubing are connected such that airflow from each tunnel sampling point passes over the top of each designated syringe. When the syringe plunger is raised, a sample from the tunnel is drawn into the syringe container. The sampling procedure consists of flushing (taking and expending a sample) the syringe three times after which the test sample is taken. The draw rate is variable and generally set to be approximately 60 s.

The sampler was periodically calibrated to insure proper function of each of the check valve and tubing assemblies. The sampler intake was connected to short sections of Tygon tubing which led to a sampling manifold. The manifold, in turn, was connected to a gas cylinder having a known concentration of tracer (~200 ppm propane). The gas was turned on and a valve on the manifold opened to release the pressure produced in the manifold. The manifold was allowed to flush for ~1 min. Normal sampling procedures were carried out to insure exactly the same procedure as when taking a sample from the tunnel. Each sample was than analyzed for methane, ethane, propane and butane. Methane, ethane and butane were analyzed to insure that the Tygon had not absorbed these hydrocarbons and was not "gassing" them off. Percent error was calculated and any "bad" samples (error > 2 percent) indicated a failure in the check valve assembly and the check valve was replaced or the bad syringe was not used for sampling from the tunnel. A typical sampler calibration is shown in Table 3.15.

- Determination of Full-Scale Concentrations

To determine a corresponding full-scale concentration from the model concentrations, consider the equation for conservation of mass, or,

$$\left[\int_{-\infty}^{\infty}\int \frac{\chi u}{q}\, dydz\right]_m = \left[\int_{-\infty}^{\infty}\int \frac{\chi u}{q}\, dydz\right]_p = 1.$$

Since $(dy)_m = \frac{(H_b)_m}{(H_b)_p}(dy)_p$ and $(dz)_m = \frac{(H_b)_m}{(H_b)_p}(dz)_p$, the equation can be rearranged to give

$$\int_{-\infty}^{\infty}\int \left[\left(\frac{\chi u}{q}\right)_p - \left(\frac{\chi u}{q}\right)_m \frac{(H_b^2)_m}{(H_b^2)_p}\right] (dydz)_p = 0$$

For this equality to be true requires

$$\left(\frac{\chi u}{q}\right)_p = \left(\frac{\chi u}{q}\right)_m \frac{(H_b^2)_m}{(H_b^2)_p} \tag{3.4}$$

or

$$\left(\frac{\chi u}{q}\, H_b^{\,2}\right)_m = \left(\frac{\chi u H_b^2}{q}\right)_p.$$

Solving for χ_p and letting $u = u_r$, $q = \chi_o \frac{\pi D_i^{\,2}}{4} u_s$, and recognizing that $\left(\frac{H_b}{D_i}\right)_m = \left(\frac{H_b}{D_i}\right)_p$ yields the following equation which can be used to calculate prototype concentrations

$$\chi_p = K_m \left[\frac{\chi_o\, Q}{u\, H_b^{\,2}}\right]_p$$

where

$$K_m = \left(\frac{\chi u}{q}\, H_b^2\right)_m = \left(\frac{\chi u H_b^2}{\chi_o Q}\right) = \frac{4D}{\pi R}\left(\frac{H_b}{D_i}\right)^2 \tag{3.5}$$

- Center of Mass and Variance

The concentration data for the ADCT were computer processed to obtain the center of mass $(\bar{z})$ and the standard deviation $(\sigma_z$ or $\sigma_y)$.

The parameters were determined by numerically integrating the following equations over the height (and width, where appropriate) of the concentration profiles:

$$Q' = \int_0^\infty K dz \tag{3.6}$$

$$\bar{z} = (1/Q') \int_0^\infty z K dz \tag{3.7}$$

$$\sigma_z^2 = (1/Q') \int_0^\infty (z-\bar{z})^2 \, K dz \tag{3.8}$$

The numerical integration was obtained using the trapezoidal rule.

- Averaging Times

To determine the averaging time for the predicted concentrations from wind-tunnel experiments the dispersion parameters--σ_y and σ_z--for the undisturbed flow in the wind tunnel were compared to those used for numerical modeling studies in the atmosphere. The dispersion rates used in the atmosphere are referred to as the Pasquill-Gifford curves and are given in Turner (1970) and modified values are given in Pasquill (1974, 1976). The results of this comparison as discussed in Section 6 showed that the σ_y and σ_z values in the wind tunnel compare (when multiplied by the length scaling factor 120) with those expected for the atmosphere. Hence, the method used for converting numerical model predictions to different averaging times should also be used for converting the wind-tunnel tests.

The EPA guideline series for evaluating new stationary sources (Budney, 1977) conservatively assumes that the Pasquill-Gifford σ_y and σ_z values represent 1-hour average values. To convert to a 3-hour value multiply by 0.9 ± 0.1 and if aerodynamic disturbances are a problem the factor should be as high as 1.

Generally, steady-state average concentrations measured in the wind tunnel are thought to correspond to a 10- or 15- minute average in the atmosphere (Snyder, 1979). This line of reasoning is based on the observed energy spectrum of the wind in the atmosphere. This spectrum shows a null in the frequency range from 1 to 3 cycles per hour. Frequencies below this null represent meandering of the wind, diurnal fluctuations, and passage of weather systems and cannot be simulated in the wind tunnel. The frequencies above this null represent the fluctuations due to roughness, buildings and other local effects and are well simulated in the tunnel. This part of the spectrum will be simulated in the tunnel as long as the wind direction and speed characteristics remain stationary in the atmosphere which is typically 10 to 15 minutes. At many locations, however, persistent winds of 3 or more hours may occur. For these cases, the wind tunnel averaging time would correspond to the atmospheric averaging time. For the more typical cases, the wind-tunnel results would have to be corrected for the large scale motion using power law relations such as given by Hino (1968) or Turner (1970).

3.5 Velocity Measurements - Single Wire

A single film sensor was used to obtain profiles of mean and longitudinal turbulence intensity for each series of tests. The measurements were performed to 1) monitor and set flow conditions, 2) document the flow conditions in the wind tunnel, and 3) for use in calculating surface roughness, power law exponent and Reynolds stress. Instrumentation used for this portion of the study included 1) a Thermo-Systems, Inc. (TSI) 1050 series anemometer, 2) a TSI Model 1210 hot-film sensor, 3) a type 120 Equibar pressure meter and pitot tube, and 4) a TSI Model 1125 calibrator for velocity calibration.

Since all tests were conducted under neutral stratification no detailed temperature measurements were required. The techniques used to obtain the velocity data with this assortment of equipment and data processing techniques will now be discussed in more detail.

- Hot-Film Anemometry--Principle of Operation and Calibration Technique

The transducer used for measuring velocities for this study was a 1210 hot-film sensor. The sensor consists of a platinum film on a single quartz fiber. The diameter of the sensor is 0.0025 cm. The sensor has the capability of resolving one component of velocity in turbulent flow fields.

The basic theory of operation is based on the physical principle that the heat transfer from the wire equals the heat supplied to the wire by the anemometer or in equation form (see Hinze, 1975).

$$I^2R_H = \pi \ell k_g (T_w - T_g)\ Nu \tag{3.9}$$

where

I = current through wire

k_g = heat conductivity of gas

ℓ = length of wire

T_w = temperature of wire

T_g = temperature of gas

Nu = Nusselt Number

$$= F\left(Re,\ Pr,\ Gr\ \frac{T_w - T_g}{T_g},\ \frac{\ell}{d}\right)$$

$$Re = \frac{ud}{\nu_g}$$

$$Pr = \frac{Cp\ \mu_g}{k_g}$$

$$Gr = \frac{gd^{\,3}(T_w - T_g)}{\nu_g^{\,2}\ T_g}$$

d = diameter of wire

R_H = operating resistance of wire

For most wind-tunnel applications an empirical equation evolved by Kramers as reported in Hinze (1975) is adequate for representing Nu for a Reynolds number range $0.01 < Re < 1000$, or

$$Nu = 0.42\ Pr^{0.2} + 0.56\ Pr^{0.33}\ Re^{0.5} \qquad (3.10)$$

Free convection from the wire can be neglected for $Re > 0.5$ when

$$Gr\ Pr < 10^{-4}$$

Alternately buoyancy may be neglected when

$$Gr < Re^3$$

The temperature dependence of the resistance of the wire is assumed to follow the ensuing relation

$$R_H = R_o\ [1 + b_1\ (T_w - T_o) + b_2\ (T_w - T_o)^2 + \ldots] \qquad (3.11)$$

where b_i are temperature coefficients. Normally the higher order terms are neglected and

$$R_w = R_o\ [1 + b_1\ (T_w - T_o)]$$

Substituting the appropriate relations yields the following equation

$$\frac{I^2\ R_w}{R_w - R_c} = A + B\ (\rho_c u)^n \qquad (3.12)$$

where

R_c = resistance of wire at calibration temperature

ρ_c = density of air at calibration temperature

$$A = \frac{\pi \ell k_f}{b_1 R_o} 0.42(Pr)^{0.2}$$

$$B = \frac{\pi \ell k_f}{b_1 R_o} 0.57(Pr)^{0.33} \left(\frac{d}{\mu}\right)^{0.5}$$

For this study A, B and n were obtained by calibrating the wire over a range of known velocities and determing A, B and n by a least-squares analysis. Since the calibration temperature of the wire is nearly equal to the temperature in the wind tunnel, no corrections for temperature were applied. Hence, the following equation was used to calculate the instantaneous velocity.

$$u = \left[\frac{\frac{I^2 R_w}{R_w - R_c} - A}{B}\right]^{1/n} \tag{3.13}$$

Calibration of the hot film was performed with the Model 1125 TSI calibrator and a type 120 Equibar pressure meter where the following relation applies:

$$u = \sqrt{\frac{2\Delta P R_m T_a}{P_a}} \tag{3.14}$$

Typical calibration curves are shown in Figure 3.5-1. A calibration was performed at the beginning of each day's measurement.

After the wire was calibrated, the desired flow condition was set in the wind tunnel. The free stream velocity was monitored with the type 120 Equibar pressure meter and pitot tube. Once the desired condition at the reference height was obtained the pressure meter setting was recorded and used to set and monitor the tunnel conditions for all remaining tests. During all subsequent velocity and concentration measurements care was taken to ensure the pressure meter reading remained constant.

- Data Collection

For the atmospheric dispersion comparability test (ADCT) velocity profiles were measured at nine locations. The profiles were taken at locations shown in Figure 3.2-4. This set of data was obtained to document the boundary layer growth and horizontal homogeneity of the wind tunnel.

For the routine concentration measurement tests (RCMT) velocity profiles in the vertical were obtained over the location marked 0 on Building 302 as shown in Figure 3.2-2. A horizontal profile was taken at a height of 0.3 m (36 m, prototype) across the tunnel above point 0. These data were used to document the vertical and horizontal distribution of velocity and turbulence for each test.

The manner of collecting the data was as follows:

1. The hot-film probe was attached to a carriage.
2. The bottom height of the profile was set to the desired initial height.
3. A vertical distribution of velocity was obtained using a vertically traversing mechanism which gave a voltage output corresponding to the height of the wire above the ground.
4. The signals from the anemometer and potentiometer device indicating height were fed directly to a Hewlett-Packard Series 1000 Real Time Executive Data Acquisition System.
5. Samples were stored digitally in the computer at a rate of 208.3 samples per second, and
6. The computer program converted each voltage into a velocity (m/s) using the equation:

$$u = \left[\frac{\frac{E^2}{R_H(R_H - R_c)} - A}{B} \right]^{1/n} \qquad (3.15)$$

At this point the program computes several useful quantities using the following equations:

$$\bar{u} = 1/N \sum_{i=1}^{N} u_i \qquad (3.16)$$

$$\overline{u'^2} = \frac{1}{N-1} \sum_{i=1}^{N} (u_i - \bar{u})^2 \qquad (3.17)$$

where N is the number of velocities considered (a 30 second average was taken, hence 6016 samples were obtained). The mean velocity and turbulence intensity at each measurement height were stored on a file in addition to being returned to the operator at the wind tunnel on a remote terminal.

A spectral analysis at three heights and two wind speeds was also conducted. The spectrum is computed using a Fast Fourier Transfer on the HP1000 computer. The basic definition of the spectrum, F(n), is given by the following equation:

$$F(n) = \int_{-\infty}^{\infty} u^2(t) e^{-i2\pi nt} \, dt$$

The data are plotted and tabulated in this report as $n \frac{F(n)}{\overline{u'^2}}$ versus $\frac{nz}{\bar{u}}$.

3.6 Velocity Measurement - Split Film

Split film anemometry techniques were used to attain four components of turbulence: $\overline{u'^2}$, $\overline{w'^2}$, $\overline{v'^2}$ and u^*. The purpose of these measurements was to compare vertical distributions and relations among turbulence qualities in the wind tunnel to those characteristic of a neutral atmosphere. The following subsections discuss the principle of operation, calibration technique, equipment set-up and data collection procedure.

- Split Film Principle of Operation and Calibration Technique

The transducer used for measuring wind tunnel velocities during this study was a Model 1287 Split Film Sensor. The sensor consists of two electrically independent platinum films on a single quartz fiber. The diameter of the sensor is 0.015 cm (0.006 in.). The sensor shown in Figure 3.6-1 has the capability of resolving two components of velocity (u and w or u and v depending on how the probe is configured in the wind tunnel) in high turbulence fields. For an ideal sensor, the heat transfer from each film is equal with the wind velocity directed at the split. As the velocity deviates from the split, the difference in heat transfer rate to the environment of the upper film and the lower film increases to a maximum when the vector is directed at the face of the upper film. The difference is directly related to the velocity (magnitude and direction) component perpendicular to the plane of the split. Thus the total heat transfer on both films gives a measure of the magnitude of the velocity vector perpendicular to the sensor.

According to Hinze (1975) and TSI Technical Bulletin TB20 the above physical phenomena can be described by the following:

$$u_N = f(Q_1 + K^2 Q_2) \qquad (3.5\text{-}1)$$

or, to put it in a "King's Law" form:

$$E_1{}^2 + K^2 E_2{}^2 = [A + B (u_N)^n] (T_w - T_g) \qquad (3.5\text{-}2)$$

where

Q_1 = heat transfer from film #1 to the environment

Q_2 = heat transfer from film #2 to the environment

K = correction for non-perfect matching of sensor $\left[\frac{R_{H_1}}{R_{H_2}}\right]^{1/2}$

A, B = "constants" depending primarily on composition of fluids

u_N = velocity component normal to the sensor

T_w = surface temperature of sensor

T_g = environment or gas temperature

n = constant

The second relation for the sensor is

$$E_1^{\ 2} - K^2 E_2^{\ 2} = f(u_N) \sin \theta \qquad (3.5\text{-}3)$$

where

$f(u_N)$ = function of u_N

θ = angle between plane of splits and the velocity vector u_N.

From Equation 3.5-2 the value of u_N can be determined, then using Equation 3.5-3 and values of E_1, E_2, u_N, K and $f(u_N)$ the value for θ is found. If u_2 is defined as the velocity component normal to the plane of the split and u_1 perpendicular to the sensor in the plane of the split, the following relations apply for u_1 and u_2

$$u_2 = u_N \sin \theta$$

$$u_1 = \sqrt{u_N^{\ 2} - u_2^2}$$

In the ideal case the above equations give the correct measurement for variations in θ up to ± 90°. With u_1 aligned with the mean flow, only fluctuations large enough to cause flow reversals would cause data problems.

- Anemometer

The anemometer, which controls the current flow for each film, operates on the principle of a feed-back loop in conjunction with a Wheatstone bridge. The purpose of the feed-back loop is to maintain the films at constant temperatures (resistances). If the velocity past the films increases, the sensor cools off thus lowering the films' resistances. The feed-back loop immediately senses this imbalance in the bridge and increases the current through the films. Since current increases and resistance remains constant, the bridge voltage drop increases. This voltage is monitored and used to calibrate the sensor.

- Initial Set-up

First the sensor cleanliness was checked by careful visual inspection. If cleaning was required, the sensor would be dipped into alcohol.

Each film was then connected to a constant temperature anemometer. The films were initially set at overheat ratios (ratio of operating resistance to "cold" resistance) of about 1.5. After the anemometers were turned on, which allows a current to pass through the films, one film was maintained at the fixed overheat ratio of 1.5 while the second film was adjusted so that the indicated voltages E_1 and E_2 are nearly equal. The split film was then placed in a flow that was parallel to the plane of the splits.

For this configuration $E_1^2 - K^2 E_2^2 = 0$ if the two films are perfectly matched. Hence $K = \frac{E_1}{E_2}$ should not vary with velocity. By a trial and error approach a ratio of $\frac{E_1}{E_2} = K$ was found that did not vary with velocity over the range of speeds to be studied.

- Split Film Calibration

In order to relate E_1 and E_2 to u_N and θ a calibration of the sensor was performed so that the constants A, B and n in Equation 3.5-3 could be found. Calibration of the split film was performed with a TSI Model 1125 Flow Calibrator for higher free stream velocity (from 2 to 4 m/s) and a Matheson Mass Flow Meter for lower free stream velocity (below 2 m/s). The calibration procedure consisted of setting the approach angle and magnitude of the wind velocity and recording the voltages from films 1 and 2. The procedure continued with different velocities and angles that encompassed the range anticipated inside the wind tunnel.

The maximum angle was 22.5° with at least four different velocities for each angle. Thereafter the constants A, B and n as well as $f(u_N)$ were found by a least squares technique. A typical calibration is shown in Figure 3.6-2.

- Data Collection

After calibration the sensor was carried into the wind tunnel. The split film sensor was attached to a carriage which could be manually moved along the wind tunnel. A vertically traversing mechanism was also an integral part of the carriage. This mechanism allowed for the positioning of the split film at various heights from outside of the wind tunnel. A digital carriage control was attached to the vertically traversing mechanism and its output was used to monitor the height of the sensor. Data were collected vertically at location D in Figure 3.2-5 for free stream velocity of 1.94 m/s. In addition a profile across the tunnel was performed at a height of 10 cm and a distance downwind corresponding to location D in Figure 3.2-5. For each type of profile (vertical or horizontal) the film was positioned in the following two manners 1) vertically to collect $\bar{u}$, $\bar{w}$, u', w' and $\sqrt{\overline{u'v'}}$ and 2) horizontally to collect $\bar{u}$, $\bar{v}$, u', v' and $u*$.

These quantities were calculated using real time computer interaction and the following equations

$$\bar{u} \text{ (or } \bar{w},\ \bar{v}) = \frac{1}{N} \sum_{i=1}^{N} (u_i)$$

$$u' = \overline{u'^2} \text{ (or } \overline{w'^2},\ \overline{v'^2}) = \frac{1}{N-1} \sum_{i=1}^{N} (u_i - \bar{u})^2$$

$$u* = \sqrt{\overline{u'w'}} = \left[\frac{1}{N-1} \sum_{i=1}^{N} (u_i - \bar{u})\ (w_i - \bar{w}) \right]^{1/2}$$

where N is the number of velocities considered. The data were obtained by sampling 500 times per second for a 30 sec duration. For each measurement two samples were obtained and averaged together. In effect each data point represented the average of two 30 s average velocity components.

3.7 Volume Flow and Back Pressure Measurements

One of the more important variables in the study was the volume flow rate of tracer gas through the model stacks. At the beginning of the study a set of volume flow rates was specified for each run and stack. Initially, the flow settings on the rotameters giving the desired flow rate were estimated from the manufacturer's supplied curves. Table 3.16 gives a list of the rotameters used and their characteristics. Various parameters affect the manufacturer's curve, such as ambient temperature T_a and pressure P_a as well as the back pressure ΔP in the line; hence the true values of the volume flow had to be determined after completion of the study. To make sure the correct volume flow rates could be determined after testing the ambient pressure and temperature, as well as back pressure, was measured for each test. Table 3.14 shows the ambient pressure and temperature for each run and Table 3.17 shows the back pressure measurements which were obtained for each test as well as the back pressure during Flowrator calibration.

After testing was complete each Flowrator was calibrated using the same tubing connections and stacks as during the tests to insure that the back pressures were the same for the calibration as for the experiments. Flow calibration was carried out using two techniques. For those flows low enough a soap bubble technique was used; whereas for the larger flow rates an alternate technique had to be devised. For these flows a 43.6 liter cylinder of compressed air was used. The initial pressure in the cylinder was measured (approximately equal to 1000 psi ± 0.5 psi). Thereafter gas was allowed to run through the Flowrator and stacks at the rate used during testing. After a certain period of time, which was monitored with a stop watch, the gas was turned off and the final pressure (say, 800 psi) in the cylinder monitored. The value of the total volume flow of gas released through the Flowrator was computed using the relation:

$$V_c = V_o \frac{\Delta P}{P_a}$$

where

V_o = 43.6 liters

ΔP = change in pressure from start to end of testing

P_a = atmospheric pressure in room

The calibrated flow rate Q_c was then determined by dividing the total amount of air released through the Flowrator by the total elapsed time

(τ or $Q_c = V_c/\tau$). Table 3.18 gives the results of all Flowrator calibrations.

The volume flow rates in Table 3.18 represent the values at the indicated ambient pressure and temperature as well as back pressure. To correct for variations in ambient temperature and pressure from day to day, the following equation was used (for Flowrators having negligible back pressure ΔP variation):

$$Q_a = Q_c \frac{P_c}{T_c} \frac{T_a}{P_a} \tag{3.7-1}$$

where the subscripts c and a mean calibration and actual test conditions. For those tests where the back pressure during testing was significantly different than that during calibration, the following equation was used:

$$Q_a = Q_c \frac{P_c}{T_c} \frac{T_a}{P_a} \sqrt{\left(\frac{P_a + \Delta P_a}{P_c + \Delta P_c}\right) \frac{T_c}{T_a}} \quad . \tag{3.7-2}$$

To determine which equation to use for correcting the calibration flow rates, ambient temperature, ambient pressure and back pressure measurements were taken prior to or after each tracer gas routine concentration measurement test. The results of the back pressure measurements are given in Table 3.17. As is evident from the table, the only flow rates requiring back pressure correction are for Flowrators A and C (see Table 3.16 for description). Thus for Flowrators A and C Equation Equation 3.7-2 was used to obtain the operating flow rate. Equation 3.7-1 was used for all other Flowrators. Table 3.14 gives the operating flow rates along with the measured or assumed ambient pressure and temperature. Also indicated in the table are those runs for which a back pressure correction has been applied.

4.0 BOUNDARY LAYER MEASUREMENT RESULTS

4.1 Atmospheric Dispersion Comparability Test (ADCT)

The procedures for collecting the velocity measurements on this test are described in Section 3.5 and 3.6. Two procedures were employed. The first entailed the use of a hot film sensor for obtaining mean and turbulent intensity magnitudes of the longitudinal velocity at several locations and speeds. Also longitudinal spectra were measured with this wire at one location. The second procedure involved the use of a split film sensor to obtain the following information, $\bar{u}$, u', v', w', and u^*. The details of the results of these measurements will now be discussed.

- Reynolds Number Test - Hot Film

To test whether the dimensionless velocity and turbulence profiles change with wind speed or Reynolds number, velocity and turbulence intensity profiles were obtained at location D (see Figure 3.2-5) for five wind speeds. The wind speeds varied from 1 to 5 m/s.

Figure 4.1-1 shows a plot of all velocity and turbulence intensity profiles at free stream speeds of 1, 1.5, 2, 3 and 5 m/s. The mean velocity profiles have all been non-dimensionalized by the free stream velocity. As can be seen all profiles follow a similar trend. The profiles which show the least conformance to the overall pattern are the 1 and 5 m/s cases. Overall the results suggest the Reynolds number independence may be achieved down to a free stream velocity as low as 1 m/s.

- Longitudinal Boundary Layer Variation - Hot Film Sensor

To test the longitudinal homogeneity of the boundary layer mean velocity and turbulence intensity profiles were taken down the center of the tunnel at locations A, B, C and D as shown in Figure 3.2-5.

The locations were 4.9, 7.3, 9.9 and 12.5 m downwind of the boundary layer trip.

Figure 4.1-2 shows these profiles - both mean velocity and turbulence intensity. The mean velocity profiles show little deviation at the four locations. The turbulence intensity profile at location A does show some effect of the spires and boundary layer trip in that increased levels of turbulence are observed. Overall the results suggest that the boundary was longitudinally homogeneous down the center of the tunnel.

- Lateral Boundary Layer Variation - Hot Film Sensor

Profiles of mean velocity and turbulence intensity where taken across the tunnel at locations H, G, D, F and E at a distance of 9.9 m from the boundary layer trip. The lateral distance between each point was 0.61 m as shown in Figure 3.2-5. The profiles are plotted in Figure 4.1-3. There appears to be a general tendency for the speeds and turbulence intensities to be lower on the G and H side of the tunnel. The variation across the tunnel does appear to be acceptable.

- Lateral Variation of Boundary Layer Characteristics - Split Film Sensor

To better assess the lateral variation of boundary layer characteristics, the split film sensor was used to take a profile of $\bar{u}$, u', v', w', and u^* across the tunnel at location D at a height of 10 cm. To obtain v' and w' two profiles had to be taken with the wire oriented in a vertical and horizontal position respectively. The results of the measurements are given in Tables 4.1 and 4.2 as well as shown in Figures 4.1-4 and 4.1-5. Figure 4.1-4 shows the lateral profile of mean velocity across the tunnel at a height of 10 cm for a free stream velocity of 1.94 m/s. The profile was taken twice, once with the wire vertical and once with the wire horizontal. As can be seen the results for both profiles are nearly identical. Also the variation in mean velocity across the tunnel between 1 and 3 m is negligible. A slight speed up is noticed on the north side of the tunnel.

Figure 4.1-5 shows the profiles of u', v', w' and $u*$ across the tunnel at a height of 10 cm for a free stream velocity of 1.94 m/s. Between about 0.6 and 3 m the lateral variation in these quantities is insignificant except for the u' component. Although, if the one data point that is high were deleted, the same could be said for the u' component. The mean ratios between 0.6 to 3 m of $u'/u*$, $v'/u*$ and $w'/u*$ are 2.06, 1.57 and 1.21 respectively. Pasquill (1974) says these values are commonly observed to be as follows for the atmosphere:

$$\frac{u'}{u*} - 2.1 - 2.9$$

$$\frac{v'}{u*} - 1.3 - 2.6$$

$$\frac{w'}{u*} - 1.25.$$

The agreement between atmosphere and laboratory is excellent at 10 cm. These results suggest that the tunnel will model the atmospheric boundary layer and the lateral homogeneity is acceptible.

- Boundary Layer Characteristics - Split Film Sensor

Vertical profiles of $\bar{u}$, u', v', w' and $u*$ were obtained at location D to assess the boundary layer characteristics. Two profiles were taken at free stream velocities of 1.9 m/s, one with the wire oriented vertically (for $\bar{u}$, u' and v') and the other with the wire horizontal (for $\bar{u}$, u', w', $u*$). Another profile was taken with the wire horizontal ($\bar{u}$, u', w' and $u*$) at a free stream velocity of 4 m/s.

The results are given in Tables 4.3, 4.4 and 4.5 and shown in Figure 4.1-6. The mean velocity and turbulence profiles when non-dimensionalized agree remarkably from test to test. The ratios of $\frac{u'}{u*}$, $\frac{v'}{u*}$ and $\frac{w'}{u*}$ are 2.06, 1.61 and 1.16 for the 1.9 m/s case and 2.15 $(\frac{u'}{u*})$, 1.22 $(\frac{w'}{u*})$ for the 4 m/s case. This again shows the invariance of the boundary layer characteristics with wind speed and also the close agreement between the wind tunnel and atmosphere. This agreement is seen by referring to the Pasquill (1974) values as given above.

- Spectra Measurements - Hot Film Sensor

Longitudinal velocity spectra data were collected at a height of 10 cm, 20 cm and 125 cm and free stream velocities of 2 and 3 m/s. Figures 4.1-7 through 4.1-9 show the results. The data are plotted $\frac{n\ F(n)}{(u')^2}$ versus $\frac{nz}{\bar{u}}$ where z and $\bar{u}$ are the local height and mean velocity. For comparison the Davenport spectrum, which was given by Davenport (1961, 1968) as:

$$\frac{n\ F(n)}{(u')^2} = \frac{2}{3}\ \frac{x^2}{(1 + x^2)^{4/3}}, \quad x = \frac{1200n}{\bar{u}_{10}},$$

is plotted on the graphs where $\bar{u}_{10}$ is speed at a height of 10 m. The agreement between the wind tunnel spectra and Davenport spectra at 10 and 20 cm heights is good. At 125 cm the agreement is not acceptable and is probably due to the remoteness of this data from the ground where viscous dissipation is strong and local isotropy of turbulence is approached.

- Summary of Boundary Layer Characteristics

To summarize the boundary layer characteristics obtained with the hot film sensor, Table 4.6 was prepared. This table gives the u*, z_o, d and n values for each profile obtained by fitting the data by least squares to the following formula:

$$\frac{\bar{u}}{u*} = \frac{1}{k} \ln \left[\frac{z-d}{z_o}\right]$$

$$\left(\frac{\bar{u}}{\bar{u}_\infty}\right) = \left(\frac{z}{z_\infty}\right)^n$$

From the table average values of 0.10 m/s, 0.10 cm, 0.24 cm for $u*$, z_o, n are observed. The average ratio of $\frac{u*}{\bar{u}_\infty} = 0.05$.

The split film data is summarized in Table 4.7. The ratio of $\frac{u*}{\bar{u}_\infty}$ as obtained by the split film is equal to 0.06 and agrees acceptably with that obtained using the hot film. This acts as a double check on the measurement techniques and implies that the data are valid. Also the tables show that turbulence characteristics in the tunnel are similar to those expected for the atmosphere.

In summary, the boundary results presented here confirm that the atmospheric boundary layer has been adequately reproduced in the CSU Environmental Wind Tunnel. Consequently, diffusion measurements should also be similar between field and laboratory.

4.2 Routine Concentration Measurement Tests (RCMT)

During the RCMT mean velocity and turbulence intensity profiles were taken over location 0 (see Figure 3.2-2) on building 302. In addition a lateral profile was taken across the tunnel over location 0 at a height of 0.3 m.

Figures 4.2-1 through 4.2-7 show the respective mean velocity and turbulence intensity profiles for the following wind directions: 1) southwest - Phase I, 2) southwest - Phase II, 3) west, 4) northwest, 5) northeast, 6) east, and 7) south. In all cases the profiles appear displaced by approximately 8 cm which is close to the height of the building upon which the profiles were taken. The profiles were taken at three speeds - 2, 3 and 4 m/s in the free stream. As can be seen the dimensionless profiles of mean velocity and turbulence intensity for a given wind direction appear invariant with wind speed.

All of the profiles were analyzed as discussed in Section 4.8 to obtain z_o, $u*$, d and n. The results are given in Table 4.8. For all tests the displacement height (d) ranges between 5.3 and 10.6 cm (6.4 to 12.7 m on prototype), the surface roughness factor ranges between 0.05 and 5.5 mm (0.6 and 6.6 cm on prototype) and the power law exponent - which has little meaning for a displaced profile - ranges from 0.3 to 1.0. The ratio of $u*/u_r$ for a given wind direction remains relatively invariant and ranges from 0.05 to 0.11 for all wind directions.

The variation of mean velocity over point 0 at 0.3 m across the tunnel is shown in Figure 4.2-8 for each wind direction (except southwest - Phase I). As can be seen each profile is different which reflects the changing nature of the surface roughness (buildings) with wind direction. For these tests a horizontally homogeneous boundary is not expected and was not observed. Figure 4.2-9 shows a similar plot of turbulence intensity across the tunnel. Again the effect of the irregular surface can be seen by the non-horizontal homogeneity of the boundary layer.

5. CONCENTRATION MEASUREMENT RESULTS

5.1 Atmospheric Dispersion Comparability Test (ADCT)

To determine whether the wind tunnel dispersion parameters (σ_y and σ_z) agree with those for the atmosphere, the vertical and horizontal concentration profiles that were obtained in the wind tunnel as discussed in Section 3.4 were analyzed. As a review, two tests were run at the 61 cm distance using wind speeds of 1 and 3 m/s in the free stream and one test at 122 cm and 183 cm both at free stream velocities of 3 m/s. Horizontal and vertical concentration profiles were obtained and analyzed for σ_y and σ_z to assess the variability in these parameters with wind speed and downwind distance. If Reynolds number is not a problem in the wind tunnel these parameters should be equal for different wind speeds and should vary with distance as observed in the atmosphere for a similar condition. The atmospheric values for σ_y and σ_z are often assumed to follow the Pasquill-Gifford curves as given in Turner (1970). However, Pasquill (1976) has recommended a different method for computing these parameters.

For σ_y Pasquill recommends the following formula for sampling times up to 1 hour:

$$\sigma_y = i_y \, x f(x) \tag{5.1}$$

where $f(x)$ is defined as follows:

x(km)	0.1	0.2	0.4	1.0	2.0	4.0
f(x)	0.8	0.7	0.65	0.6	0.5	0.4

For this study the turbulence intensity in the lateral direction (i_y) was measured using a split-film anemometer as discussed in Section 4.6. The value for i_y in that section was found to be approximately 0.15.

Figure 5.1-1 shows the observed σ_y values in the wind tunnel which have been scaled to the corresponding atmospheric values, in comparison with the predicted curve using a turbulence intensity value in the lateral direction of 0.12. The actual measured lateral turbulence intensity of 0.15 was not used since the comparison was not as good. The reason for the disagreement is more likely due to a difference in the function f(x) than recommended by Pasquill instead of an error in i_y. As can be seen from Figure 5.1-1 the variation of σ_y with distance follows the slope of the curve for the atmosphere and is slightly less than the value predicted for the atmosphere with the lateral turbulence intensity of 0.12. Also evident in the figure is the good agreement between the σ_y values for the 1 and 3 m/s cases.

For σ_z Pasquill (1976) recommends using the Turner workbook curves when the surface roughness is 3 cm. For other roughnesses he recommends using nomograms or equations in Pasquill (1974). The equation used here for σ_z is:

$$\sigma_z = 0.038\ x^{0.76} \tag{5.2}$$

where x is in kilometers and the constants were derived from Pasquill (1974) for a 10 cm roughness value. The 10 cm roughness value was chosen based upon the analysis of the velocity profiles obtained as discussed in Section 4.7.

Figure 5.1-2 shows the observed variation of σ_z versus distance in the wind tunnel (scaled to corresponding full scale values) in comparison to the prediction using the Pasquill equation for a surface roughness factor of 10 cm. As can be seen, the observed σ_z compares well at 73 (61 cm in model) and 150 m (122 cm in model); however, at

220 m (182 cm in model) the comparison is not as satisfactory. The reason for the disagreement at the 220 m distance is that the σ_z values were computed by integrating the observed concentration distribution. At a far enough distance downwind from the source, the plume reflects from the surface and does not have a Gaussian shape. From this point and beyond the σ_z computed using the integral approach would be less than that if you had a true Gaussian distribution.

Figure 5.1-3 shows the horizontal concentration profiles as observed in the wind tunnel. The data are presented in the from of $D = \frac{\chi \bar{u}_h}{q}$ for the prototype. The first set of data in Figure 5.1-3 shows the results for the two wind speeds 1 and 3 m/s. As expected the two independent sets of data agree quite closely when plotted in this form. The invariance of D with wind speed implies Reynolds number independence. The vertical concentration distribution as measured in the wind tunnel are shown on Figure 5.1-4. Again the close agreement in the D values for the 1 and 3 m/s is evident.

To assess whether the dispersion in the wind tunnel compares to the commonly used Gaussian diffusion equations, predictions were made using the following equation:

$$D = \frac{1}{2\pi\sigma_y\sigma_z} \exp\left[-\frac{1}{2}\left(\frac{y}{\sigma_y}\right)^2\right] \left\{\exp\left[-\frac{1}{2}\left(\frac{H-z}{\sigma_z}\right)^2\right] + \exp\left[-\frac{1}{2}\left(\frac{H+z}{\sigma_z}\right)^2\right]\right\} \qquad (5.3)$$

The σ_y and σ_z values were computed using Equation 5.1 with the i_y value taken to be equal to 0.115. This is the value which gave the best fit to the observed σ_y in the wind tunnel. The σ_z values used were those as predicted using Equation 5.2 and the plume height H was set equal to the release height of 10.5 cm. Figures 5.1-3 and 5.1-4 show the predicted concentration distributions and the observed distributions in the wind tunnel. The actual numerical values are given in Tables 5.1 through 5.8. As can be seen in Figure 5.1-3 the Gaussian prediction compares quite closely at the 61 cm distance. However, at 122 and 183 cm the Gaussian model underpredicts by a factor from 60 to 100 percent. The shape of the observed data, however, does conform quite closely to the Gaussian distribution. Figure 5.1-4 shows that the vertical prediction agrees much more closely than the horizontal predictions. This is true at all downwind distances. However, from this figure it appears that the assumed plume height of 10.5 cm is slightly high. At 60 cm the plume obviously appears to be lower than 10.5 cm. If a lower plume height were input into Equation 5.3, the predictions for the horizontal distributions would be closer. Regardless, the close agreement using the rough estimates of the Gaussian model inputs confirms that the wind tunnel dispersion characteristics compare favorably with those expected for the atmosphere.

5.2 Reynolds Number Independence Test

To determine the minimum wind speed for conducting routine concentration measurement tests, a gas was released from the 10.5 cm horizontal elevated source upwind of the block building shown in Figure 5.2-1. Concentrations were measured at the building roof, the downwind wall and on the ground downwind of the building at the locations shown in Figure 5.2-1. Tests were run with free stream velocities of 1, 2 and 3 m/s and flow rates through the horizontal release of 80, 175 and 293.3 cm^3/s. For this series of tests, concentrations were obtained differently than discussed in Section 4.4. The same equipment was used except the samples were taken directly from the tunnel to the gas chromatograph. Using this method the values of the tracer gas concentration measurements are approximately 4 second averages. Hence to insure that a steady state value was obtained for these tests, 20 samples were measured at each point and averaged together. In this manner an accurate assessment of the variation in concentration at the three locations (top and bottom of building and downwind of building) could be made.

The results of the concentration measurements are summarized in Table 5.9. In the table the run number versus the corresponding Reynolds number and dimensionless concentrations K at the top and bottom locations on the building and at the ground are given. The concentrations do not vary significantly between the runs designated 2 and 3 or for Reynolds numbers above 14,000. In fact, the concentrations do not vary significantly on the ground for any of the runs. On the building the most significant variance in concentration with Reynolds number is shown for the sample on the lee side of the building annotated "bottom." For the low Reynolds number test the dimensionless concentration is 0.046, whereas for the higher Reynolds test the concentrations were 0.055 and 0.060. On top of the building the concentrations for all tests were within 10 percent of each other. Above 2 m/s or a Reynolds number of 14,000, the values do not change at the various locations by more than 10 percent. Based on these results it is concluded that tests could be run with free stream wind speeds of 2 m/s or greater with confidence that Reynolds number independence is achieved. To run at the lower speed, more tests would be required to confirm Reynolds number independence.

REFERENCES

Budney, L. J., "Procedures for Evaluating Air Quality Impact of New Stationary Sources," Guidelines for Air Quality Maintenance Planning and Analysis, Volume 10 (OAQPS No. 1.2-029R) Environmental Protection Agency, Research Triangle Park, North Carolina, 27711, July 1977.

Cermak, J. E., "Applications of Fluid Mechanics to Wind Engineering," presented at Winter Annual Meeting of ASME, New York, November 17-21, 1974.

Csanady, G. T., Turbulent Diffusion in the Environment, D. Reidel Publishing Company, Doudrecht, Holland, 1973.

Davenport, A. G., "The Spectrum of Horizontal Gustiness near the Ground in High Winds," Quarterly Journal of Royal Meteorological Society, Vol. 87, No. 372, 1961.

Davenport, A. G. and N. Isyumov, "The Application of the Boundary Layer Wind Tunnel to the Prediction of Wind Loading," Proceedings from Wind Effects on Buildings and Structures, University of Toronto Press, Canada, 1968.

Hino, M., "Maximum Ground-Level Concentration and Sampling Time," Atmospheric Environment, Vol. 2, Pergamon Press, pp. 149-165, 1968.

Hinze, O. J., Turbulence, 2nd Edition, McGraw-Hill, Inc., 1975.

Hoult, D. P. and J. Weil, "Turbulent Plume in a Laminar Cross Flow," Atmospheric Environment, Vol. 6, pp. 513-531, 1972.

Pasquill, F., Atmospheric Diffusion, 2nd Edition, John Wiley and Sons, New York, 1974.

Pasquill, F., "Atmospheric Dispersion Parameters in Gaussian Plume Modeling, Part II," EPA Report No. EPA-600/4-76-0360, 1976.

Schlichting, H., Boundary Layer Theory, McGraw-Hill, Inc., New York, 1968.

Slade, D. H., Meteorology and Atomic Energy, U.S. Atomic Energy Commission, Division of Technical Information, 955 p., 1963.

Snyder, W. H., "Similarity Criteria for the Application of Fluid Models to the Study of Air Pollution Meteorology," Boundary Layer Meteorology, Vol. 3, pp. 113-134, 1972.

Snyder, W. H., "Guideline for Fluid Modeling of Atmospheric Diffusion," USEPA Report EPA-450/4-79-016, draft dated June 1979.

Sutton, O. G., Micrometeorology, McGraw-Hill, Inc., New York, 1953.

Taylor, G. I., "Diffusion by Continuous Movements," Proceedings, London Meteorological Society, Vol. 20, pp. 196-211, 1921.

Turner, P. B., Workbook of Atmospheric Dispersion Estimates, U.S. Department of Health, Education and Welfare, Public Health Service Publ. No. 999, Cincinnati, Ohio, AP-26, 88 p., 1970.

TABLES

Table 3.1. Wind-tunnel test conditions* for the Atmospheric Dispersion Comparability Test and Reynolds number test.

Run #	$\overline{u}_\infty$ (m/s)	$\overline{u}_h$ (m/s)	Q - Flow rate from stack (cm^3/s)
1	1.0	0.60	80.0
2	2.0	1.22	175.00
3	3.0	1.92	293.3

*Stack height equal to 10.5 cm and diameter equal to 1.27 cm.

Table 3.2. Model parameters* for Kodak Park test.

Parameters	Building								
	301	302	303	304					
				4	5	6	7	8	9
1. Stack diameter Inside D_i (cm)	1.15	1.18	1.18	0.69	0.69	0.69	0.56	0.55	0.55
Outside D_o (cm)	1.27	1.27	1.28	0.80	0.80	0.80	0.63	0.63	0.63
2. Building height H_b (cm)	6.61								
3. Stack height h (cm)	11.43								
4. Exit temperature T_s (°K)	293								
5. Ambient temperature T_a (°K)	293								
6. Stack gas molecular weight - m_s (g)	28.9								
7. Ambient pressure P_a (mb)	820.82 mb (24.56 inHg)								
8. Boundary layer height - z (m)	1.0								
9. Reference height z_r (m)	0.38								
10. Roughness height k_s (cm)	7.62								
11. Friction velocity ratio - $u_*/\bar{u}_r$	0.07								

*Those parameters which changed from run to run (such as exit velocity, volume flow, ambient velocity) are given in Tables 3.4 and 3.15.

Table 3.3. Prototype parameters for Kodak Park tests.

Parameters	Building								
	301*	302*	303*	304					
				4	5	6	7	8	
1. Stack diameter - D_i (m)	1.40	1.40	1.40	0.91	0.91	0.91	0.61	0.61	0
2. Stack height - h (m)	13.72	13.72	13.72	13.72	13.72	13.72	13.72	13.72	13
3. Exit velocity - u_s (m/s)	15.6	13.6	14.8	24.0	24.8	23.2	21.9	24.3	24
4. Volume flow - Q (m^3/s)	48.0	41.9	45.6	15.6	16.1	15.1	6.4	7.1	7
5. Building height - H_b (m)					7.93				
6. Exit temperature - T_s (°K)					293				
7. Ambient temperature - T_a (°K)					293				
8. Ambient pressure - P_a (mb)					1000				
9. Boundary layer height - z_∞ (m)					120				
10. Reference height or anemometer height - z_r (m)					45.72				
11. Roughness height - k_s (m)					9.1				
12. Friction velocity ratio - $u_\infty/\bar{u}_r$					0.07				

*Double flue on these buildings.

Table 3.4. Velocity ratios and reference wind speeds for each test.

RUN NO.	WIND DIRECTION	REF VEL $\bar{u}_r$ (m/s)	VELOCITY RATIO (u_s/u_r)			
			301	302	303	304
			n=2	2	2	1
1*	SW+	1.58	7.67	6.33	7.19	11.48
2*		3.11	3.89	3.21	3.66	5.83
3*		1.58	3.27	1.98	2.26	2.39
4*		2.37	1.38	0.96	1.03	1.19
5*		2.37	0.54	0.44	0.47	0.56
6		1.58	7.67	6.33	7.19	11.48
7		3.11	3.89	3.21	3.66	5.83
8		1.58	3.27	1.98	2.26	2.39
9		2.37	1.38	0.96	1.03	1.19
10		2.37	0.54	0.44	0.47	0.56
1*	SW	1.58	7.67	6.32	7.21	11.47
2*		3.05	3.98	3.28	3.73	5.95
3*		1.58	3.27	1.97	2.25	2.38
4*		2.38	1.39	0.96	1.02	1.19
5		1.58	7.71	6.37	7.24	11.56
6		3.05	3.98	3.28	3.74	5.95
7		1.58	3.27	1.98	2.22	2.39
8		2.38	1.38	0.95	1.02	1.18
9	W	1.56	7.79	6.39	7.26	16.94
10		2.98	4.07	3.35	3.81	6.08
11		1.56	3.28	1.99	2.26	2.40
12		2.31	1.41	0.97	1.04	1.20
13	NW	1.56	7.76	6.40	7.80	11.63
14		2.92	4.07	3.44	4.03	6.02
15		1.56	3.31	2.01	2.29	2.42
16		2.34	1.40	0.97	1.04	1.20
17	NE	1.72	7.13	5.92	6.81	10.73
18		3.26	3.75	3.10	3.58	5.63
19		1.72	3.02	1.83	2.08	2.20
20		2.39	1.38	0.95	1.02	1.19
21	E	1.64	7.07	6.10	7.07	11.08
22		3.34	3.48	3.01	3.48	5.46
23		1.64	3.15	1.91	2.17	2.30
24		2.38	1.38	0.95	1.02	1.18
25	S	1.55	7.50	6.51	7.52	11.81
26		3.07	3.79	3.30	3.80	5.99
27		1.55	3.36	2.04	2.32	2.46
28		2.31	1.44	0.99	1.06	1.23

*Future building configuration.
+The first series of tests for this wind direction.

Table 3.5. Release locations.

Stack Name	Building	Easting(ft)	Northing(ft)	Elevation (ft, MSL)	Height above Grade (ft)
J-1	301	745,878	1,166,789	300	45
J-2		745,881	1,166,786	300	45
H-1	302	745,878	1,166,894	300	45
H-2		745,881	1,166,891	300	45
G-1	303	745,834	1,167,019	300	45
G-2		745,841	1,167,019	300	45
A	304-7	745,838	1,167,144	300	45
B	304-8	745,881	1,167,144	300	45
C	304-9	745,900	1,167,144	300	45
D	304-4	745,845	1,167,078	300	45
E	304-5	745,909	1,167,078	300	45
F	304-6	745,981	1,167,078	300	45

Table 3.6. Description of information portrayed on color slides.

Slide Number	Slide Description
1	Building section of model before placed in tunnel
2	Building section of model before placed in tunnel
3	Setup for exit velocity and back pressure tests
4	Unassembled model sections
5	Unassembled model sections
6	Preparation of stacks
7	Preparation of stacks
8	Preparation of stacks
9	Studying Kodak blueprints
10	Unpacking and assembling model sections
11	Dr. Cermak testing flow visualization
12	Engineers analyzing results
13	Studying velocity profile set up conditions
14	Examination of spires
15	Instrument setup for velocity profile tests
16	Setting up for velocity profile
17	Velocity profile setup in tunnel spires and roughness
18	Boundary layer test - free stream velocity of 1 m/s, 1/25 second shutter speed
19	Boundary layer test - free stream velocity of 1 m/s, 1/16 second shutter speed
20	Boundary layer test - free stream velocity of 2 m/s, 1/25 second shutter speed
21	Boundary layer test - free stream velocity of 2 m/s, 1/16 second shutter speed
22	Boundary layer test - free stream velocity of 3 m/s, 1/25 second shutter speed
23	Boundary layer test - free stream velocity of 3 m/s, 1/16 second shutter speed
24	Model in tunnel for SW wind direction looking in
25	Close-up of source complex in future configuration looking from the north
26	Close-up of buildings 301 through 304
27	Source complex from north
28	Close-up of roofs of buildings 302, 303 and 304

Table 3.6. Description of information portrayed on color slides.

Slide Number	Run Number	Wind Direction	Configuration	Velocity Ratio-301	Stack Operating 301	304-7
30	1*	SW 225^{o}	F	7.31		X
31	1J*				X	
32					X	
33	2*			3.70		X
34	2J*				X	
35	3*			1.83		X
36	3J*				X	
37	4*			0.94		X
38	4J*				X	
39	5*			0.46		X
40	5J*				x	
53	6*		P	7.31		X
54	6J*				X	
55	7*			3.70		X
56	7J*				X	
57	8*			1.83		X
58	8J*				X	
59	9*			0.94		X
60	9J*				X	
61	10*			0.46		X
62	10J*				X	
41	5A	SW 225^{o}	P	7.31	X	
42	5J					X
43	6A			3.70	X	
44	6J					X
45	7A			1.83	X	
46	7J					X
47	8A			0.94	X	
48	8J					X
49	9	W 270^{o}	P	7.31		X
50	9J				X	
51	10			3.70		X
52	10J				X	

*Designates tests conducted between 5-12-79 and 5-22-79.

Table 3.6. Description of information portrayed on color slides.

Slide Number	Run Number	Wind Direction	Configuration	Velocity Ratio-301	Stack Operating 301	304-7
63	11			1.83		X
64	11J				X	
65	12			0.94		X
66	12J				X	
67	13A	NW 315°	P	7.31		X
68	13J				X	
69						X
70	14A			3.70		X
71	14J				X	
72	15A			1.83		X
73	15J				X	
74	16A			0.94		X
75	16J				X	
76	17A	NE 45°	P	7.31		X
77						X
78	17J				X	
79	18A			3.70		X
80	18J				X	
81	19A			1.83		X
82	19J				X	
83	20A			0.94		X
84	20J				X	
85	21A	E 90°	P	7.30		X
86	21J				X	
87	22A			3.70		X
88	22J				X	
89	23A			1.83		X
90	23J				X	
91	24A			0.94		X
92	24J				X	
93	25A	S 180°	P	7.31		X
94	25J				X	
95	26A			3.70		X
96	26J				X	

Table 3.6. Description of information portrayed on color slides.

Slide Number	Run Number	Wind Direction	Configuration	Velocity Ratio-301	Stack Operating 301	
					301	304-7
97	27A			1.83		X
98	27J				X	
99	28A			0.94		X
100	28J				X	

Table 3.7. Description of information on black and white photographs.

Photo Number	Photo Description
1	Kodak building model section
2	Checking exit velocities of stacks
3	Unpacked model sections
4	Unpacked model sections
5	Roughness used for boundary layer tests
6	Release probe for boundary layer tests
7	Roughness used for boundary layer tests
8	Release probe for boundary layer tests
9	Release probe for boundary layer tests
10	Boundary layer test - free stream velocity of 1 m/s, 1/25 second shutter speed
11	Boundary layer test - free stream velocity of 1 m/s, 1/16 second shutter speed
12	Boundary layer test - free stream velocity of 2 m/s, 1/25 second shutter speed
13	Boundary layer test - free stream velocity of 2 m/s, 1/25 second shutter speed
14	Boundary layer test - free stream velocity of 2 m/s, 1/16 second shutter speed
15	Boundary layer test - free stream velocity of 3 m/s, 1/25 second shutter speed
16	Boundary layer test - free stream velocity of 3 m/s, 1/16 second shutter speed
46	Equipment setup
52	Installing SW wind direction
61	Equipment setup
62	Installing SW wind direction
63	Looking downwind in tunnel, SW wind direction

Table 3.7. Description of information on black and white photographs.

Photo Number	Photo Description
64	Looking downwind in tunnel, SW wind direction
65	Looking downwind in tunnel, SW wind direction
66	Looking upwind in tunnel, SW wind direction
67	Looking upwind in tunnel, SW wind direction
68	Looking downwind in tunnel, SW wind direction
69	Sampling rake
85	Tunnel air inlet
86	North side of tunnel
87	South side of tunnel, camera hood
88	South side of tunnel, camera hood
89	North side of tunnel
90	Small flow rators
91	Method of tube connection to building model
92	Equipment setup
93	Sampler and gas chromatograph
94	Large and small flow rators
95	Downwind view in tunnel, SW wind direction
96	Large and small flow rators
97	Sampling rake
98	Upwind view in tunnel, SW wind direction
99	Model in tunnel
100	Small flow rators
101	Tunnel setup, South West wind direction
206	Tunnel setup, South wind direction
207	Tunnel setup, East wind direction

Table 3.7. Description of information on black and white photographs.

Photo Number	Photo Description
208	Tunnel setup, North East wind direction
209	Tunnel setup, East wind direction
210	Small flow rators and pressure gauge
211	Tunnel setup, North East wind direction
212	Sampler
213	Gas chromatograph and Integrator

Table 3.7. Description of information on black and white photographs.

Photo Number	Run Number	Wind Direction	Config-uration	Velocity Ratio-301	Stack Operating 301	304-7
17	1*	SW 225	F	7.31		X
18						X
19	1J*				X	
20					X	
21	2*			3.70		X
22						X
23	2J*				X	
24					X	
25	3*			1.83		X
26						X
27	3J*				X	
28					X	
29	4*			0.94		X
30						X
31	4J*				X	
32					X	
33	5*			0.46		X
34						X
35	5J*				X	
36					X	
37	6*		P	7.31		X
38						X
39	6J*				X	
40					X	
41	7*			3.70		X
42						X
43	7J*				X	
44					X	
45					X	
47	8*			1.83		X
48						X
49	8J*				X	
50					X	
51					X	

Table 3.7. Description of information on black and white photographs.

Photo Number	Run Number	Wind Direction	Config-uration	Velocity Ratio-301	Stack Operating 301	304-7
53	9*			0.94		X
54						X
55	9J*				X	
56					X	
57	10*			0.46		X
58						X
59	10J*				X	
60					X	
103	4A	SW 225	F	0.94		X
104	5A		P	7.31	X	
105					X	
106	5J					X
107						X
108	6A	SW 225	P	3.70	X	
109					X	
110	6J					X
111						X
112	7A			1.83	X	
113					X	
114	7J					X
115						X
116	8A			0.94	X	
117					X	
118	8J					X
119						X
120	9	W 270^{o}	P	7.31		X
121						X
122	9J				X	
124	10			3.70		X
125						X
126	10J				X	
127					X	
128	11			1.83		X

Table 3.7. Description of information on black and white photographs.

Photo Number	Run Number	Wind Direction	Configuration	Velocity Ratio-301	Stack Operating 301	304-7
129						X
130	11J				X	
131					X	
132	12			0.94		X
133						X
134	12J				X	
135					X	
136	13A	NW 315°	P	7.31		X
137						X
138	13J				X	
139					X	
140					X	
142	14A			3.70		X
144	14J				X	
145					X	
146	15A			1.83		X
147						X
148	15J				X	
149					X	
150	16A			0.94		X
151						X
152	16J				X	
153					X	
154	17A	NE 45°	P	7.31		X
155						X
156						X
158	17J	NE 45	P	7.31	X	
159					X	
160	18A			3.70		X
161						X
162	18J				X	
163					X	
164	19A			1.83		X
165						X

Table 3.7. Description of information on black and white photographs.

Photo Number	Run Number	Wind Direction	Config-uration	Velocity Ratio-301	Stack Operating 301	304-7
166	19J				X	
167					X	
169					X	
170	20A			0.94		X
171						X
172	20J				X	
173					X	
175	21A	E 90°	P	7.31		X
177	21J				X	
178	22A					X
179						X
181	22J				X	
182	23A			3.70		X
183						X
184	23J				X	
185					X	
186	24A			1.83		X
187						X
188	24J				X	
189					X	
190	25A	S 180°	P	7.31		X
191						X
192	25J				X	
193					X	
194	26A			3.70		X
195						X
196	26J				X	
197					X	
198	27A			1.83		X
199						X
200	27J				X	
201					X	
202	28A			0.94		X
203						X

Table 3.7. Description of information on black and white photographs.

Photo Number	Run Number	Wind Direction	Config-uration	Velocity Ratio-310	Stack Operating 301	304-7
204	28J				X	
205					X	

Table 3.8. Building sampling locations.

Sample Point No.	Easting(ft)	Northing(ft)	Elevation(ft)
BW01	745,875	1,166,784	267
BW02	745,875	1,166,890	267
BW03	745,830	1,166,995	267
BW04	745,827	1,167,105	267
BW05	745,830	1,167,252	264
BW06	745,832	1,167,400	265
BW07	745,892	1,166,757	267
BW08	745,922	1,167,137	277
BW09	745,995	1,167,322	270
BW10	746,010	1,167,435	270
BW11	746,050	1,166,740	267
BW12	746,122	1,166,784	267
BW13	746,071	1,166,887	262
BW14	746,071	1,166,995	268
BW15	746,112	1,167,105	268
BW16	746,136	1,167,254	267
BW17	746,136	1,167,376	269
BR18	745,892	1,166,784	281
BR19	745,894	1,166,890	281
BR20	745,847	1,166,992	281
BR21	745,847	1,167,105	291
BR22	745,887	1,167,252	281
BR23	745,896	1,167,400	283
BR24	746,050	1,166,784	281
BR25	746,047	1,166,890	281
BR26	746,046	1,166,995	291
BR27	746,045	1,167,105	291
BR28	746,024	1,167,254	281
BR29	746,005	1,167,322	308
BR30	746,025	1,167,399	288
BR31	746,105	1,167,254	295
BR32	746,101	1,167,343	288

Table 3.9a. Ground-level sampling locations for a) southwest wind direction.

Sample Point	Easting(ft)	Northing(ft)	Elevation(ft)
PG01	746,400	1,167,870	247
PG02	746,400	1,167,690	246
PG03	746,400	1,167,500	246
PG04	746,400	1,167,370	246
PG05	746,320	1,167,590	248
PG06	746,230	1,167,670	250
PG07	746,225	1,166,970	252
PG08	746,165	1,167,030	252
PG09	746,120	1,167,080	252
PG10	746,020	1,167,202	252
PG11	745,941	1,167,294	253
PG12	746,325	1,167,031	252
PG13	746,259	1,167,100	252
PG14	746,206	1,167,159	249
PG15	746,231	1,167,325	250
PG16	746,013	1,167,375	287

Table 3.9b. Ground points sampling locations for b) west wind direction.

Sample Point	Easting(ft)	Northing(ft)	Elevation(ft)
PG01	746,397	1,167,250	247
PG02	746,397	1,167,125	246
PG03	746,397	1,167,000	246
PG04	746,397	1,166,875	247
PG05	746,397	1,166,750	250
PG06	746,397	1,166,625	245
PG07	746,228	1,167,250	249
PG08	746,228	1,167,125	249
PG09	746,228	1,167,000	252
PG10	746,228	1,166,875	256
PG11	746,228	1,166,750	260
PG12	746,228	1,166,625	264
PG13	746,191	1,167,250	249
PG14	746,191	1,167,125	251
PG15	746,191	1,167,000	252
PG16	746,191	1,166,875	255
PG17	746,191	1,166,750	255
PG18	746,191	1,166,625	245

Table 3.9c. Ground sampling locations for c) northwest wind direction.

Sample Point	Easting(ft)	Northing(ft)	Elevation(ft)
PG01	746,419	1,166,806	247
PG02	746,356	1,166,734	260
PG03	746,288	1,166,163	263
PG04	746,219	1,166,591	260
PG05	746,147	1,166,519	260
PG06	746,075	1,166,447	261
PG07	746,366	1,166,863	254
PG08	746,297	1,166,794	256
PG09	746,228	1,166,725	258
PG10	746,156	1,166,650	250
PG11	746,088	1,166,578	242
PG12	746,016	1,166,506	260
PG13	746,306	1,166,666	252
PG14	746,238	1,166,841	254
PG15	746,169	1,166,775	255
PG16	746,100	1,166,706	256
PG17	746,025	1,166,638	250
PG18	745,956	1,166,566	252

Table 3.9d. Ground sampling locations for d) northeast wind direction.

Sample Point	Easting(ft)	Northing(ft)	Elevation(ft)
PG01	745,853	1,166,538	261
PG02	745,794	1,166,616	252
PG03	745,713	1,166,681	254
PG04	745,628	1,166,756	257
PG05	745,553	1,166,825	256
PG06	745,488	1,166,900	255
PG07	745,909	1,166,603	244
PG08	745,841	1,166,669	254
PG09	745,759	1,166,744	254
PG10	745,681	1,166,813	254
PG11	745,606	1,166,878	255
PG12	745,538	1,166,950	255
PG13	745,959	1,166,663	254
PG14	745,894	1,166,738	254
PG15	745,819	1,166,806	255
PG16	745,744	1,166,881	253
PG17	745,672	1,166,950	255
PG18	745,600	1,167,009	255

Table 3.9e. Ground sampling locations for e) east wind direction.

Sample Point	Easting(ft)	Northing(ft)	Elevation(ft)
PG01	745,578	1,166,688	257
PG02	745,578	1,166,784	257
PG03	745,578	1,166,834	255
PG04	745,578	1,166,988	252
PG05	745,578	1,167,088	249
PG06	745,578	1,167,188	246
PG07	745,678	1,166,688	254
PG08	745,678	1,166,784	255
PG09	745,678	1,166,834	256
PG10	745,678	1,166,988	254
PG11	745,678	1,167,088	277
PG12	745,678	1,167,188	248
PG13	745,778	1,166,688	254
PG14	745,778	1,166,784	254
PG15	745,778	1,166,834	255
PG16	745,778	1,166,988	255
PG17	745,778	1,167,088	255
PG18	745,778	1,167,188	254

Table 3.9f. Ground sampling locations for f) south wind direction.

Sample Point	Easting(ft)	Northing(ft)	Elevation(ft)
PG01	745,703	1,167,303	250
PG02	745,772	1,167,303	252
PG03	745,841	1,167,303	252
PG04	745,909	1,167,303	253
PG05	745,981	1,167,303	253
PG06	746,047	1,167,303	253
PG07	745,703	1,167,269	253
PG08	745,772	1,167,269	253
PG09	745,841	1,167,269	253
PG10	745,909	1,167,269	253
PG11	745,981	1,167,269	253
PG12	746,047	1,167,269	253
PG13	745,703	1,167,191	249
PG14	745,772	1,167,191	252
PG15	745,841	1,167,191	254
PG16	745,909	1,167,191	254
PG17	745,981	1,167,191	254
PG18	746,047	1,167,191	250

Table 3.10a. Near rake sampling locations for a) southwest wind direction.

Sample Point	Easting (ft)	Northing(ft)	Elevation Base (ft)	Elevation Row 2 (ft)	Elevation Row 3 (ft)	Elevation Row 4 (ft)	Elevation Row 5 (ft)	Elevation Row 6 (ft)
NG03	746,075	1,167,509	250	-23* 275	-43* 300	-63* 350	-83* 400	
NG04	746,106	1,167,472	250	-24 275	-44 300	-64 350	-84 400	-104* 450
NG05	746,137	1,167,434	250	-25 275	-45 300	-65 350	-85 400	-105 450
NG06	746,167	1,167,397	250	-26 275	-46 300	-66 350	-86 400	-106 450
NG07	746,198	1,167,359	245	-27 270	-47 295	-67 345	-87 395	-107 445
NG08	746,229	1,167,322	245	-28 270	-48 295	-68 345	-88 395	-108 445
NG09	746,260	1,167,285	245	-29 270	-49 295	-69 345	-89 395	-109 445
NG10	746,290	1,167,247	245	-30 270	-50 295	-70 345	-90 395	-110 445
NG11	746,321	1,167,210	245	-31 270	-51 295	-71 345	-91 395	-111 445
NG12	746,352	1,167,172	245	-32 270	-52 295	-72 345	-92 395	-112 445
NG13	746,382	1,167,135	245	-33 270	-53 295	-73 345	-93 395	-113 445
NG14	746,413	1,167,097	245	-34 270	-54 295	-74 345	-94 395	

*This number is the sampling point number used for computer processing. Full number is N-23, N-24, etc.

Table 3.10b. Near rake sampling locations for b) west wind direction.

Sample Point	Easting (ft)	Northing(ft)	Elevation Base (ft)	Elevation Row 2 (ft)	Elevation Row 3 (ft)	Elevation Row 4 (ft)	Elevation Row 5 (ft)	Elevation Row 6 (ft)
NG03	746,425	1,167,187	247	-23* 272	-43* 297	-63* 347	-83* 397	
NG04	746,425	1,167,137	247	-24 272	-44 297	-64 347	-84 397	-104* 447
NG05	746,425	1,167,087	247	-25 272	-45 297	-65 347	-85 397	-105 447
NG06	746,425	1,167,037	247	-26 272	-46 297	-66 347	-86 397	-106 447
NG07	746,425	1,166,987	246	-27 271	-47 296	-67 346	-87 396	-107 446
NG08	746,425	1,166,937	246	-28 271	-48 296	-68 346	-88 396	-108 446
NG09	746,425	1,166,887	246	-29 271	-49 296	-69 346	-89 396	-109 446
NG10	746,425	1,166,837	246	-30 271	-50 296	-70 346	-90 396	-110 446
NG11	746,425	1,166,787	247	-31 272	-51 297	-71 347	-91 397	-111 447
NG12	746,425	1,166,737	247	-32 272	-52 297	-72 347	-92 397	-112 447
NG13	746,425	1,166,687	247	-33 272	-53 297	-73 347	-93 397	-113 447
NG14	746,425	1,166,637	247	-34 272	-54 297	-74 347	-94 397	

*This number is the sampling point number used for computer processing. Full number is N-23, N-24, etc.

Table 3.10c. Near rake sampling locations for c) northwest wind direction.

Sample Point	Easting (ft)	Northing(ft)	Elevation Base (ft)	Elevation Row 2 (ft)	Elevation Row 3 (ft)	Elevation Row 4 (ft)	Elevation Row 5 (ft)	Elevation Row 6 (ft)
NG03	746,444	1,166,741	247	-23* 272	-43* 297	-63* 347	-83* 397	
NG04	746,409	1,166,705	247	-24 272	-44 297	-64 347	-84 397	-104* 447
NG05	746,375	1,166,669	252	-25 277	-45 302	-65 352	-85 402	-105 452
NG06	746,340	1,166,633	260	-26 285	-46 310	-66 360	-86 410	-106 460
NG07	746,305	1,166,597	261	-27 286	-47 311	-67 361	-87 411	-107 461
NG08	746,271	1,166,561	261	-28 286	-48 311	-68 361	-88 411	-108 461
NG09	746,236	1,166,524	261	-29 286	-49 311	-69 361	-89 411	-109 461
NG10	746,202	1,166,488	261	-30 286	-50 311	-70 361	-90 411	-110 461
NG11	746,167	1,166,452	261	-31 286	-51 311	-71 361	-91 411	-111 461
NG12	746,132	1,166,416	261	-32 286	-52 311	-72 361	-92 411	-112 461
NG13	746,098	1,166,380	261	-33 286	-53 311	-73 361	-93 411	-113 461
NG14	746,063	1,166,344	261	-34 286	-54 311	-74 361	-94 411	

*This number is the sampling point number used for computer processing. The full number is N-23, N-24, etc.

Table 3.10d. Near rake sampling locations for d) northwest wind direction.

Sample Point	Easting (ft)	Northing(ft)	Elevation Base (ft)	Elevation Row 2 (ft)		Elevation Row 3 (ft)		Elevation Row 4 (ft)		Elevation Row 5 (ft)		Elevation Row 6 (ft)	
NG03	745,722	1,166,438	260	-23*	285	-43*	310	-63*	360	-83*	410		
NG04	745,688	1,166,473	260	-24	285	-44	310	-64	360	-84	410	-104*	460
NG05	745,653	1,166,508	260	-25	285	-45	310	-65	360	-85	410	-105	460
NG06	745,619	1,166,544	250	-26	275	-46	300	-66	350	-86	400	-106	450
NG07	745,584	1,166,579	250	-27	275	-47	300	-67	350	-87	400	-107	450
NG08	745,550	1,166,614	252	-28	277	-48	302	-68	352	-88	402	-108	452
NG09	745,516	1,166,649	252	-29	277	-49	302	-69	352	-89	402	-109	452
NG10	745,481	1,166,684	252	-30	277	-50	302	-70	352	-90	402	-110	452
NG11	745,447	1,166,719	252	-31	277	-51	302	-71	352	-91	402	-111	452
NG12	745,413	1,166,755	252	-32	277	-52	302	-72	352	-92	402	-112	452
NG13	745,378	1,166,790	250	-33	275	-53	300	-73	350	-93	400	-113	450
NG14	745,344	1,166,825	248	-34	273	-54	298	-74	348	-94	398		

*This number is the sampling point number used for computer processing. The full number is N-23, N-24, etc.

Table 3.10e. Near rake sampling locations for e) east wind direction.

Sample Point	Easting (ft)	Northing(ft)	Elevation Base (ft)	Elevation Row 2 (ft)	Elevation Row 3 (ft)	Elevation Row 4 (ft)	Elevation Row 5 (ft)	Elevation Row 6 (ft)
NG03	745,494	1,166,700	254	-23* 279	-43* 304	-63* 354	-83* 404	
NG04	745,492	1,166,751	255	-24 280	-44 305	-64 355	-84 405	-104* 455
NG05	745,491	1,166,802	256	-25 281	-45 306	-65 356	-85 406	-105 456
NG06	745.489	1,166,852	255	-26 280	-46 305	-66 355	-86 405	-106 455
NG07	745,487	1,166,903	255	-27 280	-47 305	-67 355	-87 405	-107 455
NG08	745,485	1,166,954	252	-28 277	-48 302	-68 352	-88 402	-108 452
NG09	745,484	1,167,005	250	-29 275	-49 300	-69 350	-89 400	-109 450
NG10	745,482	1,167,056	256	-30 281	-50 307	-70 357	-90 407	-110 457
NG11	745,480	1,167,107	262	-31 287	-51 312	-71 362	-91 412	-111 462
NG12	745,478	1,167,157	246	-32 271	-52 296	-72 346	-92 396	-112 446
NG13	745,477	1,167,208	246	-33 271	-53 296	-73 346	-93 396	-113 446
NG14	745,475	1,167,259	274	-34 299	-54 324	-74 374	-94 424	

*This number is the sampling point number used for computer processing. The full number is N-23, N-24, etc.

Table 3.10f. Near rake sampling locations for f) south wind direction.

Sample Point	Easting (ft)	Northing(ft)	Elevation Base (ft)	Elevation Row 2 (ft)	Elevation Row 3 (ft)	Elevation Row 4 (ft)	Elevation Row 5 (ft)	Elevation Row 6 (ft)
NG03	745,597	1,167,397	245	-23* 270	-43* 295	-63* 345	-83* 395	
NG04	745,648	1,167,397	246	-24 271	-44 296	-64 346	-84 396	-104* 446
NG05	745,699	1,167,397	250	-25 275	-45 300	-65 350	-85 400	-105 450
NG06	745,749	1,167,397	250	-26 275	-46 300	-66 350	-86 400	-106 450
NG07	745,800	1,167,397	250	-27 275	-47 300	-67 350	-87 400	-107 450
NG08	745,850	1,167,397	250	-28 275	-48 300	-68 350	-88 400	-108 450
NG09	745,901	1,167,397	250	-29 275	-49 300	-69 350	-89 400	-109 450
NG10	745,951	1,167,397	250	-30 275	-50 300	-70 350	-90 400	-110 450
NG11	746,002	1,167,397	287	-31 312	-51 337	-71 387	-91 437	-111 487
NG12	746,052	1,167,397	287	-32 312	-52 337	-72 387	-92 437	-112 487
NG13	746,103	1,167,397	298	-33 323	-53 348	-73 398	-93 448	-113 498
NG14	746,153	1,167,397	250	-34 275	-54 300	-74 350	-94 400	

*This number is the sampling point number used for computer processing. The full number is N-23, N-24, etc.

Table 3.11a. Far rake sampling locations for a) southwest wind direction.

Sample Point	Easting (ft)	Northing (ft)	Elevation Base (ft)	Elevation Row 2 (ft)	Elevation Row 3 (ft)	Elevation Row 4 (ft)	Elevation Row 5 (ft)	Elevation Row 6 (ft)
FG03	746,441	1,167,841	280	-23* 305	-43* 330	-63* 380	-83* 430	
FG04	746,473	1,167,801	280	-24 305	-44 330	-64 380	-84 430	-104* 480
FG05	746,505	1,167,760	280	-25 305	-45 330	-65 380	-85 430	-105 480
FG06	746,537	1,167,720	280	-26 305	-46 330	-66 380	-86 430	-106 480
FG07	746,569	1,167,679	270	-27 295	-47 320	-67 370	-87 420	-107 470
FG08	746,600	1,167,639	270	-28 295	-48 320	-68 370	-88 420	-108 470
FG09	746,632	1,167,598	270	-29 295	-49 320	-69 370	-89 420	-109 470
FG10	746,641	1,167,558	270	-30 295	-50 320	-70 370	-90 420	-110 470
FG11	746,696	1,167,517	270	-31 295	-51 320	-71 370	-91 420	-111 470
FG12	746,728	1,167,477	270	-32 295	-52 320	-72 370	-92 420	-112 470
FG13	746,760	1,167,436	270	-33 295	-53 320	-73 370	-93 420	-113 470
FG14	746,792	1,167,396	270	-34 295	-54 320	-74 370	-94 420	

*This number is the sampling point number used for computer processing. The full number is N-23, N-24 etc.

Table 3.11b. Far rake sampling locations for b) west wind direction.

Sample Point	Easting (ft)	Northing (ft)	Elevation Base (ft)	Elevation Row 2 (ft)		Elevation Row 3 (ft)		Elevation Row 4 (ft)		Elevation Row 5 (ft)		Elevation Row 6 (ft)	
FG03	746,906	1,167,187	270	-23*	295	-43*	320	-63*	370	-83*	420		
FG04	746,906	1,167,137	246	-24	271	-44	296	-64	346	-84	396	-104*	446
FG05	746,906	1,167,087	268	-25	293	-45	318	-65	368	-85	418	-105	468
FG06	746,906	1,167,037	268	-26	293	-46	318	-66	368	-86	418	-106	468
FG07	746,906	1,166,987	268	-27	293	-47	318	-67	368	-87	418	-107	468
FG08	746,906	1,166,937	268	-28	293	-48	318	-68	368	-88	418	-108	468
FG09	746,906	1,166,887	268	-29	293	-49	318	-69	368	-89	418	-109	468
FG10	746,906	1,166,837	246	-30	271	-50	296	-70	346	-90	396	-110	446
FG11	746,906	1,166,787	270	-31	295	-51	320	-71	370	-91	420	-111	470
FG12	746,906	1,166,737	270	-32	295	-52	320	-72	370	-92	420	-112	470
FG13	746,906	1,166,687	270	-33	295	-53	320	-73	370	-93	420	-113	470
FG14	746,906	1,166,637	270	-34	295	-54	320	-74	370	-94	420		

*This number is the sampling point number used for computer processing. The full number is N-23, N-24, etc.

Table 3.11c. Far rake sampling locations for c) northwest wind direction.

Sample Point	Easting (ft)	Northing(ft)	Elevation Base (ft)	Elevation Row 2 (ft)	Elevation Row 3 (ft)	Elevation Row 4 (ft)	Elevation Row 5 (ft)	Elevation Row 6 (ft)
FG03	746,788	1,166,406	263	-23* 288	-43* 313	-63* 363	-83* 413	
FG04	746,750	1,166,369	263	-24 288	-44 313	-64 363	-84 413	-104* 463
FG05	746,713	1,166,332	263	-25 288	-45 313	-65 363	-85 413	-105 463
FG06	746,675	1,166,295	263	-26 288	-46 313	-66 363	-86 413	-106 463
FG07	746,638	1,166,258	263	-27 288	-47 313	-67 363	-87 413	-107 463
FG08	746,600	1,166,221	263	-28 288	-48 313	-68 363	-88 413	-108 463
FG09	746,563	1,166,185	263	-29 288	-49 313	-69 363	-89 413	-109 463
FG10	746,525	1,166,148	263	-30 288	-50 313	-70 363	-90 413	-110 463
FG11	746,488	1,166,111	261	-31 286	-51 311	-71 361	-91 411	-111 461
FG12	746,450	1,166,074	258	-32 283	-52 308	-72 358	-92 408	-112 458
FG13	746,413	1,166,037	260	-33 285	-53 310	-73 360	-93 410	-113 460
FG14	746,375	1,166,000	260	-34 285	-54 310	-74 360	-94 410	

*This number is the sampling point number used for computer processing. The full number is N-23, N-24, etc.

Table 3.11d. Far rake sampling locations for d) northeast wind direction.

Sample Point	Easting (ft)	Northing(ft)	Elevation Base (ft)	Elevation Row 2 (ft)	Elevation Row 3 (ft)	Elevation Row 4 (ft)	Elevation Row 5 (ft)	Elevation Row 6 (ft)
FG03	745,384	1,166,113	259	-23* 284	-43* 309	-63* 359	-83* 409	
FG04	745,348	1,166,147	260	-24 285	-44 310	-64 360	-84 410	-104* 460
FG05	745,313	1,166,181	261	-25 286	-45 311	-65 361	-85 411	-105 461
FG06	745,277	1,166,214	261	-26 286	-46 311	-66 361	-86 411	-106 461
FG07	745,241	1,166,248	260	-27 285	-47 310	-67 360	-87 410	-107 460
FG08	745,205	1,166,282	254	-28 279	-48 304	-68 354	-88 404	-108 454
FG09	745,170	1,166,316	248	-29 273	-49 298	-69 348	-89 398	-109 448
FG10	745,134	1,166,349	247	-30 272	-50 297	-70 347	-90 397	-110 447
FG11	745,098	1,166,383	245	-31 270	-51 295	-71 345	-91 395	-111 445
FG12	745,062	1,166,417	246	-32 271	-52 296	-72 346	-92 396	-112 446
FG13	745,027	1,166,451	248	-33 273	-53 298	-73 348	-93 398	-113 448
FG14	744,991	1,166,484	248	-34 273	-54 298	-74 348	-94 398	

*This number is the sampling point number used for computer processing. The full number is N-23, N-24, etc.

Table 3.11e. Far rake sampling locations for e) east wind direction.

Sample Point	Easting (ft)	Northing(ft)	Elevation Base (ft)	Elevation Row 2 (ft)	Elevation Row 3 (ft)	Elevation Row 4 (ft)	Elevation Row 5 (ft)	Elevation Row 6 (ft)
FG03	745,019	1,166,700	247	-23* 272	-43* 297	-63* 347	-83* 397	
FG04	745,019	1,166,751	247	-24 272	-44 297	-64 347	-84 397	-104* 447
FG05	745,019	1,166,802	274	-25 299	-45 324	-65 374	-85 424	-105 474
FG06	745,019	1,166,853	247	-26 272	-46 297	-66 347	-86 397	-106 447
FG07	745,019	1,166,905	246	-27 271	-47 296	-67 346	-87 396	-107 446
FG08	745,019	1,166,956	244	-28 269	-48 294	-68 344	-88 394	-108 444
FG09	745,019	1,167,007	243	-29 268	-49 293	-69 343	-89 393	-109 443
FG10	745,019	1,167,058	243	-30 268	-50 293	-70 343	-90 393	-110 443
FG11	745,019	1,167,109	265	-31 290	-51 315	-71 365	-91 415	-111 465
FG12	745,019	1,167,160	243	-32 268	-52 293	-72 343	-92 393	-112 443
FG13	745,019	1,167,211	243	-33 268	-53 293	-73 343	-93 393	-113 443
FG14	745,019	1,167,263	274	-34 299	-54 324	-74 374	-94 424	

*This number is the sampling point number used for computer processing. The full number is N-23, N-24, etc.

Table 3.11f. Far rake sampling locations for f) south wind direction.

Sample Point	Easting (ft)	Northing (ft)	Elevation Base (ft)	Elevation Row 2 (ft)	Elevation Row 3 (ft)	Elevation Row 4 (ft)	Elevation Row 5 (ft)	Elevation Row 6 (ft)
FG03	745,597	1,167,875	245	-23* 270	-43* 295	-63* 345	-83* 395	
FG04	745,648	1,167,875	246	-24 271	-44 296	-64 346	-84 396	-104* 446
FG05	745,699	1,167,875	248	-25 273	-45 298	-65 348	-85 398	-105 448
FG06	745,749	1,167,875	250	-26 275	-46 300	-66 350	-86 400	-106 450
FG07	745,800	1,167,875	250	-27 275	-47 300	-67 350	-87 400	-107 450
FG08	745,850	1,167,875	250	-28 275	-48 300	-68 350	-88 400	-108 450
FG09	745,901	1,167,875	250	-29 275	-49 300	-69 350	-89 400	-109 450
FG10	745,951	1,167,875	250	-30 275	-50 300	-70 350	-90 400	-110 450
FG11	746,002	1,167,875	250	-31 275	-51 300	-71 350	-91 400	-111 450
FG12	746,052	1,167,875	250	-32 275	-52 300	-72 350	-92 400	-112 450
FG13	746,103	1,167,875	250	-33 275	-53 300	-73 350	-93 400	-113 450
FG14	746,153	1,167,875	250	-34 275	-54 300	-74 350	-94 400	

*This number is the sampling point number used for computer processing. The full number is N-23, N-24, etc.

Table 3.12. Key giving the sampling point configuration corresponding to each run number.

Run #	Letter	Sampling Points*
1-8	A	NG03-NG08 B1-15 (ex 5, 6)
	B	NG09-NG14 B16-29 (ex 22, 23, 28)
	C	FG09-FG14 B5, 6, 22, 23, 28, 30-32 P1-4
	D	FG03-FG08 P5-16
9-12	A	NG03-NG08 B1-15 (ex 5, 6)
	B	NG09-NG14 B16-29 (ex 22, 23, 28)
	C	FG09-FG14 B30-32 P1-9
	D	FG03-FG08 P10-18
13-16	A	NG03-NG08 B1-15 (ex 5, 6)
	B	NG09-NG14 B16-30 (ex 22, 23, 28)
	C	FG09-FG14 B31-32 P1-9
	D	FG03-FG08 P10-18
17-20	A	NG03-NG08
	B	NG09-NG14
	C	FG09-FG14
	D	FG03-FG08 P10-18
	E	B1-32 (ex 5, 6, 13, 22, 23) P1-9

Table 3.12. Key giving the sampling point configuration corresponding to each run number.

Run #	Letter	Sampling Points*
21-24	A	NG03-NG08 B1-15 (ex 5, 6)
	B	NG09-NG14 B16-30 (ex 22, 23, 28)
	C	FG09-FG14 B31, 32 P1-9
	D	FG03-FG08 P10-18
25-28	A	NG03-NG08 B1-15 (ex 5, 6)
	B	NG09-NG14 B16-31 (ex 22, 23, 28)
	C	FG09-FG14 B32 P1-9
	D	FG03-FG08 P10-18
1-10	A	BG03-NG13
(First test series)	B	B1-33
	C	FG03-FG12
	D	P1-9

*NG03-NG08 means those ground points and all points at a greater elevation on the ladder, i.e.:

NG03	NG04
N-23	N-24
N-43	N-44
N-63	N-64
N-83	N-84
	N-104

Table 3.13. Tracer gas mixture certifications.

SCIENTIFIC GAS PRODUCTS INC.

2330 HAMILTON BLVD., SOUTH PLAINFIELD, NJ 07080 (201) 754-7700
3325 WESTSIDE DRIVE, PASADENA, TX 77502 (713) 947-2222
LAKESIDE OFFICE BLDG. NORTH AVE., WAKEFIELD, MA 01880 (617) 245-8707
115 WEST BRIDGE ST., BRIGHTON, CO 80601 (303) 659-3500
3395 DE LA CRUZ BLVD., SANTA CLARA, CA 95050 (408) 988-3600

Date 5-15-79

COLORADO STATE UNIVERSITY
FT. COLLINS, CO 80521

Cust. P.O. 34008 F

Inv. No. 401770

Q.C. No.

CERTIFICATION

CYLINDER NO.	COMPONENT	REQUESTED	ACTUAL
USN-H4531	METHANE	15%	16.1%
	CARBON DIOXIDE	16.9%	16.4%
	NITROGEN	Balance	Balance
TW-103404	SAME	SAME	SAME
1A-7524	CARBON DIOXIDE	3.7%	3.85%
	ETHANE	10%	10.2%
	NITROGEN	Balance	Balance
H-1261022	SAME	SAME	SAME
A-2863	PROPANE	10%	10.2%
	HELIUM	2.9%	2.9%
	NITROGEN	Balance	Balance
AF-159513	PROPANE	10%	10.2%
	HELIUM	2.9%	2.8%
	NITROGEN	Balance	Balance
V-11143	BUTANE	10%	9.8%
	HELIUM	8.8%	9.24%
	NITROGEN		
1C-1504	BUTANE	10%	9.8%
	HELIUM	8.8%	9.24%
	NITROGEN	Balance	Balance
1A-4001	METHANE	15%	15.2%
	CARBON DIOXIDE	16.9%	14.5%
	NITROGEN	Balance	Balance
1A-7602	METHANE	15%	15.2%
	CARBON DIOXIDE	16.9%	14.3%
	NITROGEN	Balance	Balance
A-5803	ETHANE	10%	10.2%
	CARBON DIOXIDE	3.7%	3.77%
	NITROGEN	Balance	Balance
1A-3328	ETHANE	10%	9.8%
	CARBON DIOXIDE	3.7%	3.65%
	NITROGEN	Balance	Balance
1C-1278	PROPANE	10%	10.8%
	HELIUM	2.9%	3.7%
	NITROGEN	Balance	Balance
1A-2444	PROPANE	10%	10.8%
	HELIUM	2.9%	3.7%
	NITROGEN	Balance	Balance
1C-1004	BUTANE	10%	9.2%
W-1552	HELIUM	8.8%	9.6%
	NITROGEN	Balance	Balance

All values are in Mole percent unless otherwise noted.

Accuracy tolerance on all values greater than 100 ppm within ± 2% unless otherwise stated.

Don Fred
Don Fred

ANALYST

SUPERVISOR

Table 3.14a. Test conditions for building 301.

RUN NUMBER	GAS	FLOW TYPE	RATOR SETTING	SOURCE (1) STRENGTH (%)	CALIBRATION (2) FACTOR (PPM/μVS) (X10^{-4})	BOTTLE NUMBER	BACK-GROUND (μVS)	TEMP (°C)	PRESSURE (in Hg)	VOLUME FLOW (ℓ/MIN)
1A*	ETHANE	1-A	16.55	10.2/10.2	1.0603	3	36930	23	24.63+	152.38*
B*	BUTANE			9.20/9.2	1.2214	1	78520	23	24.63	152.38*
C*	ETHANE	1-A	16.55	10.2/10.2	1.1238	3	58480	23	24.63	152.38*
D*				10.2/10.2	1.1238	3	58480	23	24.63	152.38*
2A*		1-A	16.55	10.2/10.2	1.0603	3	43190	23	24.63	152.38*
B*	BUTANE			9.2/9.2	1.2214	1	117040	23	24.63	152.38*
C*	ETHANE	1-A	16.55	10.2/10.2	1.1238	3	41660	23	24.63	152.38*
D*				10.2/10.2	1.1238	3	41600	23	24.63	152.38*
3A*		3-G	131	10.2/10.2	1.0603	3	23920	23	24.63	65.01
B*	METHANE			16.4/15.2	1.2214	2	48110	23	24.63	65.01
C*	BUTANE			9.7/10.0	1.2054	5	0	23	24.63	65.01
D*	ETHANE			10.2/10.2	1.1238	3	34930	23	24.63	65.01
4A*		3-G	102	10.2/10.2	1.1501	3	14930	23	24.63	41.43
B*				10.2/10.2	1.0979	2	27530	23	24.63	41.43
C*				10.2/10.2	1.2054	3	31260	23	24.63	41.43
D*				10.2/10.2	1.1238	3	22750	23	24.63	41.43
5A*		3-G	56.5	10.2/10.2	1.1501	3	19620	23	24.63	16.01
B*				10.2/10.2	1.1716	2	22410	23	24.63	16.01
C*				10.2/10.2	1.2054	3	15920	23	24.63	16.01
D*				10.2/10.2	1.2054	3	15920	23	24.63	16.01
6A*		1-A	16.55	10.2/10.2	1.0603	3	9510	23	24.63	152.38*
B*				10.2/10.2	1.1716	2	195250	23	24.63	152.38*
C*				10.2/10.2	1.1238	3	27880	23	24.63	152.38*
D*				10.2/10.2	1.1716	2	116730	23	24.63	152.38*
7A*		1-A	16.55	10.2/10.2	1.0603	3	39730	23	24.63	152.38*
B*				10.2/10.2	1.1716	2	185140	23	24.63	152.38*
C*				10.2/10.2	1.1238	3	41280	23	24.63	152.38*
D*				10.2/10.2	1.0726	3	336230	23	24.63	152.38*
8A*		3-G	131	10.2/10.2	1.2050	4	12490	23	24.63	65.01
B*				10.2/10.2	1.1716	2	61410	23	24.63	65.01
C*				10.2/10.2	1.2054	3	28830	23	24.63	65.01
D*				10.2/10.2	1.0726	3	92410	23	24.63	65.01

(1) The first number is the requested gas mixture and the second the certified or corrected gas mixture.
(2) For propane.
* Back pressure correction applied.

Table 3.14a. Test conditions for building 301.

RUN NUMBER	GAS	FLOW TYPE	RATOR SETTING	SOURCE(1) STRENGTH (%)	CALIBRATION(2) FACTOR (PPM/μVS) ($X10^{-4}$)	BOTTLE NUMBER	BACK-GROUND (μVS)	TEMP (°C)	PRESSURE (in Hg)	VOLUME FLOW (ℓ/MIN)
7A	ETHANE	3-G	131.0	10.2/10.2	1.2935	4	18575	24	24.63	65.23
B				9.4/10.0	1.2801	5	14410	26	24.65	65.62
C				9.4/10.0	1.2752	5	34020	19	24.52	64.42
D				9.4/10.0	1.2752	5	13750	21.1	24.50	64.94
8A		3-G	102.0	10.2/10.2	1.2935	4	29350	24	24.63	41.57
B				9.4/10.0	1.2801	5	10215	22	24.65	41.26
C				9.4/10.0	1.2752	5	5850	20	24.52	41.20
D				9.4/10.0	1.2752	5	24620	21.1	24.50	41.38
9A		1-A	16.55	9.2/10.0	0.9682	6	2690	28	24.67	154.30*
B				9.6/10.0	0.9582	7	15440	23	24.95	152.00*
C				9.6/10.0	0.9582	7	35040	23	24.88	152.25*
D				9.6/10.0	0.9532	7	47460	24	24.85	152.62*
10A		1-A	16.55	9.6/10.0	0.9682	7	18910	27.5	24.67	154.17*
B				9.6/10.0	0.9582	7	13540	23	25.00	151.82*
C				9.6/10.0	0.9582	7	10340	24	24.80	152.80*
D				9.6/10.0	0.9532	7	11400	26	24.85	151.59*
11A		3-G	131.0	9.6/10.0	0.9532	7	850	25.0	24.80	65.00
B				9.6/10.0	0.9582	7	14610	22.5	24.93	64.12
C				9.6/10.0	0.9582	7	15030	23	24.95	64.18
D				9.6/10.0	0.9532	7	14490	22	24.90	64.09
12A		3-G	102.0	9.6/10.0	0.9532	7	5510	28	24.80	41.84
B				9.6/10.0	0.9739	7	23920	23	24.89	41.00
C				9.6/10.0	0.9532	7	13380	21	24.90	40.71
D				9.6/10.0	0.9532	7	10880	20	24.90	40.57
13A		1-A	16.55	10.2/10.0	0.9141	8	36250	29	24.80	153.35*
B				10.2/10.0	0.8977	8	30100	26	24.94	152.08*
C				10.4/10.0	0.9057	9	42320	23	24.94	151.32*
D				10.4/10.0	0.9057	9	2890	27	24.90	152.48*
14A		1-A	16.55	10.2/10.0	0.9141	8	15140	27	24.80	152.84*
B				10.2/10.0	0.8977	8	24470	27.5	28.5	141.09*
C				10.4/10.0	0.9057	9	30020	25	24.94	151.83*
D				10.4/10.0	0.9057	9	21980	26	24.90	152.23*

(1) The first number is the requested gas mixture and the second the certified or corrected gas mixture.
(2) For propane.

Table 3.14a. Test conditions for building 301.

RUN NUMBER	GAS	FLOW TYPE	RATOR SETTING	SOURCE (1) STRENGTH (%)	CALIBRATION (2) FACTOR (PPM/μVS) ($\times 10^{-4}$)	BOTTLE NUMBER	BACK-GROUND (μVS)	TEMP (°C)	PRESSURE (in Hg)	VOLUME FLOW (ℓ/MIN)
9A*	ETHANE	3-G	102	10.2/10.2	1.1501	4	19750	23	24.63	41.43
B*				10.2/10.2	1.1716	2	32520	23	24.63	41.43
C*				10.2/10.2	1.1553	3	17850	23	24.63	41.43
D*				10.2/10.2	1.0726	3	104470	23	24.63	41.43
10A*		3-G	56.5	10.2/10.2	1.1501	4	18850	23	24.63	16.01
B*				10.2/10.2	1.1716	2	22130	23	24.63	16.01
C*				10.2/10.2	1.1553	3	187800	23	24.63	16.01
D*				10.2/10.2	1.0726	3	162590	23	24.63	16.01
1A		1-A	16.55	10.2/10.2	1.3020	4	60360	23	24.70	152.54*
B				9.4/10.0	1.2865	5	45670	22	24.60	152.65*
C				9.4/10.0	1.2865	5	9460	22	24.55	152.83*
D				9.2/10.0	0.9574	6	114790	24	24.59	153.20*
2A		1-A	16.55	10.2/10.2	1.3020	4	10125	28	24.70	153.82*
B				9.4/10.0	1.2865	5	35020	21.2	24.60	152.44*
C				9.4/10.0	1.2865	5	32910	21	24.60	152.39*
D				9.2/10.0	0.9565	6	16155	23	24.73	152.43*
3A		3-G	131.0	10.2/10.2	1.2935	4	8140	25	24.63	65.45*
B				9.4/10.0	1.2801	5	28780	24	24.65	65.18
C				9.2/10.0	0.9407	6	18720	21.9	24.84	64.22
D				9.2/10.2	0.9574	6	10120	19	24.73	63.87
4A		3-G	102.0	10.2/10.2	1.2935	4	10650	25.5	24.60	41.83
B				9.4/10.0	1.2935	5	6110	24.5	24.60	41.69
C				9.2/10.0	0.9407	6	11625	23	24.84	41.08
D				9.4/10.0	1.2752	5	11740	21.2	24.50	41.40
5A		1-A	16.55	10.2/10.2	1.3020	4	5045	29	24.70	154.08*
B				9.4/10.0	1.2801	5	15500	23.5	24.65	152.85*
C				9.4/10.0	1.2865	5	10025	22.5	24.55	152.96*
D				9.2/10.0	0.9574	6	66330	25.6	24.63	153.47*
6A		1-A	16.55	10.2/10.2	1.2935	4	81615	25	24.63	153.31*
B				9.4/10.0	1.2801	5	3445	23.5	24.65	152.85*
C				9.4/10.0	1.2865	5	15330	23	24.55	153.09*
D				9.2/10.0	0.9574	6	30690	23.5	24.82	152.24*

(1) The first number is the requested gas mixture and the second the certified or corrected gas mixture.
(2) For propane.
* Back pressure correction applied.

Table 3.14a. Test conditions for building 301.

RUN NUMBER	GAS	FLOW TYPE	RATOR SETTING	SOURCE (1) STRENGTH (%)	CALIBRATION (2) FACTOR (PPM/μVS) ($X10^{-4}$)	BOTTLE NUMBER	BACK-GROUND (μVS)	TEMP (°C)	PRESSURE (in Hg)	VOLUME FLOW (ℓ/MIN)
15A	ETHANE	3-G	131.0	10.2/10.0	0.8977	8	13230	24.5	24.94	64.53
B				10.2/10.0	0.8977	8	14790	26	24.90	64.96
C				10.2/10.0	0.8977	8	5520	25	24.93	64.66
D				10.4/10.0	0.9057	9	8220	27	24.75	65.57
16A		3-G	102.0	10.2/10.0	0.8977	8	10330	24.5	24.95	41.11
B				10.2/10.0	0.8977	8	8620	27	24.82	41.67
C				10.2/10.0	0.9057	8	8070	23	24.91	40.97
D				10.4/10.0	0.9057	9	8240	27	24.90	41.54
17A		1-A	16.55	10.4/10.0	0.9301	9	52560	27	24.20	155.43*
B				10.4/10.0	0.9301	9	30380	26	24.65	153.50*
C				11.0/10.0	0.9184	10	6810	28	24.58	154.27*
D				11.0/10.0	1.2116	10	4780	27	24.64	153.79*
E				11.0/10.0	1.2116	10	11870	27	24.77	153.31*
18A		1-A	16.55	10.4/10.0	0.9301	9	40590	27	24.75	153.39*
B				10.4/10.0	0.9301	9	81720	27	24.65	153.75*
C				11.0/10.0	0.9184	10	7320	27.5	24.60	154.06*
D				11.0/10.0	0.9119	10	1250	27.5	24.65	153.88*
E				11.0/10.0	1.2116	10	52480	27.5	24.77	153.44*
19A		3-G	131.0	10.4/10.0	0.9301	9	15000	24.5	24.73	65.08
B				10.4/10.0	0.9184	9	27340	24	24.64	65.21
C				10.4/10.0	0.9184	9	3000	25.5	24.66	65.48
D				11.0/10.0	0.9119	10	23540	24.5	24.67	65.23
E				11.0/10.0	0.9119	10	5980	26	24.77	65.30
20A		3-G	102.0	10.4/10.0	0.9301	9	8790	26	24.74	41.67
B				10.4/10.0	0.9184	9	10470	24	24.65	41.54
C				10.4/10.0	0.9184	9	4820	25	24.65	41.68
D				11.0/10.0	0.9119	10	59800	26.5	24.70	41.80
E				11.0/10.0	1.1935	10	12210	24.5	24.75	41.44
21A		1-A	16.55	11.0/10.0	1.2186	10	18150	27	24.81	146.28*
B				10.7/10.0	1.2182	11	12080	26.5	24.90	145.87*
C				10.7/10.0	1.2182	11	41660	26	24.92	145.68*
D				10.7/10.0	1.2186	11	12150	26	24.84	145.94*

(1) The first number is the requested gas mixture and the second the certified or corrected gas mixture.
(2) For propane.
* Back pressure correction applied.

Table 3.14a. Test conditions for building 301.

RUN NUMBER	GAS	FLOW TYPE	RATOR SETTING	SOURCE (1) STRENGTH (%)	CALIBRATION (2) FACTOR (PPM/μVS) (X10-4)	BOTTLE NUMBER	BACK-GROUND (μVS)	TEMP (°C)	PRESSURE (in Hg)	VOLUME FLOW (ℓ/MIN)
22A	ETHANE	1-A	16.55	10.7/10.0	1.2186	11	28300	26	24.90	145.75*
B				10.7/10.0	1.2182	11	3640	27	24.90	145.99*
C				10.7/10.0	1.2182	11	490	27	24.8	146.31*
D				10.7/10.0	1.2064	11	2840	29	24.80	146.80*
23A		3-G	131.10	10.7/10.0	1.2186	11	16920	25	24.91	64.72
B				10.7/10.0	1.2182	11	11520	25	24.90	64.74
C				10.7/10.0	1.2064	11	3120	24	24.82	64.73
D				10.7/10.0	1.2064	11	8610	27	24.82	65.39
24A		3-G	102.0	10.7/10.0	1.2182	11	10860	25	24.90	41.26
B				10.7/10.0	1.2182	11	5980	24	24.91	41.10
C				10.7/10.0	1.2064	11	21360	23	24.82	41.11
D				10.7/10.0	1.2064	11	2420	27.5	24.80	41.77
25A		1-A	16.55	10.7/10.0	1.1992	11	2830	29	24.80	146.53*
B				10.7/10.0	1.2908	11	25080	25	24.87	145.33*
C				10.8/10.0	1.2908	12	10020	30	24.89	146.48*
D				10.8/10.0	1.2035	12	48990	29	24.77	146.62*
26A		1-A	16.55	10.7/10.0	1.1992	11	1710	30	24.80	146.77*
B				10.7/10.0	1.2908	11	19680	28	24.88	146.03*
C				10.8/10.0	1.2908	12	5070	30	24.76	146.90*
D				10.8/10.0	1.2035	12	22360	28	24.77	146.38*
27A		3-G	131.0	10.7/10.0	1.1992	11	3140	29	24.75	66.01
B				10.7/10.0	1.2908	11	8410	26	24.83	65.14
C				10.8/10.0	1.2908	12	2230	29	24.80	65.87
D				10.8/10.0	1.2035	12	4780	27	24.80	65.44
28A		3-G	102.0	10.7/10.0	1.1992	11	8080	25.6	24.77	41.56
B				10.7/10.0	1.1992	11	1140	27	24.80	41.70
C				10.8/10.0	1.2908	12	4590	30	24.81	42.10
D				10.8/10.0	1.2035	12	4390	27	24.77	41.75

(1) The first number is requested gas mixture and the second the certified or corrected gas mixture.
(2) For propane.
* Back pressure correction applied.

Table 3.14b. Test conditions for building 302.

RUN NUMBER	GAS	FLOW TYPE	RATOR SETTING	SOURCE(1) STRENGTH (%)	CALIBRATION(2) FACTOR (PPM/μVS) ($X10^{-4}$)	BOTTLE NUMBER	BACK-GROUND (μVS)	TEMP (°C)	PRESSURE (in Hg)	VOLUME FLOW (ℓ/MIN)
1A*	PROPANE	1-B	14.55	10.11/10.0	1.0603	5	10220	23	24.63	131.25
B*				10.8/10.8	1.2214	1	84650	23	24.63	131.25
C*				10.2/10.2	1.1238	4	105250	23	24.63	131.25
D*				10.2/10.2	1.1238	4	105250	23	24.63	131.25
2A*		1-B	14.55	10.1/10.0	1.0603	5	41540	23	24.63	131.25
B*				10.8/10.8	1.2214	1	124700	23	24.63	131.25
C*				10.2/10.2	1.1238	4	46260	23	24.63	131.25
D*				10.2/10.2	1.1238	4	46260	23	24.63	131.25
3A*		3-H	116	10.1/10.0	1.0603	5	30990	23	24.63	41.15
B*				10.8/10.8	1.2214	1	20040	23	24.63	41.15
C*				10.2/10.2	1.2054	4	20450	23	24.63	41.15
D*				10.2/10.2	1.1238	4	46290	23	24.63	41.15
4A*		3-H	90	10.1/10.0	1.1501	5	101950	23	24.63	29.80
B*				10.8/10.8	1.0979	1	39010	23	24.63	29.80
C*				10.2/10.2	1.2054	4	42450	23	24.63	29.80
D*				10.2/10.2	1.1238	4	34600	23	24.63	29.80
5A*		3-H	49.5	10.1/10.0	1.1501	5	76980	23	24.63	13.67
B*				10.8/10.8	1.1716	2	25860	23	24.63	13.67
C*				10.2/10.2	1.2054	4	16400	23	24.63	13.67
D*				10.2/10.2	1.2054	4	16400	23	24.63	13.67
6A*		1-B	14.55	10.1/10.0	1.0603	5	38850	23	24.63	131.25
B*				10.8/10.8	1.1716	2	1062170	23	24.63	131.25
C*				10.1/10.0	1.1238	5	41820	23	24.63	131.25
D*				10.8/10.8	1.1716	2	149220	23	24.63	131.25
7A*		1-B	14.55	10.1/10.0	1.0603	5	32190	23	24.63	131.25
B*				10.8/10.8	1.1716	2	544310	23	24.63	131.25
C*				10.2/10.2	1.1238	4	50290	23	24.63	131.25
D*				10.8/10.8	1.0726	2	345980	23	24.63	131.25
8A*		3-H	116	10.1/10.0	1.2050	5	40730	23	24.63	41.15
B*				10.8/10.8	1.1716	2	97900	23	24.63	41.15
C*				10.2/10.2	1.2054	4	41320	23	24.63	41.15
D*				10.2/10.2	1.0726	4	99250	23	24.63	41.15

(1) The first number is the requested gas mixture and the second the certified or corrected gas mixture.
(2) For propane.

Table 3.14b. Test conditions for building 302.

RUN NUMBER	GAS	FLOW TYPE	RATOR SETTING	SOURCE (1) STRENGTH (%)	CALIBRATION (2) FACTOR (PPM/μVS) ($X10^{-4}$)	BOTTLE NUMBER	BACK-GROUND (μVS)	TEMP (°C)	PRESSURE (in Hg)	VOLUME FLOW (ℓ/MIN)
7A	PROPANE	3-H	116.0	10.4/10.0	1.2935	7	37660	24	24.63	41.29
B				10.4/10.0	1.2801	7	26390	26	24.65	41.53
C				10.4/10.0	1.2752	8	23275	19	24.52	40.77
D				5.95/10.0	1.2752	D.N.	15900	21.1	24.50	41.10
8A		3-H	90.0	10.4/10.0	1.2935	7	42870	24	24.63	29.90
B				10.4/10.0	1.2801	7	27715	22	24.65	29.67
C				5.95/10.0	1.2752	D.N.	12745	20	24.52	29.63
D				5.95/10.0	1.2752	D.N.	28660	21.1	24.50	29.76
9A		1-B	14.55	9.80/10.0	0.9682	10	22100	28	24.67	133.25
B				9.80/10.0	0.9582	10	15070	23	24.95	129.57
C				9.75/10.0	0.9582	12	57620	23	24.88	129.94
D				9.75/10.0	0.9532	12	47660	24	24.85	130.53
10A		1-B	14.55	9.80/10.0	0.9682	10	27580	27.5	24.67	133.03
B				9.80/10.0	0.9582	10	14120	23	25.00	129.31
C				9.80/10.0	0.9582	10	13790	24	24.80	130.79
D				9.75/10.0	0.9532	12	15980	26	24.85	131.41
11A		3-H	116.0	9.75/10.0	0.9532	12	5350	25.0	24.80	41.14
B				9.80/10.0	0.9582	10	9930	22.5	24.93	40.58
C				9.75/10.0	0.9582	12	28300	23	24.95	40.62
D				9.75/10.0	0.9532	12	14560	22	24.90	40.56
12A		3-H	90.0	9.75/10.0	0.9532	12	7470	28	24.80	30.09
B				9.80/10.0	0.9739	10	20140	23	24.89	29.49
C				9.75/10.0	0.9532	12	13100	21	24.90	29.28
D				9.76/10.0	0.9532	12	10280	20	24.90	29.18
13A		1-B	14.55	9.75/10.0	0.9141	12	37630	29	24.80	132.56
B				9.54/10.0	0.8977	13	31330	26	24.94	130.94
C				9.54/10.0	0.9057	13	51630	23	24.94	129.62
D				10.60/10.0	0.9057	14	5620	27	24.90	131.58
14A		1-B	14.55	9.54/10.0	0.9141	13	17260	27	24.80	132.12
B				9.54/10.0	0.8977	13	27510	27.5	24.50	133.96
C				9.54/10.0	0.9057	13	16730	25	24.94	130.50
D				10.6 /10.0	0.9057	14	19250	26	24.90	131.15

(1) The first number is requested gas mixture and the second the certified or corrected gas mixture.
(2) For propane.

Table 3.14b. Test conditions for building 302.

RUN NUMBER	GAS	FLOW TYPE	RATOR SETTING	SOURCE (1) STRENGTH (%)	CALIBRATION (2) FACTOR (PPM/μVS) ($X10^{-4}$)	BOTTLE NUMBER	BACK-GROUND (μVS)	TEMP (°C)	PRESSURE (in Hg)	VOLUME FLOW (ℓ/MIN)
9A*	PROPANE	3-H	90	10.1/10.0	1.1501	5	53640	23	24.63	29.80
B*				10.8/10.8	1.1716	2	42180	23	24.63	29.80
C*				10.2/10.2	1.1553	4	42940	23	24.63	29.80
D*				10.2/10.2	1.0726	3	112810	23	24.63	29.80
10A*		3-H	49.5	10.1/10.0	1.1501	5	12200	23	24.63	13.67
B*				10.8/10.8	1.1716	2	29120	23	24.63	13.67
C*				10.2/10.2	1.1553	4	142020	23	24.63	13.67
D*				10.2/10.2	1.0726	3	163540	23	24.63	13.67
1A		1-B	14.55	10.4/10.0	1.3020	6	200770	22	24.70	130.44
B				10.4/10.0	1.2865	8	47270	22	24.60	130.97
C				10.4/10.0	1.2865	8	18820	22	24.55	131.24
D				10.4/10.0	0.9574	9	142810	24	24.59	131.91
2A		1-B	14.55	10.4/10.0	1.3020	6	130405	28	24.70	133.09
B				10.4/10.0	1.2865	8	39205	21.2	24.60	130.62
C				10.4/10.0	1.2865	8	47300	21	24.60	130.53
D				10.4/10.0	0.9565	9	14295	23	24.73	130.72
3A		3-H	116.0	10.4/10.0	1.2935	7	33830	25	24.63	41.43
B				10.4/10.0	1.2801	7	36285	24	24.65	41.25
C				9.8/10.0	0.9407	10	18285	21.9	24.84	40.65
D				5.95/5.95	0.9574	D.N.	12700	19	24.73	40.43
4A		3-H	90.0	10.4/10.0	1.2935	7	36825	25.5	24.60	30.09
B				10.4/10.0	1.2935	7	31410	24.5	24.60	30.00
C				9.8/10.0	0.9407	10	15045	23	24.84	29.55
D				5.95/5.95	1.2752	D.N.	17690	21.1	24.50	29.76
5A		1-B	14.55	10.4/10.0	1.3020	6	103690	29	24.70	133.53
B				10.4/10.0	1.2801	7	32590	23.5	24.65	131.37
C				10.4/10.0	1.2865	8	25915	22.5	24.55	131.46
D				10.4/10.0	0.9574	9	41420	25.6	24.63	132.41
6A		1-B	14.55	10.4/10.0	1.2935	7	133445	25	24.63	132.14
B				10.4/10.0	1.2801	7	15420	23.5	24.65	131.37
C				10.4/10.0	1.2865	8	31380	23	24.55	131.68
D				10.4/10.0	0.9574	9	37035	23.5	24.82	130.47

(1) The first number is the requested gas mixture and the second the certified or corrected gas mixture.
(2) For propane.

Table 3.14b. Test conditions for building 302.

RUN NUMBER	GAS	FLOW TYPE	RATOR SETTING	SOURCE (1) STRENGTH (%)	CALIBRATION (2) FACTOR (PPM/μVS) ($X10^{-4}$)	BOTTLE NUMBER	BACK-GROUND (μVS)	TEMP (°C)	PRESSURE (in Hg)	VOLUME FLOW (ℓ/MIN)
15A	PROPANE	3-H	116.0	9.54/10.0	0.8977	13	10690	24.5	24.94	40.84
B				9.54/10.0	0.8977	13	15260	26	24.90	41.11
C				9.54/10.0	0.8977	13	6130	25	24.93	40.93
D				10.60/10.0	0.9057	14	11800	27	24.75	41.50
16A		3-H	90.0	9.54/10.0	0.8977	13	10520	24.5	24.95	29.57
B				9.54/10.0	0.8977	13	13900	27	24.82	29.97
C				9.54/10.0	0.9057	13	6670	23	24.91	29.46
D				10.60/10.0	0.9057	14	8230	27	24.90	29.87
17A		1-B	14.55	10.60/10.0	0.9301	14	98320	27	24.20	135.39
B				10.60/10.0	0.9301	14	54490	26	24.65	132.48
C				10.55/10.0	0.9184	11	4200	28	24.58	133.74
D				10.55/10.0	1.2116	11	18900	27	24.64	132.97
E				10.41/10.0	1.2116	15	26680	27	24.77	132.28
18A		1-B	14.55	10.60/10.0	0.9301	14	65790	27	24.75	132.38
B				10.60/10.0	0.9301	14	110050	27	24.65	132.92
C				10.55/10.0	0.9184	11	18680	27.5	24.60	133.41
D				10.41/10.0	0.9119	15	2050	27.5	24.65	133.14
E				10.41/10.0	1.2116	15	92290	27.5	24.77	132.50
19A		3-H	116.0	10.60/10.0	0.9301	14	233840	24.5	24.73	41.19
B				10.60/10.0	0.9184	14	24160	24	24.64	41.27
C				10.60/10.0	0.9184	14	8379	25.5	24.66	41.45
D				10.55/10.0	0.9119	11	30730	24.5	24.67	41.29
E				10.41/10.0	0.9119	15	10750	26	24.77	41.38
20A		3-H	90.0	10.60/10.0	0.9301	14	125730	26	24.74	29.93
B				10.60/10.0	0.9184	14	15880	24	24.65	29.88
C				10.60/10.0	0.9184	14	10660	25	24.65	29.98
D				10.55/10.0	0.9119	11	68690	26.5	24.70	30.07
E				10.41/10.0	1.1935	15	19470	24.5	24.75	29.80
21A		1-B	14.55	10.55/10.0	1.2186	11	73200	27	24.81	132.06
B				10.41/10.0	1.2182	15	7110	26.5	24.90	131.37
C				10.64/10.0	1.2182	16	49920	26	24.92	131.04
D				10.64/10.0	1.2186	16	15210	26	24.84	131.46

(1) The first number is requested gas mixture and the second the certified or corrected gas mixture.
(2) For propane.

Table 3.14b. Test conditions for building 302.

RUN NUMBER	GAS	FLOW TYPE	RATOR SETTING	SOURCE (1) STRENGTH (%)	CALIBRATION (2) FACTOR (PPM/μVS) ($X10^{-4}$)	BOTTLE NUMBER	BACK-GROUND (μVS)	TEMP (°C)	PRESSURE (in Hg)	VOLUME FLOW (ℓ/MIN)
22A	PROPANE	1-B	14.55	10.41/10.0	1.2186	15	46890	26	24.90	131.15
B				10.41/10.0	1.2182	15	5410	27	24.90	131.58
C				10.41/10.0	1.2182	15	4510	27	24.8	132.12
D				10.64/10.0	1.2064	16	7370	29	24.80	133.00
23A		3-H	116.0	10.41/10.0	1.2186	15	24370	25	24.91	40.96
B				10.41/10.0	1.2182	15	9510	25	24.90	40.98
C				10.64/10.0	1.2064	16	34890	24	24.82	40.97
D				10.64/10.0	1.2064	16	6310	27	24.82	41.38
24A		3-H	90.0	10.41/10.0	1.2182	15	16540	25	24.90	29.67
B				10.41/10.0	1.2182	15	11540	24	24.91	29.56
C				10.64/10.0	1.2064	16	21460	23	24.82	29.57
D				10.64/10.0	1.2064	16	4170	27.5	24.80	30.04
25A		1-B	14.55	10.64/10.0	1.1992	16	7840	29	24.80	133.00
B				10.64/10.0	1.2908	16	33230	25	24.87	130.87
C				11.07/10.0	1.2908	17	12750	30	24.89	132.95
D				11.02/10.0	1.2035	18	69460	29	24.77	133.16
26A		1-B	14.55	10.64/10.0	1.1992	16	5130	30	24.80	133.44
B				10.64/10.0	1.2908	16	24750	28	24.88	132.13
C				11.07/10.0	1.2908	17	14470	30	24.76	133.65
D				11.07/10.0	1.2035	17	32660	28	24.77	132.72
27A		3-H	116.0	10.64/10.0	1.1992	16	5070	29	24.75	41.76
B				10.64/10.0	1.2908	16	6980	26	24.83	41.23
C				11.07/10.0	1.2908	17	4140	29	24.80	41.69
D				11.07/10.0	1.2035	17	4370	27	24.80	41.42
28A		3-H	90.0	10.64/10.0	1.1992	16	8230	25.6	24.77	29.89
B				10.64/10.0	1.1992	16	2000	27	24.80	29.99
C				11.07/10.0	1.2908	17	5830	30	24.81	30.28
D				11.07/10.0	1.2035	17	5640	27	24.77	30.03

(1) The first number is requested gas mixture and the second the certified or corrected gas mixture.
(2) For propane.

Table 3.14c. Test conditions for building 303.

RUN NUMBER	GAS	FLOW TYPE	RATOR SETTING	SOURCE(1) STRENGTH (%)	CALIBRATION(2) FACTOR (PPM/μVS) ($X10^{-4}$)	BOTTLE NUMBER	BACK-GROUND (μVS)	TEMP (°C)	PRESSURE (in Hg)	VOLUME FLOW (ℓ/MIN)
1A*	METHANE	1-C	15.75	17.4/16.1	1.0603	4	33030	23	24.63	149.28*
B*				16.4/15.2	1.2214	2	129150	23	24.63	149.28*
C*				17.4/16.1	1.1238	4	28680	23	24.63	149.28*
D*				17.4/16.1	1.1238	4	28680	23	24.63	149.28*
2A*		1-C	15.75	17.4/16.1	1.0603	4	36370	23	24.63	149.28*
B*				16.4/15.2	1.2214	2	142410	23	24.63	149.28*
C*				17.4/16.1	1.1238	4	28750	23	24.63	149.28*
D*				17.4/16.1	1.1238	4	28750	23	24.63	149.28*
3A*		3-I	124.5	17.4/16.1	1.0603	4	21240	23	24.63	46.83
B*				16.4/15.2	1.2214	2	34070	23	24.63	46.83
C*				17.4/161	1.2054	4	18580	23	24.63	46.83
D*				17.4/16.1	1.1238	4	31950	23	24.63	46.83
4A*		3-I	97	17.4/16.1	1.1501	4	17780	23	24.63	31.93
B*				16.4/15.2	1.0979	2	45150	23	24.63	31.93
C*				17.4/16.1	1.2054	4	33290	23	24.63	31.93
D*				17.4/16.1	1.238	4	23180	23	24.63	31.93
5A*		3-I	53.5	17.4/16.1	1.1501	4	23880	23	24.63	14.69
B*				16.4/15.2	1.1716	2	24910	23	24.63	14.69
C*				17.4/16.1	1.2054	4	16530	23	24.63	14.69
D*				17.4/16.1	1.2054	4	16530	23	24.63	14.69
6A*		1-C	15.75	17.4/16.1	1.0603	4	8900	23	24.63	149.28*
B*				17.4/16.1	1.1716	3	364520	23	24.63	149.28*
C*				17.4/16.1	1.1238	4	21720	23	24.63	149.28*
D*				17.4/16.1	1.1716	3	96440	23	24.63	149.28*
7A*		1-C	15.75	17.4/16.1	1.0603	4	29270	23	24.63	149.28*
B*				16.4/15.2	1.1716	2	276120	23	24.63	149.28*
C*				17.4/16.1	1.1238	4	28820	23	24.63	149.28*
D*				17.5/16.1	1.0726	4	358600	23	24.63	149.28*
8A*		3-I	124.5	16.7/15.0	1.2050	5	12830	23	24.63	46.83
B*				16.4/15.2	1.1716	2	123900	23	24.63	46.83
C*				17.4/16.1	1.2054	4	33640	23	24.63	46.83
D*				17.4/16.1	1.0726	4	91310	23	24.63	46.83

(1) The first number is requested gas mixture and the second the certified or corrected gas mixture.
(2) For propane
* Back pressure correction applied.

Table 3.14c. Test conditions for building 303.

RUN NUMBER	GAS	FLOW TYPE	RATOR SETTING	SOURCE(1) STRENGTH (%)	CALIBRATION(2) FACTOR (PPM/μVS) ($X10^{-4}$)	BOTTLE NUMBER	BACK-GROUND (μVS)	TEMP (°C)	PRESSURE (in Hg)	VOLUME FLOW (ℓ/MIN)
7A	METHANE	3-I	124.5	16.7/15.0	1.2935	5	16075	24	24.63	46.99
B				16.7/15.0	1.2801	5	12725	26	24.60	47.36
C				16.7/15.0	1.2752	6	21840	19	24.52	46.40
D				16.7/15.0	1.2752	6	12680	21.1	24.50	43.50
8A		3-I	97.0	16.7/15.0	1.2935	5	14370	24	24.63	32.04
B				16.7/15.0	1.2801	5	10315	22	24.65	31.80
C				16.7/15.0	1.2752	6	11665	20	24.52	31.75
D				16.7/15.0	1.2752	6	21630	21.1	24.50	31.89
9A		1-C	15.75	16.7/15.0	0.9682	6	24010	28	24.67	150.18*
B				16.7/15.0	0.9582	6	23100	23	24.95	147.99*
C				16.7/15.0	0.9582	6	31910	23	24.88	148.22*
D				16.7/15.0	0.9532	7	48140	24	24.85	148.57*
10A		1-C	15.75	16.7/15.0	0.9682	6	29690	27.5	24.67	150.05*
B				16.7/15.0	0.9582	6	17070	23	25.00	147.82*
C				16.7/15.0	0.9582	6	15710	24	24.80	148.74*
D				16.7/15.0	0.9532	7	15540	26	24.85	149.07*
11A		3-I	124.5	16.7/15.0	0.9532	7	6440	25	24.80	46.82
B				16.7/15.0	0.9582	6	16820	22.5	24.93	46.19
C				16.7/15.0	0.9582	6	20460	23	24.95	46.23
D				16.7/15.0	0.9532	6	16790	22	24.90	46.16
12A		3-I	97.0	16.7/15.0	0.9532	7	10040	28	24.80	32.25
B				16.7/15.0	0.9739	6	24050	23	24.89	31.60
C				16.7/15.0	0.9532	6	15960	21	24.90	31.37
D				16.7/15.0	0.9532	6	14490	20	24.90	31.26
13A		1-C	15.75	16.7/15.0	0.9141	7	35560	29	24.80	158.62*
B				16.7/15.0	0.8977	7	38620	26	24.94	157.30*
C				16.7/15.0	0.9057	8	54870	23	24.94	156.51*
D				16.7/15.0	0.9057	8	8590	27	24.90	157.71*
14A		1-C	15.75	16.7/15.0	0.9141	7	17720	27	24.80	158.10*
B				16.7/15.0	0.8977	7	30050	27.5	28.5	145.54*
C				16.7/15.0	0.9057	8	33840	25	24.94	157.03*
D				16.7/15.0	0.9057	8	28630	26	24.90	157.45*

(1) The first number is requested gas mixture and the second the certified or corrected gas mixture.
(2) For propane.

Table 3.14c. Test conditions for building 303.

RUN NUMBER	GAS	FLOW TYPE	RATOR SETTING	SOURCE(1) STRENGTH (%)	CALIBRATION(2) FACTOR (PPM/μVS) ($\times 10^{-4}$)	BOTTLE NUMBER	BACK-GROUND (μVS)	TEMP (°C)	PRESSURE (in Hg)	VOLUME FLOW (ℓ/MIN)
9A*	METHANE	3-I	97	16.7/15.0	1.1501	5	18380	23	24.63	31.93
B*				16.4/15.2	1.1716	2	34860	23	24.63	31.93
C*				17.4/16.1	1.1553	4	23120	23	24.63	31.93
D*				17.4/16.1	1.0726	4	105270	23	24.63	31.93
10A*		3-I	5.34	17.4/16.1	1.1501	4	24080	23	24.63	14.69
B*				16.4/15.2	1.1716	2	23960	23	24.63	14.69
C*				17.4/16.1	1.1553	4	92240	23	24.63	14.69
D*				17.4/16.1	1.0726	4	183050	23	24.63	14.69
1A		1-C	15.75	16.7/15.0	1.3020	5	47960	22	24.70	149.11*
B				16.7/15.0	1.2865	6	49330	22	24.60	149.45*
C				16.7/15.0	1.2865	6	10360	22	24.55	149.63*
D				16.7/15.0	0.9574	7	107410	24	24.59	149.99*
2A		1-C	15.75	16.7/15.0	1.3020	5	13080	28	24.70	150.62*
B				16.7/15.0	1.2865	6	31400	21.2	24.60	149.25*
C				16.7/15.0	1.2865	6	35280	21	24.60	149.20*
D				16.7/15.0	0.9565	6	30070	23	24.73	149.26*
3A		3-I	124.5	16.7/15.0	1.2935	5	9905	25	24.63	47.14
B				16.7/15.0	1.2801	5	22790	24	24.65	46.95
C				16.7/15.0	0.9407	6	19100	21.9	24.84	46.26
D				16.7/15.0	0.9574	6	10565	19	24.73	46.01
4A		3-I	97.0	16.7/15.0	1.2935	5	12125	25.5	24.60	32.24
B				16.7/15.0	1.2935	5	8680	24.5	24.60	32.13
C				16.7/15.0	0.9407	6	15310	23	24.84	31.66
D				16.7/15.0	1.2752	6	11945	21.1	24.50	31.89
5A		1-C	15.75	16.7/15.0	1.3020	5	7965	29	24.70	150.87
B				16.7/15.0	1.2801	5	14075	23.5	24.65	149.66
C				16.7/15.0	1.2865	6	9190	22.5	24.55	149.75
D				16.7/15.0	0.9574	6	29585	25.6	24.63	150.26
6A		1-C	15.75	16.7/15.0	1.2935	5	70530	25	24.63	150.11
B				16.7/15.0	1.2901	5	6455	23.5	24.65	149.66
C				16.7/15.0	1.2865	6	17210	23	24.55	149.88
D				16.7/15.0	0.9574	6	36575	23.5	24.82	149.08

(1) The first number is requested gas mixture and the second the certified or corrected gas mixture.
(2) For propane.
* Back pressure correction applied.

Table 3.14c. Test conditions for building 303.

RUN NUMBER	GAS	FLOW TYPE	RATOR SETTING	SOURCE(1) STRENGTH (%)	CALIBRATION(2) FACTOR (PPM/μVS) ($X10^{-4}$)	BOTTLE NUMBER	BACK-GROUND (μVS)	TEMP (°C)	PRESSURE (in Hg)	VOLUME FLOW (ℓ/MIN)
15A	METHANE	3-I	124.5	16.7/15.0	0.8977	7	12050	24.5	24.94	46.48
B				16.7/15.0	0.8977	7	18140	26	24.90	46.79
C				16.7/15.0	0.8977	7	9690	25	24.93	46.58
D				16.7/15.0	0.9057	8	11730	27	24.75	47.23
16A		3-I	97.0	16.7/15.0	0.8977	7	15400	24.5	24.95	31.68
B				16.7/15.0	0.8977	7	14500	27	24.82	32.11
C				16.7/15.0	0.9057	7	14810	23	24.91	31.57
D				16.7/15.0	0.9057	8	12220	27	24.90	32.01
17A		1-C	15.75	16.7/15.0	0.9301	8	27150	27	24.20	155.04*
B				16.7/15.0	0.9301	8	32580	26	24.65	153.14*
C				16.7/15.0	0.9184	8	12520	28	24.58	153.90*
D				16.6/15.0	1.2116	9	8190	27	24.64	153.43*
E				16.6/15.0	1.2116	9	12860	27	24.77	152.96*
18A		1-C	15.75	16.7/15.0	0.9301	8	32760	27	24.75	153.03*
B				16.7/15.0	0.9301	8	78680	27	24.60	153.57*
C				16.7/15.0	0.9184	8	8640	27.5	24.60	153.77*
D				16.6/15.0	0.9119	9	7500	27.5	24.65	153.52*
E				16.6/15.0	1.2116	9	45060	27.5	24.77	153.09*
19A		3-I	124.5	16.7/15.0	0.9301	8	17500	24.5	24.73	46.87
B				16.7/15.0	0.9184	8	16570	24	24.64	46.97
C				16.7/15.0	0.9184	8	10800	25.5	24.66	47.17
D				16.6/15.0	0.9119	9	21970	24.5	24.67	46.99
E				16.6/15.0	0.9119	9	8950	26	24.77	47.03
20A		3-I	97.0	16.7/15.0	0.9301	8	12390	26	24.74	32.11
B				16.7/15.0	0.9184	8	16140	24	24.65	32.01
C				16.7/15.0	0.9184	8	13210	25	24.65	32.12
D				16.6/15.0	0.9119	9	45760	26.5	24.70	32.21
E				16.6/15.0	1.1935	9	11530	24.5	24.75	31.93
21A		1-C	15.75	16.6/10.0	1.2186	9	17550	27	24.81	152.61*
B				16.6/10.0	1.2182	9	19210	26.5	24.90	152.16*
C				16.6/10.0	1.2182	9	41750	26	24.92	151.96*
D				15.7/10.0	1.2186	10	16800	26	24.84	152.25*

(1) The first number is requested gas mixture and the second the certified or corrected gas mixture.
(2) For propane.
* Back pressure correction applied.

Table 3.14c. Test conditions for building 303.

RUN NUMBER	GAS	FLOW TYPE	RATOR SETTING	SOURCE(1) STRENGTH (%)	CALIBRATION(2) FACTOR (PPM/μVS) ($X10^{-4}$)	BOTTLE NUMBER	BACK-GROUND (μVS)	TEMP (°C)	PRESSURE (in Hg)	VOLUME FLOW (ℓ/MIN)
22A	METHANE	1-C	15.75	16.6/10.0	1.2186	9	22640	26	24.90	152.03*
B				16.6/10.0	1.2182	9	1800	27	24.90	152.29*
C				16.6/10.0	1.2182	9	6500	27	24.8	152.64*
D				15.7/10.0	1.2064	10	6110	29	24.80	153.15*
23A		3-I	124.5	16.6/10.0	1.2186	9	9380	25	24.91	46.61
B				16.6/10.0	1.2182	9	13950	25	24.90	46.63
C				15.7/10.0	1.2064	10	3020	24	24.82	46.63
D				15.7/10.0	1.2064	10	9120	27	24.82	47.10
24A		3-I	97.0	16.6/10.0	1.2182	9	12870	25	24.90	31.80
B				16.6/10.0	1.2182	9	10560	24	24.91	31.68
C				15.7/10.0	1.2064	10	19680	23	24.80	31.71
D				15.7/10.0	1.2064	10	3500	27.5	24.80	32.19
25A		1-C	15.75	15.7/15.0	1.1992	10	6570	29	24.80	153.41*
B				15.7/15.0	1.2908	10	30880	25	24.87	152.15*
C				15.7/15.0	1.2908	10	11400	30	24.89	153.35*
D				15.7/15.0	1.2035	10	52540	29	24.77	153.52*
26A		1-C	15.75	15.7/15.0	1.1992	10	4930	30	24.80	153.67*
B				15.7/15.0	1.2908	10	25730	28	24.88	152.87*
C				15.7/15.0	1.2908	10	3520	30	24.76	153.81*
D				15.7/15.0	1.2035	10	22800	28	24.77	153.27*
27A		3-I	124.5	15.7/15.0	1.1992	10	5680	29	24.75	47.54
B				15.7/15.0	1.2908	10	12830	26	24.83	46.92
C				15.7/15.0	1.2908	10	1000	29	24.80	47.45
D				15.7/15.0	1.2035	10	9510	27	24.80	47.14
28A		3-I	97.0	15.7/15.0	1.1992	10	10640	25.6	24.77	32.03
B				15.7/15.0	1.1992	10	0	27	24.80	32.14
C				15.7/15.0	1.2908	10	3890	30	24.81	32.45
D				15.7/15.0	1.2035	10	8890	27	24.77	32.18

(1) The first number is requested gas mixture and the second the certified or corrected gas mixture.
(2) For propane.
* Back pressure correction applied.

Table 3.14d. Test conditions for building 304.

RUN NUMBER	GAS	FLOW TYPE	RATOR SETTING	SOURCE (1) STRENGTH (%)	CALIBRATION (2) FACTOR (PPM/μVS) ($X10^{-4}$)	BOTTLE NUMBER	BACK- GROUND (μVS)	TEMP (°C)	PRESSURE (in Hg)	VOLUME FLOW (ℓ/MIN)
1A*	BUTANE	3-G	76	10.22/10.0	1.0603	6	10220	23	24.63	26.43
B*	ETHANE			10.22/10.2	1.2214	2	13520	23	24.63	26.43
C*	BUTANE			9.73/10.0	1.1238	5	32930	23	24.63	26.43
D*				9.73/10.0	1.1238	5	32930	23	24.63	26.43
2A*		3-G	76	10.22/10.0	1.0603	6	13680	23	24.63	26.43
B*	ETHANE			10.2/10.2	1.2214	2	22710	23	24.63	26.43
C*	BUTANE			9.73/10.0	1.1238	5	17470	23	24.63	26.43
D*				9.73/10.0	1.1238	5	17470	23	24.63	26.43
3A*		4-J	99.1	10.22/10.2	1.0603	6	7910	23	24.63	5.50
B*	ETHANE			10.2/10.2	1.2214	2	6040	23	24.63	5.50
C*	ETHANE			10.2/10.2	1.2054	3	1698	23	24.63	5.50
D*	BUTANE			9.73/10.0	1.1238	5	4170	23	24.63	5.50
4A*		4-J	76	10.22/10.0	1.1501	6	1380	23	24.63	4.106
B*				9.80/9.8	1.0979	3	40880	23	24.63	4.106
C*				9.73/10.0	1.2054	5	4170	23	24.63	4.106
D*				9.73/10.0	1.1238	5	2120	23	24.63	4.106
5A*		4-J	40.5	10.22/10.0	1.1501	6	1350	23	24.63	1.95
B*				9.80/9.8	1.1716	3	9980	23	24.63	1.95
C*				9.73/10.0	1.2054	5	0	23	24.63	1.95
D*				9.73/10.0	1.2054	5	0	23	24.63	1.95
6A*		3-G	76	10.22/10.0	1.0603	6	15850	23	24.63	26.43
B*				9.80/9.8	1.1716	4	25150	23	24.63	26.43
C*				10.22/10.0	1.1238	6	29310	23	24.63	26.43
D*				9.80/9.8	1.1716	4	56770	23	24.63	26.43
7A*		3-G	76	10.22/10.0	1.0603	6	15730	23	24.63	26.43
B*				9.80/9.8	1.1716	3	32110	23	24.63	26.43
C*				9.73/10.0	1.1238	5	21920	23	24.63	26.43
D*	METHANE			17.4/16.1	1.0726	4	304480	23	24.63	26.43
8A*	BUTANE	4-J	99.1	10.22/10.0	1.2050	6	1660	23	24.63	5.50
B*				9.80/9.8	1.1716	3	7030	23	24.63	5.50
C*				9.73/10.0	1.2054	5	0	23	24.63	5.50
D*				9.80/9.8	1.0726	3	12820	23	24.63	5.50

(1) The first number is the requested gas mixture and the second the certified or corrected gas mixture.
(2) For propane.

Table 3.14d. Test conditions for building 304.

RUN NUMBER	GAS	FLOW TYPE	RATOR SETTING	SOURCE (1) STRENGTH (%)	CALIBRATION (2) FACTOR (PPM/μVS) (X10^{-4})	BOTTLE NUMBER	BACK-GROUND (μVS)	TEMP (°C)	PRESSURE (in Hg)	VOLUME FLOW (ℓ/MIN)
7A	BUTANE	4-J	99.1	9.73/10.0	1.2935	7	0	24	24.63	5.52
B				9.73/10.0	1.2801	7	15235	26	24.60	5.56
C				8.91/10.0	1.2752	8	1870	19	24.52	5.45
D				8.91/10.0	1.2752	8	2560	21.1	24.50	5.50
8A		4-J	76.0	9.73/10.0	1.2935	7	2555	24	24.63	4.12
B				10.2/10.0	1.2801	6	0	22	24.65	4.09
C				8.91/10.0	1.2752	8	1295	20	24.52	4.08
D				8.91/10.0	1.2752	8	4170	21.1	24.50	4.09
9A		3-G	76.0	9.73/10.0	0.9682	10	2790	28	24.67	26.83
B				9.73/10.0	0.9582	10	0	23	24.95	26.09
C				9.59/10.0	0.9582	11	13440	23	24.88	26.16
D				9.59/10.0	0.9532	11	10500	24	24.85	26.28
10A		3-G	76.0	9.73/10.0	0.9682	10	6750	27.5	24.67	26.79
B				9.73/10.0	0.9582	10	1370	23	25.00	26.04
C				9.73/10.0	0.9582	10	0	24	24.80	26.34
D				9.59/10.0	0.9532	11	4000	26	24.85	26.46
11A		4-J	99.1	9.59/10.0	0.9532	11	0	25	24.80	5.50
B				9.73/10.0	0.9582	10	0	22.5	24.93	5.43
C				9.59/10.0	0.9582	11	7020	23	24.95	5.43
D				9.59/10.0	0.9532	11	3360	22	24.90	5.42
12A		4-J	76.0	9.59/10.0	0.9532	11	2510	28	24.80	4.15
B				9.73/10.0	0.9739	10	3490	23	24.89	4.06
C				9.59/10.0	0.9532	11	7910	21	24.90	4.03
D				9.59/10.0	0.9532	11	0	20	24.90	4.02
13A		3-G	76.0	9.59/10.0	0.9141	11	10770	29	24.80	26.78
B				9.59/10.0	0.8977	11	6920	26	24.94	26.37
C				9.70/10.0	0.9057	12	16630	23	24.94	26.10
D				9.70/10.0	0.9057	12	5150	27	24.90	26.50
14A		3-G	76.0	9.59/10.0	0.9141	11	8320	27	24.80	26.60
B				9.70/10.0	0.8977	12	9460	27.5	28.5	23.19
C				9.70/10.0	0.9057	12	3090	25	24.94	26.28
D				9.70/10.0	0.9057	12	4350	26	24.90	26.41

(1) The first number is the requested gas mixture and the second the certified or corrected gas mixture.
(2) For propane.

Table 3.14d. Test conditions for building 304.

RUN NUMBER	GAS	FLOW TYPE	RATOR SETTING	SOURCE (1) STRENGTH (%)	CALIBRATION (2) FACTOR (PPM/μVS) ($X10^{-4}$)	BOTTLE NUMBER	BACK-GROUND (μVS)	TEMP (°C)	PRESSURE (in Hg)	VOLUME FLOW (ℓ/MIN)
9A*	BUTANE	4-J	76	10.22/10.0	1.1501	6	1810	23	24.63	4.106
B*				9.80/9.8	1.1716	3	7570	23	24.63	4.106
C*	METHANE			16.7/14.38	1.1553	5	19830	23	24.63	4.106
D*	BUTANE			9.80/9.8	1.0726	3	16150	23	24.63	4.106
10A*		4-J	40.5	10.22/10.0	1.1501	6	2230	23	24.63	1.95
B*				9.80/9.8	1.1716	3	7170	23	24.63	1.95
C*	METHANE			16.70/14.38	1.1553	5	20230	23	24.63	1.95
D*	BUTANE			9.80/9.8	1.0726	4	21390	23	24.63	1.95
1A		3-G	76.0	9.73/10.0	1.3020	7	10625	22	24.70	26.27
B				8.91/10.0	1.2865	8	4185	22	24.60	26.37
C				8.91/10.0	1.2865	8	1380	22	24.55	26.43
D				9.73/10.0	0.9574	10	32965	24	24.59	26.56
2A		3-G	76.0	9.73/10.0	1.3020	7	5465	28	24.70	26.80
B				8.91/10.0	1.2865	8	2610	21.2	24.60	26.30
C				8.91/10.0	1.2865	8	5540	21	24.60	26.28
D				9.73/10.0	0.9565	9	0	23	24.73	26.32
3A		4-J	99.1	9.73/10.0	1.2935	7	0	25	24.63	5.54
B				9.73/10.0	1.2801	7	1040	24	24.65	5.52
C				9.73/10.0	0.9407	10	5835	21.9	24.84	5.43
D				8.91/10.0	0.9574	8	0	19	24.73	5.41
4A		4-J	76.0	9.73/10.0	1.2935	7	1055	25.5	24.60	4.15
B				9.73/10.0	1.2935	7	0	24.5	24.60	4.13
C				9.73/10.0	0.9407	10	4460	23	24.84	4.07
D				8.91/10.0	1.2752	8	1040	21.2	24.50	4.10
5A		3-G	76.0	9.73/10.0	1.3020	7	1205	29	24.70	26.89
B				8.91/10.0	1.2801	8	0	23.5	24.65	26.45
C				8.91/10.0	1.2865	8	1590	22.5	24.55	26.47
D				9.73/10.0	0.9574	9	22185	25.6	24.63	26.66
6A		3-G	76.0	9.73/10.0	1.2935	7	28785	25	24.63	26.61
B				8.91/10.0	1.2801	8	0	23.5	24.65	26.45
C				8.91/10.0	1.2865	8	2900	23	24.55	26.52
D				9.73/10.0	0.9574	9	18550	23.5	24.82	26.27

(1) The first number is the requested gas mixture and the second the certified or corrected gas mixture.
(2) For propane.

Table 3.14d. Test conditions for building 304.

RUN NUMBER	GAS	FLOW TYPE	RATOR SETTING	SOURCE (1) STRENGTH (%)	CALIBRATION (2) FACTOR (PPM/μVS) (X10^{-4})	BOTTLE NUMBER	BACK-GROUND (μVS)	TEMP (°C)	PRESSURE (in Hg)	VOLUME FLOW (ℓ/MIN)
15A	BUTANE	4-J	99.1	9.59/10.0	0.8977	11	2700	24.5	24.94	5.46
B				9.70/10.0	0.8977	12	3800	26	24.90	5.50
C				9.70/10.0	0.8977	12	0	25	24.93	5.47
D				9.70/10.0	0.9057	12	1810	27	24.75	5.55
16A		4-J	76.0	9.59/10.0	0.8977	11	1520	24.5	24.95	4.07
B				9.70/10.0	0.8977	12	3880	27	24.82	4.13
C				9.70/10.0	0.9057	12	0	23	24.91	4.06
D				9.70/10.0	0.9057	12	0	27	24.90	4.12
17A		3-G	76.0	9.70/10.0	0.9301	12	0	27	24.20	21.26
B				9.70/10.0	0.9301	12	0	26	24.65	26.68
C				9.92/10.0	0.9184	13	6010	28	24.58	26.93
D				9.92/10.0	1.2116	13	2000	27	24.64	26.78
E				9.92/10.0	1.2116	13	3220	27	24.77	26.78
18A		3-G	76.0	9.70/10.0	0.9301	12	0	27	24.75	26.66
B				9.70/10.0	0.9301	12	0	27	24.60	26.82
C				9.92/10.0	0.9184	13	7070	27.5	24.60	26.86
D				9.92/10.0	0.9119	13	9750	27.5	24.65	26.81
E				9.92/10.0	1.2116	13	13720	27.5	24.77	26.68
19A		4-J	99.1	9.70/10.0	0.9301	12	0	24.5	24.73	5.51
B				9.70/10.0	0.9184	12	7190	24	24.64	5.52
C				9.70/10.0	0.9184	12	0	25.5	24.66	5.54
D				9.92/10.0	0.9119	13	17030	24.5	24.67	5.52
E				9.92/10.0	0.9119	13	0	26	24.77	5.53
20A		4-J	76.0	9.70/10.0	0.9301	12	0	26	24.74	4.13
B				9.70/10.0	0.9184	12	3910	24	24.65	4.12
C				9.70/10.0	0.9184	12	2990	25	24.65	4.13
D				9.92/10.0	0.9119	13	17260	26.5	24.70	4.14
E				9.92/10.0	1.1935	13	0	24.5	24.75	4.11
21A		3-G	76.0	9.92/10.0	1.2186	13	16990	27	24.81	26.59
B				9.47/10.0	1.2182	15	3060	26.5	24.90	26.45
C				9.47/10.0	1.2182	15	13670	26	24.92	26.39
D				9.47/10.0	1.2186	15	0	26	24.84	26.47

(1) The first number is the requested gas mixture and the second the certified or corrected gas mixture.
(2) For propane.

Table 3.14d. Test conditions for building 304.

RUN NUMBER	GAS	FLOW TYPE	RATOR SETTING	SOURCE (1) STRENGTH (%)	CALIBRATION (2) FACTOR (PPM/μVS) (X10^{-4})	BOTTLE NUMBER	BACK-GROUND (μVS)	TEMP (°C)	PRESSURE (in Hg)	VOLUME FLOW (ℓ/MIN)
22A	BUTANE	3-G	76.0	9.92/10.0	1.2186	13	7320	26	24.90	26.41
B				9.47/10.0	1.2182	15	1890	27	24.90	26.50
C				9.47/10.0	1.2182	15	0	27	24.8	26.60
D				9.47/10.0	1.2064	15	4160	29	24.80	26.78
23A		4-J	99.1	9.92/10.0	1.2186	13	10350	25	24.91	5.48
B				9.92/10.0	1.2182	13	0	25	24.90	5.48
C				9.47/10.0	1.2064	15	5320	24	24.82	5.48
D				9.47/10.0	1.2064	15	0	27	24.82	5.53
24A		4-J	76.0	9.92/10.0	1.2182	13	14960	25	24.90	4.09
B				9.92/10.0	1.2182	13	0	24	24.91	4.07
C				9.47/10.0	1.2064	15	4060	23	24.80	4.08
D				9.47/10.0	1.2064	15	0	27.5	24.80	4.14
25A		3-G	76.0	9.47/10.0	1.1992	15	1540	29	24.80	26.78
B				9.47/10.0	1.2908	15	3190	25	24.87	26.35
C				9.47/10.0	1.2908	15	0	30	24.89	26.77
D				9.36/10.0	1.2035	16	9050	29	24.77	26.81
26A		3-G	76.0	9.47/10.0	1.1992	15	1770	30	24.80	26.87
B				9.47/10.0	1.2908	15	1530	28	24.88	26.61
C				9.47/10.0	1.2908	15	0	30	24.76	26.91
D				9.47/10.0	1.2035	15	4420	28	24.77	26.72
27A		4-J	99.1	9.47/10.0	1.1992	15	0	29	24.75	5.59
B				9.47/10.0	1.2908	15	0	26	24.83	5.51
C				9.47/10.0	1.2908	15	0	29	24.80	5.57
D				9.47/10.0	1.2035	15	0	27	24.80	5.54
28A		4-J	76.0	9.47/10.0	1.1992	15	0	25.6	24.77	4.12
B				9.47/10.0	1.1992	15	0	27	24.80	4.13
C				9.47/10.0	1.2908	15	0	30	24.81	4.17
D				9.47/10.0	1.2035	15	0	27	24.77	4.14

(1) The first number is the requested gas mixture and the second the certified or corrected gas mixture.
(2) For propane.

Table 3.15. Typical sampling system calibration.

Sample #	Raw Data
1	205694
2	203629
3	202588
4	204305
5	204430
6	203817
7	204636
8	204425
9	204820
10	202794
11	202874
12	203496
13	197171
14	203790
15	202432
16	202426
17	202317
18	200461
19	200372
20	201950
21	201829
22	201817
23	199365
24	201459
25	200297
26	200940
27	200012
28	200622
29	------
30	199445
31	199914
32	198845
33	198725
34	198899
35	198898
36	195163
37	198945
38	197443
39	197502
40	196235
41	196938
42	196890
43	147606
44	196634
45	196964
46	197027
47	195721
48	196414
49	196934
50	196582
Calibration	197778

*Integrated output from Gas Chromotograph in μv-s.

Table 3.16. Flowrator key.

Numeral Designated	Specific Rator	Type	Description
1	A,B,C,D	Fisher-Porter	No. LK-1735-5 Tube No. B6-35-10/77 Max. flow 782.2; min. flow 62.3 ℓ/min.
2	E	Fisher-Porter	No. LK-1735-5 Tube No. B4-21-10/77 Max. flow 70.3; min. flow 2.8 ℓ/min.
3	I.H.G	Brooks	Tube No. R-6-15-B Spherical, STL.ST. 316 Float Max. flow 43.5; min. flow 0.5 ℓ/min.
4	J	Brooks	Tube No. R-2-15-C Spherical. STL.ST. 316 Float Max. flow 7.60; min. flow 0.05 ℓ/min.

Table 3.17. Results of back pressure measurements.

Stack or Building	Flowrator No./Specification	Setting	Back Pressure (psi)							
			During Calibration	SW (Start)	SW (Finish)	W	NW	NE	E	S
301	3/G	102.0	5.05	5.05	5.05	5.05	5.05	5.05	5.05	5.05
	3/G	131.0	12.18	12.18	12.18	12.18	12.18	12.18	12.18	12.18
	1/A**	16.55	1.2	2.52	2.60	2.67	2.53	2.6	1.30	1.25
302	3/H	90.0	0.15	0.13	0.13	0.15	0.15	0.15	0.15	0.15
	3/H	116.0	0.21	0.20	0.20	0.23	0.23	0.23	0.23	0.23
	1/B	14.55	1.8	1.70	1.81	1.84	1.85	1.72	1.70	1.70
303	3/I	97.0	0.16	0.15	0.15	0.15	0.18	0.16	0.17	0.15
	3/I	124.5	0.25	0.21	0.23	0.23	0.26	0.25	0.25	0.25
	1/C**	15.75	2.3	1.70	1.76	1.66	3.30	2.29	2.25	2.30
304	4/J	76	0.21	0.26	0.20	0.21	0.35	0.23	0.21	0.30
	4/J	99.1	0.31	0.41	0.30	0.30	0.55	0.33	0.35	0.50
	3/G	76	3.35	3.35	3.35	3.35	3.35	3.35	3.35	3.35
Orifice	1/D	21.2	3.3	3.3	3.14	3.2	3.23	3.28	3.30	3.20
	2/E	50.5	0.32	0.30	0.29	0.30	0.30	0.30	0.30	*
	2/E	67.0	0.47	0.42	0.45	0.42	0.40	0.45	0.45	*
T_a(°C)			27	29	25	24	*	*	25	30.5
P_a("Hg)			24.90	24.75	24.84	24.92	*	*	24.91	24.65

*Missing

**All flow rates using these Flowrators were corrected for back pressure; the others were not.

Table 3.18. Calibration results for Flowrators.

Stack or Building	Flowrator No./ Designation	Flowrator Setting	Calibration Conditions					Calibration Volume Flow Q_c (ℓ/min)
			Ambient Temperature (°C)	Ambient Pressure ("Hg)	Start Pressure (psi)	End Pressure (psi)	Time (s)	
301	3/G	56.5	17.0	24.65	*	*	*	15.67
	3/G	102.0	26.0	25.05	1198	1140	300	41.15
	3/G	131.0	26.0	25.05	1175	1084	300	64.57
	1/A	16.55	26.5	24.92	1042	960	120	145.45
302	3/H	49.5	17.0	24.65	*	*	*	13.38
	3/H	90.0	26.5	24.92	1084	1042	300	29.80
	3/H	116.0	26.5	24.92	1413	1355	300	41.15
	1/B	14.55	26.5	24.92	1074	1000	120	131.26
303	3/I	53.5	17.0	24.65	*	*	*	14.69
	3/I	97.0	26.5	24.92	1355	1310	300	31.93
	3/I	124.5	26.5	24.92	1140	1074	300	46.83
	1/C	15.75	26.5	24.92	1310	1224	120	152.55
304	4/J	76	21.0	24.74	*	*	*	4.06†
	4/J	40.5	21.0	24.74	*	*	*	1.93
	4/J	99.1	21.0	24.74	*	*	*	5.44
	3/G	76	26	25.05	1487	1413	600	26.25
Orifice	2/E	25.0	21.1	29.9	*	*	*	17.57
	2/E	50.5	25.5	24.2	1000	962	180	45.11
	2/E	67.0	25.5	24.92	960	914	180	54.61
	1/D	21.2	25.5	24.92	1224	1048	180	208.93

*Calibration performed with soap bubble meter. Negligible back pressure was assumed for these tests.
†Linear interpolation between 40.5 and 99.1 Flowrator settings.

Table 4.1. Lateral velocity profile for a free stream velocity of 1.94 m/s with the split film in a vertical position at 10 cm from the ground.

y (m)	$\bar{u}$ (m/s)	$\bar{v}$ (m/s)	u' (m/s)	v' (m/s)	$\sqrt{\overline{u'v'}}$ (m/s)
0.457	1.2991	-0.0596	0.2223	0.1667	0.0591
0.609	1.2608	-0.0591	0.2257	0.1747	0.0436
0.914	1.1800	-0.0617	0.2299	0.1779	0.0141
1.219	1.0684	-0.0793	0.2382	0.1767	0.0839
1.524	1.0414	-0.0201	0.2180	0.1766	0.0387
1.829	1.1207	0.0100	0.2236	0.1636	0.0474
2.133	1.0581	-0.0157	0.2114	0.1741	0.0406
2.438	1.0128	0.0162	0.2145	0.1636	0.0212
2.743	1.1188	0.4485	0.2159	0.1614	0.0316
3.048	1.1093	0.0372	0.2294	0.1685	0.0367
3.200	1.1648	0.0349	0.2139	0.1600	0.0406
3.353	1.1929	0.0285	0.2185	0.1554	0.0394
3.453	1.1590	0.0178	0.2224	0.1530	0.0515
3.554	1.1576	0.0025	0.2083	0.1498	0.0223
Average between 0.61 and 3.0 m			0.223	0.171	------

Table 4.2. Lateral velocity profile across the tunnel at 10 cm from the ground with a free stream velocity of 1.94 m/s and the wire oriented horizontally.

y (m)	$\bar{u}$ (m/s)	$\bar{w}$ (m/s)	u' (m/s)	w' (m/s)	u* (m/s)
0.100	1.1154	-0.0196	0.1907	0.1379	0.0800
0.201	1.2917	-0.0265	0.2078	0.1333	0.1027
0.305	1.3337	-0.0271	0.2055	0.1304	0.0951
0.457	1.3123	-0.0225	0.2223	0.1330	0.1075
0.609	1.3105	-0.0230	0.2368	0.1359	0.1127
0.914	0.1742	-0.0245	0.2320	0.1417	0.1210
1.219	1.1344	-0.0305	0.2489	0.1342	0.1131
1.524	1.0660	-0.0046	0.2158	0.1299	0.1020
1.829	1.1576	-0.0287	0.2254	0.1346	0.1081
2.133	1.1037	-0.0138	0.2206	0.1245	0.1049
2.438	1.078	-0.0079	0.2236	0.1271	0.1093
2.743	1.1636	-0.0145	0.2164	0.1319	0.1041
3.048	1.1902	-0.0146	0.2222	0.1312	0.1079
Average from 0.61 to 3.0 m			0.227	0.132	0.109

Table 4.3. Vertical profile of $\bar{u}$, u', v' and $\sqrt{\overline{u'v'}}$ with the split film in a vertical position and a free stream velocity of 1.9 m/s.

z (m)	$\bar{u}$ (m/s)	$\bar{v}$ (m/s)	u' (m/s)	v' (m/s)	$\sqrt{\overline{u'v'}}$ (m/s)
3.54	0.646	-0.075	0.217	0.182	0.035
7.2	1.034	-0.054	0.230	0.179	0.043
7.9	1.034	-0.051	0.217	0.160	0.032
12.5	1.110	-0.050	0.213	0.163	0.037
22.3	1.323	-0.057	0.210	0.158	0.054
32.4	1.412	-0.053	0.197	0.155	0.053
42.5	1.496	-0.060	0.178	0.163	0.00
63.6	1.612	-0.064	0.180	0.156	0.047
88.0	1.770	-0.061	0.175	0.134	0.033
104.4	1.850	-0.056	0.128	0.102	0.035
118.5	1.909	-0.048	0.105	0.090	0.038
136.4	1.931	-0.029	0.081	0.071	0.037

Table 4.4. Vertical profile of $\bar{u}$, u', w' and u* with the split film in a horizontal position and a free stream velocity of 1.9 m/s.

z (cm)	$\bar{u}$ (m/s)	$\bar{w}$ (m/s)	u' (m/s)	w' (m/s)	u* (m/s)
4.1	0.735	-0.030	0.210	0.119	0.101
7.2	0.930	-0.029	0.241	0.128	0.113
13.2	1.122	-0.024	0.218	0.128	0.102
21.6	1.241	-0.032	0.194	0.127	0.098
33.1	1.337	-0.028	0.193	0.139	0.096
47.0	1.463	-0.037	0.182	0.141	0.096
62.2	1.551	-0.049	0.182	0.135	0.091
76.2	1.658	-0.049	0.177	0.124	0.087
85.5	1.762	-0.060	0.147	0.118	0.077
100.0	1.837	-0.056	0.140	0.096	0.060
113.4	1.881	-0.058	0.099	0.076	0.040
119.1	1.914	-0.062	0.090	0.080	0.038
127.3	1.941	-0.063	0.069	0.064	0.030
130.8	1.923	-0.061	0.079	0.067	0.030

Table 4.5. Vertical profile of $\bar{u}$, u', w' and u* with split film in horizontal position and a free stream velocity of 4 m/s.

z (cm)	$\bar{u}$ (m/s)	$\bar{w}$ (m/s)	u' (m/s)	w' (m/s)	u* (m/s)
3.44	1.565	0.018	0.492	0.283	0.234
5.24	1.875	-0.011	0.504	0.283	0.233
8.54	2.344	-0.038	0.463	0.281	0.215
12.04	2.530	-0.048	0.488	0.277	0.234
21.04	2.882	-0.067	0.429	0.302	0.217
32.55	3.042	-0.069	0.390	0.295	0.195
42.50	3.132	-0.094	0.370	0.298	0.189
62.63	3.391	-0.067	0.382	0.301	0.188
82.53	3.680	-0.088	0.339	0.282	0.164
98.98	3.779	-0.070	0.295	0.230	0.134
107.15	3.915	-0.070	0.283	0.224	0.132
137.54	4.045	-0.043	0.175	0.1431	0.039

Table 4.6. Summary of velocity profile analysis for boundary layer tests.

u_∞ (m/s)	Location (Point D is 0,0)	x(m)	y(m)	$u*$[1] (m/s)	z_o[1] (cm)	d (cm)	n[2]
2	A	-4.92	0.0	0.120	0.165	-0.31	0.214
	B	-2.61	0.0	0.105	0.074	1.04	0.23
	C	2.60	0.0	0.111	0.117	-0.10	0.21
	E	0.0	-1.82	0.093	0.035	2.00	0.27
	F	0.0	-0.91	0.110	0.115	1.30	0.27
	G	0.0	0.91	0.086	0.031	1.75	0.23
	H	0.0	1.82	0.093	0.059	1.69	0.26
	0	0	0	0.122	0.209	-0.077	0.24
1	0	0	0	0.052	0.11	2.0	0.35
1.5	0	0	0	0.094	0.18	0.6	0.25
2	0	0	0	0.116	0.13	0.8	0.24
3	0	0	0	0.165	0.10	1.3	0.26
5	0	0	0	0.235	0.04	1.4	0.21

[1] Least squares from following equation

$$\frac{\bar{u}}{u*} = \frac{1}{K} \ell n \left[\frac{z-d}{z_o}\right]$$

[2] Least squares from following equation

$$\left(\frac{\bar{u}}{u_\infty}\right) = \left(\frac{z}{z_\infty}\right)^n$$

Table 4.7. Summary of boundary layer characteristics as obtained with split film sensor.

Quantity \ z(cm)	$\overline{u}_\infty = 1.9$ m/s			$\overline{u}_\infty = 4.0$ m/s			Pasquill (1974)
	10	20	125	10	20	125	
$\frac{u'}{u_o^*}$	2.06	1.98	2.30	2.12	1.98	2.34	2.1 - 2.9
$\frac{v'}{u_o^*}$	1.57	1.61	2.12	-	-	-	1.3 - 2.6
$\frac{w'}{u_o^*}$	1.21	1.30	2.23	1.25	1.39	2.69	1.25
$\frac{u_o^*}{\overline{u}_\infty}$	0.057			0.059			

Table 4.8. Summary of velocity profile characteristics for scale model tests.

Wind Direction	$\bar{u}_r$ (m/s)	zo (mm)	$u^*/\bar{u}_r$	d (cm)	Re_{zo}	n	e_{zo} 1)	e_n 2)
SW - Phase I	3.11	5.34	0.101	10.3	112.14	0.952	0.217	0.159
	2.32	6.75	0.109	9.88	113.85	0.853	0.241	0.992
	1.58	5.49	0.101	10.3	58.56	0.953	0.150	0.809
SW - Phase II	3.05	2.47	0.083	10.5	41.83	0.792	0.258	0.131
	2.38	1.68	0.078	10.6	20.72	0.821	0.210	0.113
	1.58	1.63	0.077	10.6	13.26	0.782	0.150	0.691
W	2.98	0.111	0.054	10.5	1.20	0.336	0.114	0.369
	2.31	0.364	0.061	10.5	3.42	0.430	0.0619	0.384
	1.56	0.0510	0.050	10.6	0.26	0.337	0.0666	0.209
NW	2.92	5.48	0.104	5.47	111.43	0.350	0.113	0.182
	2.34	5.14	0.097	5.28	77.79	0.337	0.0500	0.117
	1.56	3.50	0.094	7.13	34.07	0.355	0.0557	0.108
NE	3.26	0.997	0.070	8.50	14.85	0.312	0.0813	0.234
	2.39	0.760	0.068	8.63	8.21	0.307	0.0449	0.166
	1.72	0.589	0.066	9.63	4.48	0.346	0.0532	0.174
E	3.34	0.287	0.050	10.4	3.60	0.402	0.127	0.506
	2.38	0.0957	0.050	10.6	0.77	0.376	0.0565	0.342
	1.64	0.318	0.062	10.0	2.14	0.344	0.0749	0.194

Table 4.8 (continued)

Wind Direction	$\bar{u}_r$ (m/s)	zo (mm)	$u^*/\bar{u}_r$	d (cm)	Re_{zo}	n	e_{zo} 1)	e_n 2)
S	3.07	3.04	0.085	9.75	52.69	0.567	0.135	0.624
	2.31	2.52	0.081	10.1	31.25	0.621	0.0920	0.579
	1.55	1.87	0.077	10.4	14.96	0.672	0.0629	0.458

1) The root-mean-square error between log-law and observation.

2) The root-mean-square error between power-law and observation.

All profile locations at point 0, coordinates (746041, 1166956).

Table 5.1. Horizontal concentration distribution for ADCT runs with $\overline{u}_\infty = 3$ m/s.

x (cm)	y (cm)	z (cm)	D x 10^3 (m^{-2}) Wind Tunnel	Gaussian Model
60.93	24.00	8.2	0.01	0.00
	18.90		0.121	0.02
	16.35		0.35	0.08
	13.70		0.95	0.26
	11.20		1.99	0.66
	8.80		2.50	1.36
	6.1		3.42	2.49
	5.0		3.42	2.99
	3.7		4.61	3.55
	2.45		4.79	3.99
	1.30		5.05	4.26
	0.00		4.85	4.37
	-1.60		4.24	4.20
	-2.75		3.82	3.70
	-4.10		3.18	3.39
	-6.35		1.81	2.38
	-8.95		0.83	1.30
	-14.30		0.20	0.20
	-19.20		0.07	0.02
	-24.20		0.03	0.00

Table 5.2. Horizontal concentration distribution for ADCT run with $\overline{u}_{\infty} = 1$ m/s.

x (cm)	y (cm)	z (cm)	$D \times 10^3$ (m^{-2})	
			Wind Tunnel	Gaussian Model
60.93	24.00	9.3	0.04	0.00
	8.80		2.69	1.36
	0.10		3.39	2.49
	3.70		2.80	3.55
	2.45		5.05	3.99
	1.30		3.91	4.26
	0.00		4.04	4.37
	-1.60		3.66	4.20
	-2.75		3.88	3.90
	-6.35		1.55	2.38
	-11.50		0.52	0.59
	-24.20		0.01	0.00

Table 5.3. Horizontal concentration distribution for ADCT runs with $\overline{u}_\infty$ = 3 m/s.

x (cm)	y (cm)	z (cm)	$D \times 10^3$ (m^{-2})	
			Wind Tunnel	Gaussian Model
121.92	24.00	7.1	0.36	0.104
	18.90		0.95	0.28
	13.70		1.47	0.61
	8.80		1.70	1.00
	6.10		2.39	1.20
	3.70		2.11	1.34
	1.30		2.18	1.41
	0.00		2.13	1.42
	-1.60		1.95	1.41
	-4.10		1.73	1.32
	-6.35		1.72	1.20
	-11.50		1.02	0.78
	-16.75		0.54	0.40
	-24.20		0.15	0.10

Table 5.4. Horizontal concentration distribution for ADCT runs with $\overline{u}_\infty = 3$ m/s.

x (cm)	y (cm)	z (cm)	$D \times 10^3$ (m^{-2})	
			Wind Tunnel	Gaussian Model
243.84	39.00	6.00	0.130	0.02
	32.10		0.24	0.08
	16.35		0.89	0.48
	8.80		1.29	0.77
	3.70		1.38	0.90
	2.45		1.42	0.91
	1.30		1.41	0.92
	0.00		1.53	0.94
	-1.60		1.41	0.92
	-2.75		1.44	0.91
	-6.35		1.30	0.84
	-16.75		0.85	0.48
	-24.20		0.42	0.22
	-39.70		0.07	0.02
	-48.55		0.05	0.00

Table 5.5. Vertical concentration distribution for ADCT runs with $\overline{u}_{\infty}$ = 3 m/s.

x (cm)	y (cm)	z (cm)	D x 10^3 (m^{-2})	
			Wind Tunnel	Gaussian Model
		0.00		0.62
60.96	0.00	3.10	1.72	1.30
		4.40	3.17	1.95
		5.65	4.07	2.69
		6.90	4.14	3.43
		8.05	4.87	4.00
		9.05	4.73	4.32
		10.45	4.31	4.40
		11.85	3.09	4.04
		14.40	1.93	2.65
		16.90	1.46	1.25
		19.20	0.44	0.47
		22.10	0.10	0.09
		24.50	0.11	0.02
		27.95	0.05	0.00
		30.25	0.01	0.00

Table 5.6. Vertical concentration measurements for ADCT runs with $\overline{u}_{\infty}$ = 3 m/s.

x (cm)	y (cm)	z (cm)	$D \times 10^3$ (m^{-2}) Wind Tunnel	Gaussian Model
60.96	0	0	1.66	0.61
		3.10	2.32	1.30
		4.40	2.60	1.95
		5.65	3.39	2.69
		6.90	4.33	3.43
		8.05	4.23	4.00
		9.05	4.63	4.32
		10.45	3.35	4.40
		11.85	3.48	4.04
		13.1	2.10	3.43
		14.4	1.69	2.65
		16.9	0.61	1.25
		19.2	0.38	0.47
		24.5	0.05	0.02
		27.95	0.01	0.00

Table 5.7. Vertical concentration distributions for ADCT runs with $\bar{u}_\infty = 3$ m/s.

x (cm)	y (cm)	z (cm)	$D \times 10^3$ (m^{-2}) Wind Tunnel	Gaussian Model
121.92	0	0.00	1.51	1.13
		3.10	1.78	1.21
		4.40	1.83	1.28
		5.65	1.59	1.35
		6.90	2.06	1.42
		8.05	1.60	1.46
		9.05	1.54	1.47
		10.45	1.44	1.46
		13.10	1.15	1.32
		16.90	0.00	0.92
		19.2	0.54	0.65
		22.1	0.53	0.37
		24.5	0.38	0.20
		27.95	0.23	0.07
		32.0	0.04	0.02
		36.9	0.00	0.00

Table 5.8. Vertical concentration distribution for ADCT runs with $\bar{u}_\infty$ = 3 m/s.

x (cm)	y (cm)	z (cm)	$D \times 10^3$ (m^{-2}) Wind Tunnel	Gaussian Model
243.84	0.00	0.00	1.30	0.94
		3.10	1.42	0.93
		4.40	1.20	0.93
		5.65	1.42	0.93
		6.90	1.20	0.92
		8.05	1.14	0.91
		9.05	0.95	0.89
		11.85	0.86	0.83
		14.40	0.69	0.74
		16.90	0.57	0.63
		19.20	0.42	0.52
		22.10	0.38	0.38
		24.50	0.27	0.27
		27.95	0.17	0.15
		32.00	0.11	0.07
		39.9	0.02	0.00

Table 5.9. Reynolds number independence test.

Run # or $\bar{u}_\infty$ (m/s)	$Re = \frac{\bar{u}_\infty H_s}{\nu}$	Dimensionless Concentration K		
		Top	Bottom	Ground
1	7,000	0.084	0.046	0.041
2	14,000	0.090	0.055	0.044
3	21,000	0.093	0.060	0.041
	MEAN	0.089	0.054	0.042

FIGURES

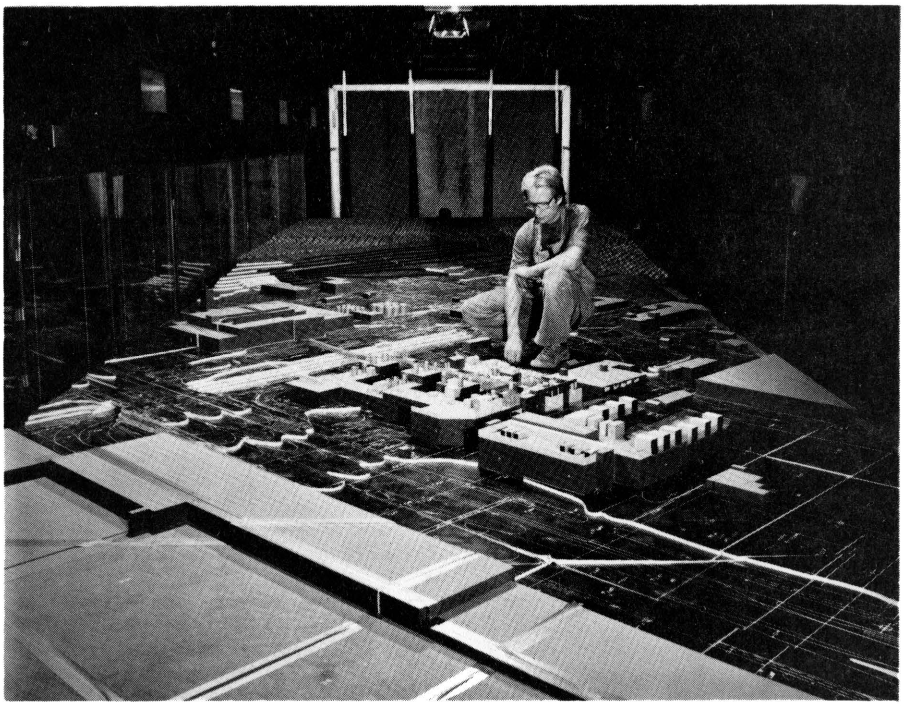

a

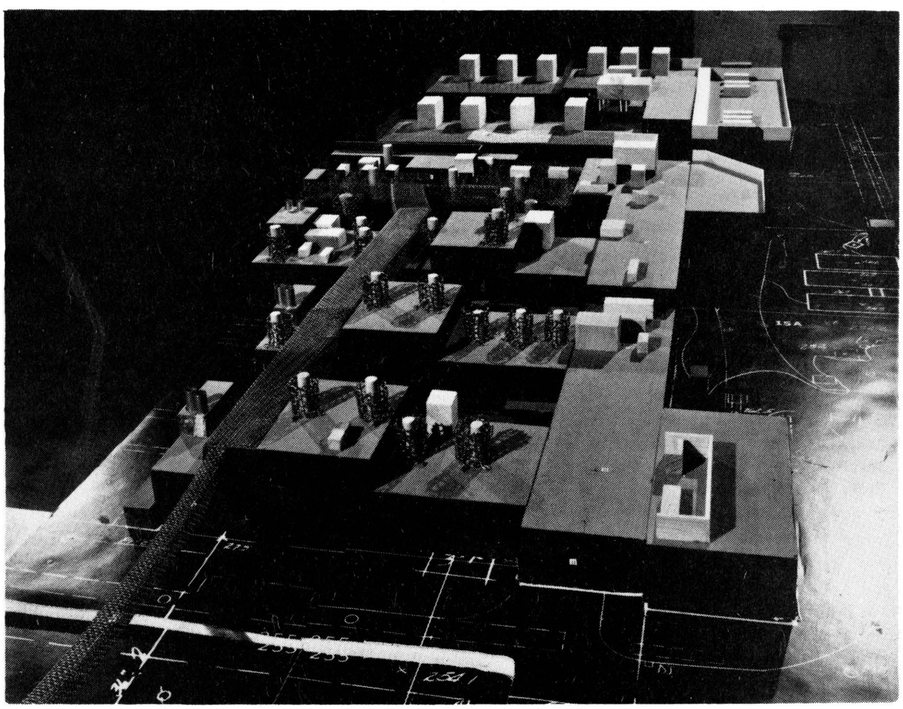

b

Figure 3.2-1. Photographs of Kodak Park Model a) positioned in wind tunnel for SW wind direction, and b) buildings 301, 302, 303, 337A, 337B and 339.

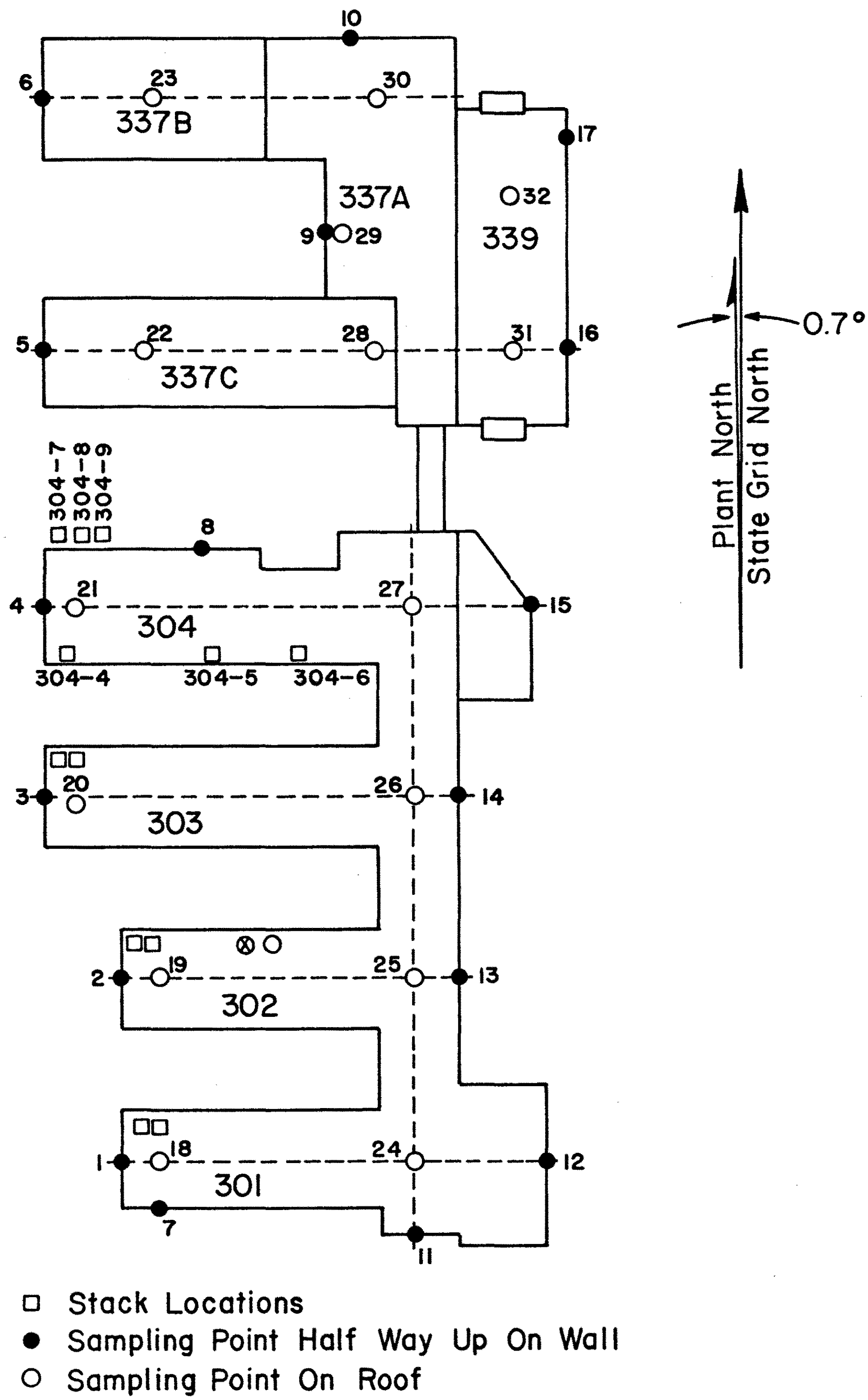

Figure 3.2-2. Sampling and stack locations for buildings 301, 302, 303, 304, 337A, 337B, 337C and 339.

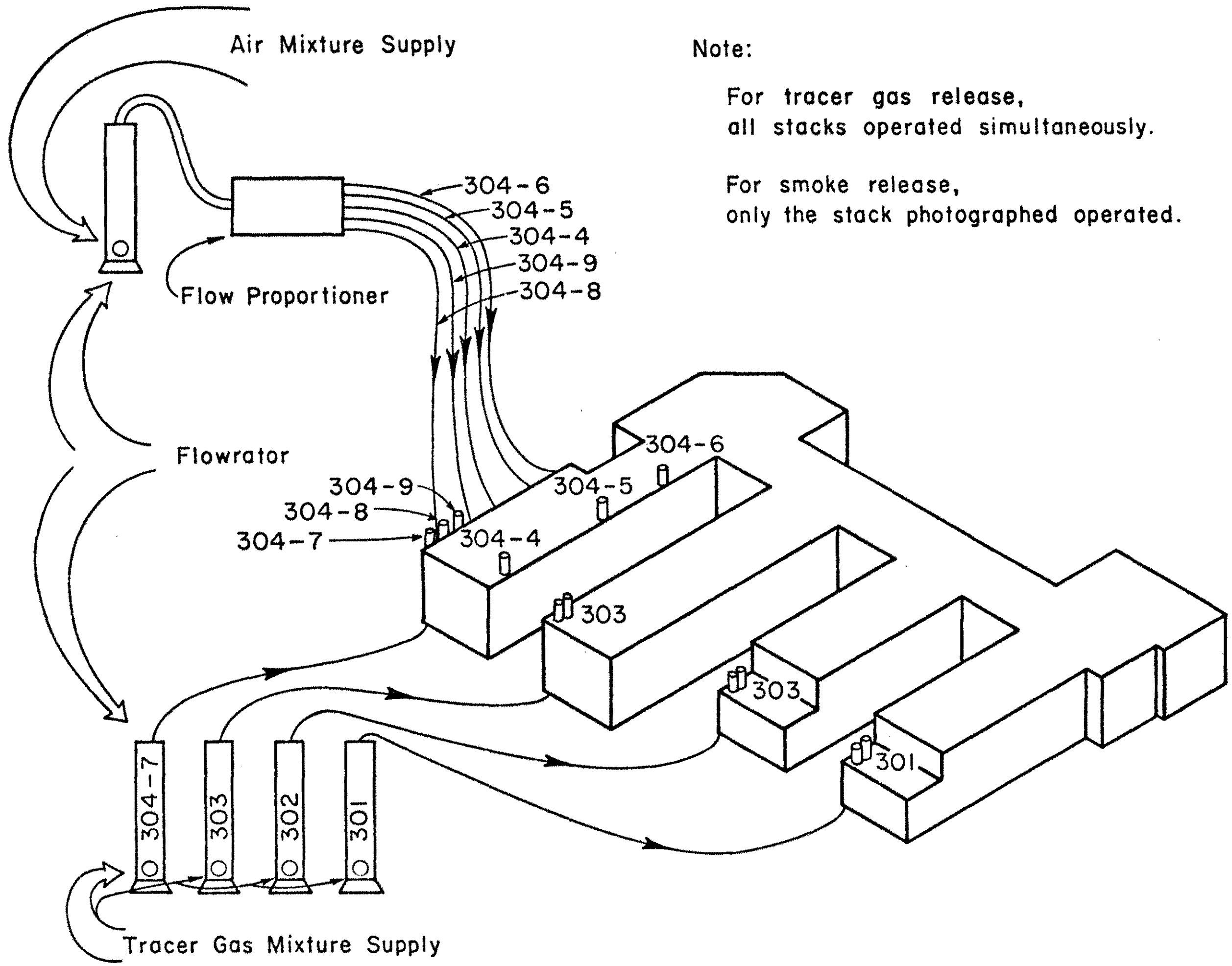

Figure 3.2-3. Schematic showing the flow system for tracer gas and smoke release.

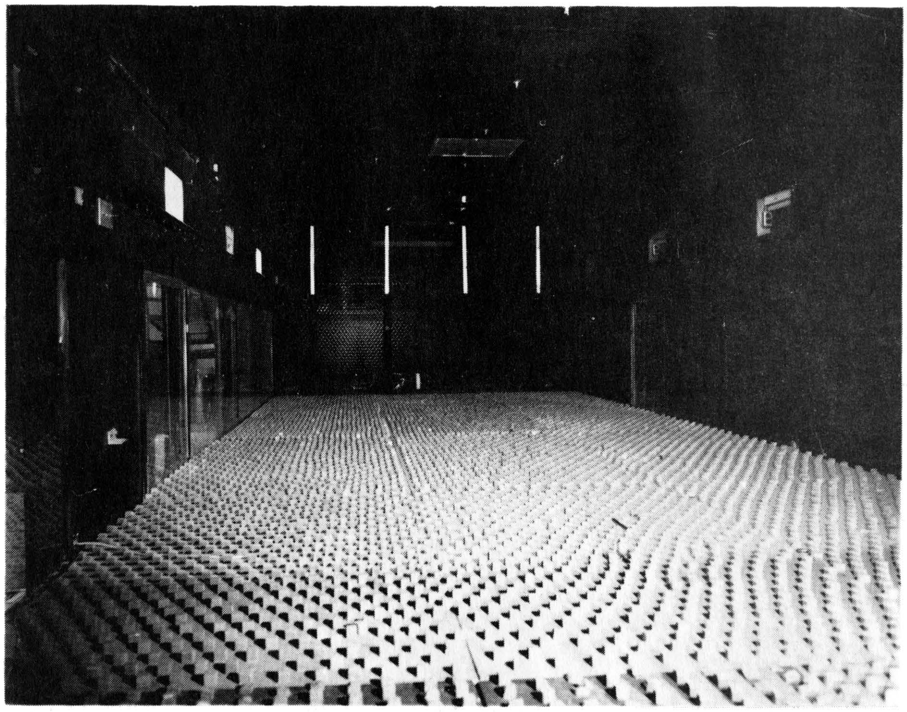

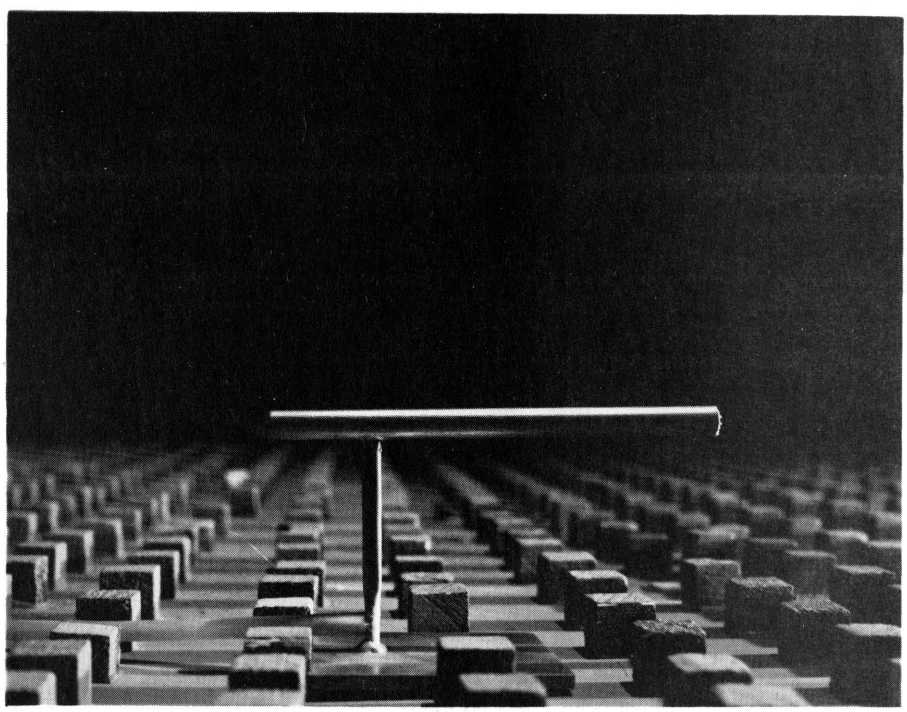

Figure 3.2-4. Photographs of a) the wind-tunnel setup, and b) release probe for ADCT.

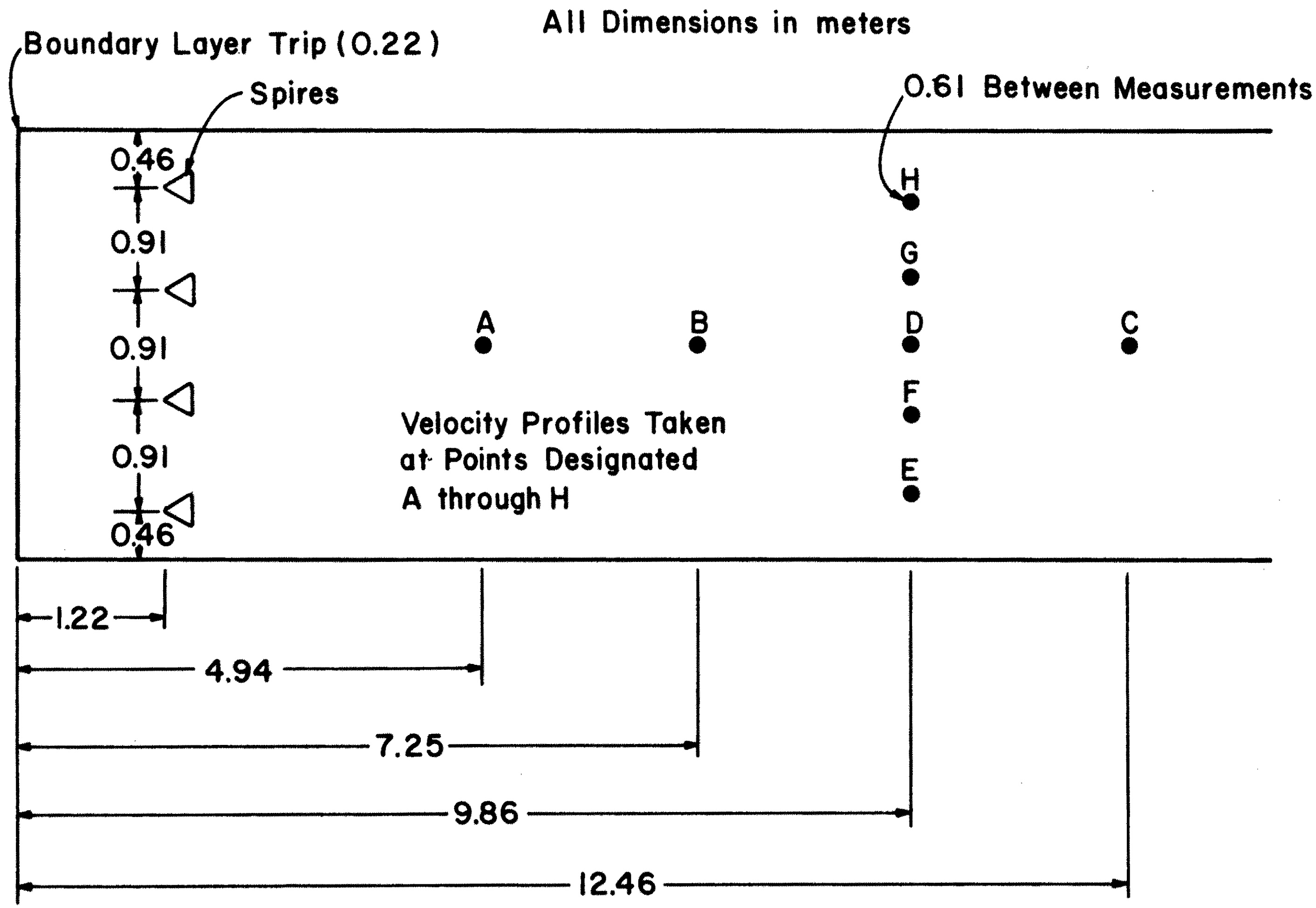

Figure 3.2-5. Wind-tunnel setup for atmospheric dispersion comparability tests and velocity profile location key.

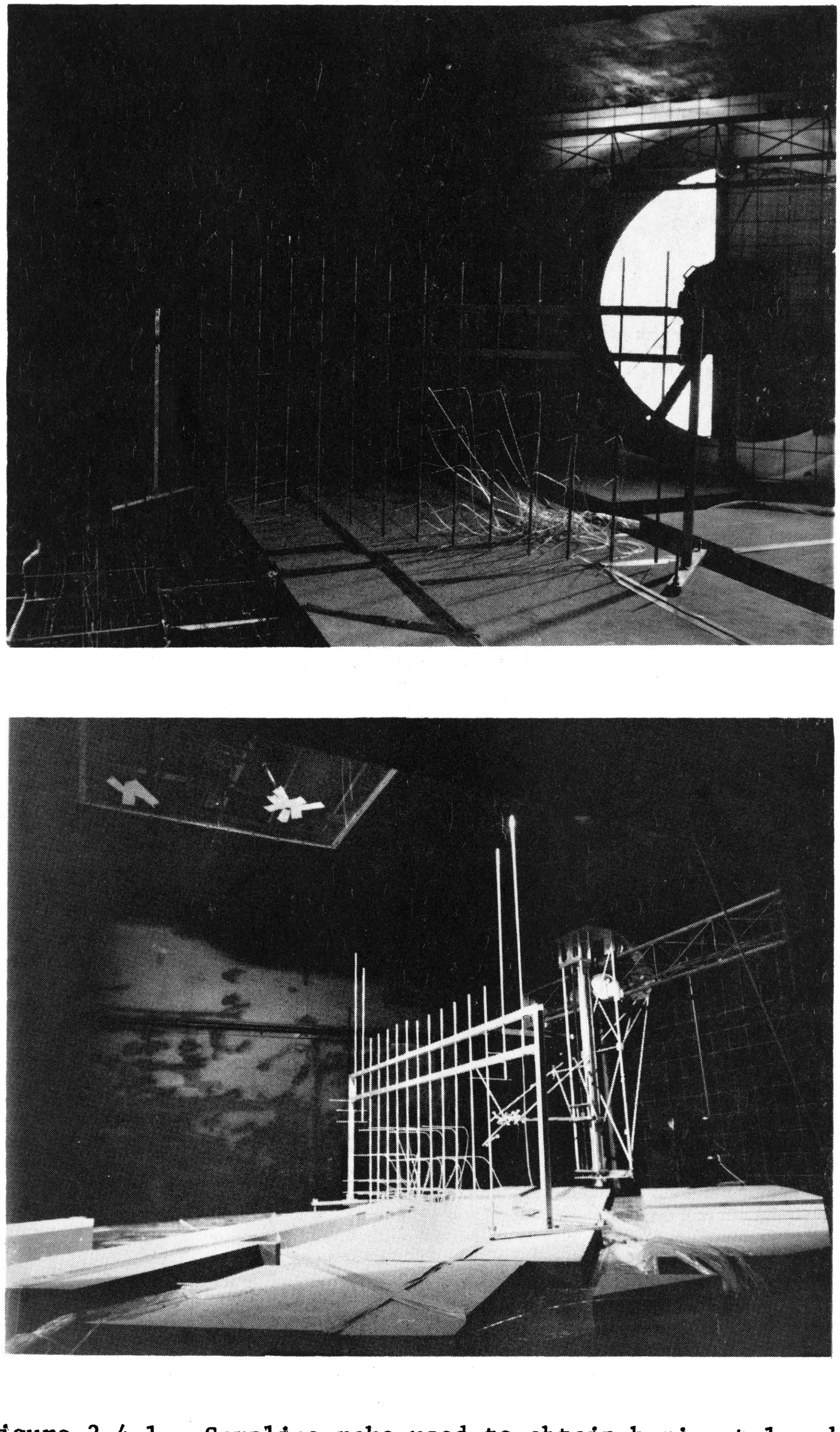

a

b

Figure 3.4-1. Sampling rake used to obtain horizontal and vertical concentration distributions for the Routine Concentration Measurement Tests.

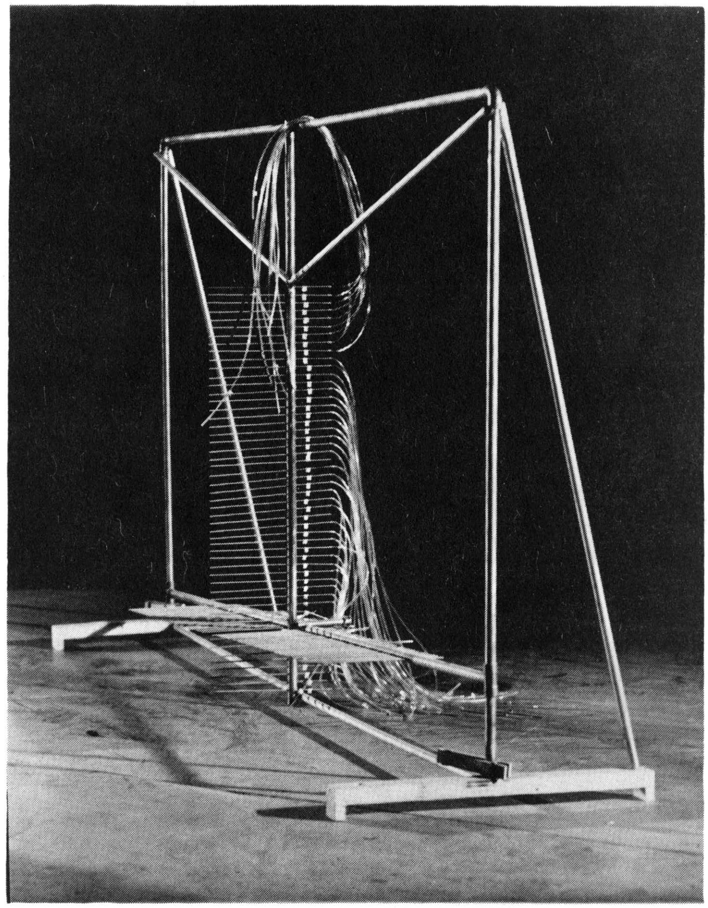

Figure 3.4-2. Sampling rake used for the ADCT tests.

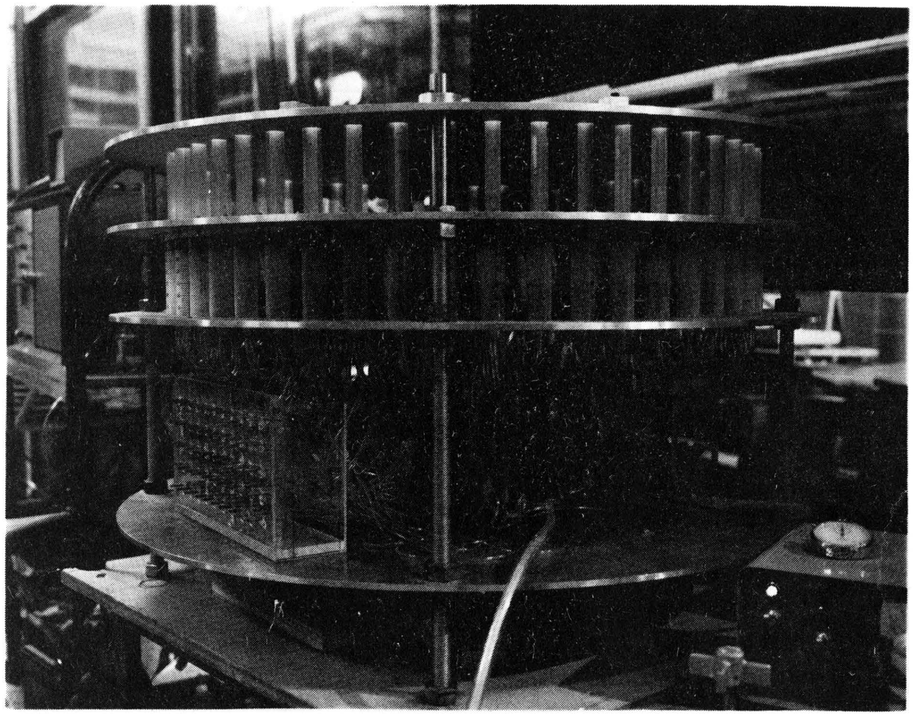

a

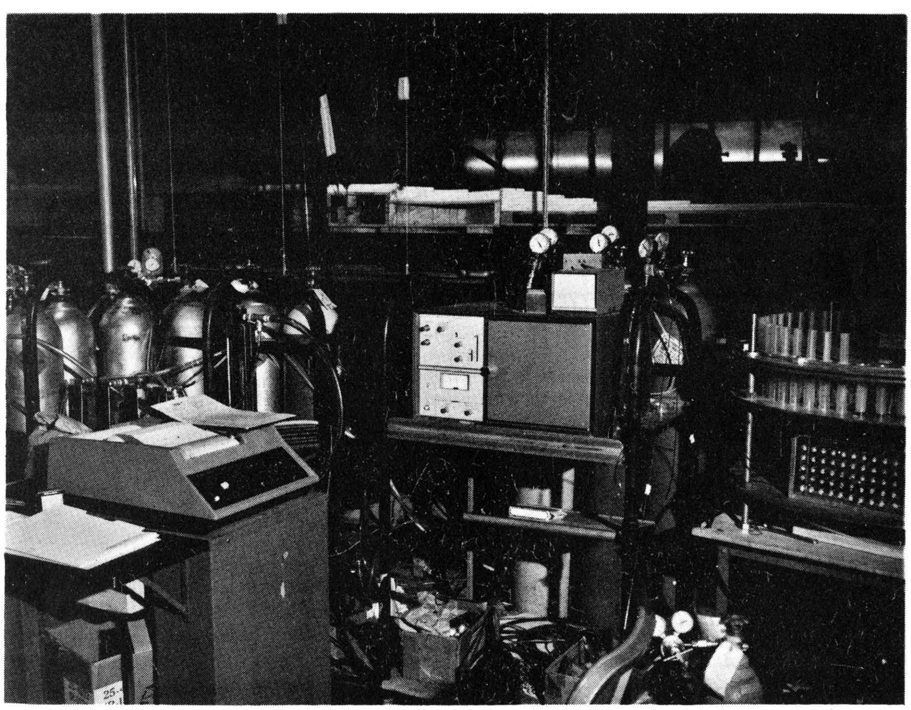

b

Figure 3.4-3. Photographs of a) the gas sampling system, and b) the HP gas chromatograph and integrator.

RUN #

Wind Direction		Calibration 1) Integrated Value 2) Standard Concentration 3) Range	
Exit Velocity - Model--301 (m/s)			
Exit Velocity - Prototype--301 (m/s)		DATE	
		TIME	
		DATA TAKER	
Configuration		RECORDER	
		Remarks:	
Velocity Ratio for 301			

Building #					
Source Strength (%)					
Bottle #					
Tracer					
Background					
Ambient Pressure					
Ambient Temperature					
Flow Rator Back Pressure					

SAMPLE #	GRID #	RANGE					
1							
2							
3							
4							
5							
6							
7							
8							
9							
10							
11							
12							
13							
14							
15							
16							
17							
18							
19							
20							
21							
22							
23							
24							
25							
26							
27							
28							
29							
30							
31							
32							
33							
34							
35							
36							
37							
38							
39							
40							
41							
42							
43							
44							
45							
46							
47							
48							
49							
50							

Figure 3.4-4. Data tabulation form.

Card #	Columns on card	Format	Description of Information
1	1-3	I3	Number (N) of samples for file
2	1-3	I3	Run number
through	4-6	I3	Wind direction
N	7-11	F5.1	Exit velocity (uncalibrated)
	12	A1	Building configuration (P-present; F-future)
	13-18	F6.4	Velocity ratio (uncalibrated)
	19	A1	Sampling configuration (N-near rake; F-far rake; B-building, P-prototype)
	20	A1	Sample designation (G-ground level; - for other)
	21-22	I2	Sample number
	23-28	I6	x - coordinate of sample
	29-35	I7	y - coordinate of sample
	36-45	E10.5	χ/χ_o for building 301
	46-55	E10.5	χ/χ_o for building 302
	56-65	E10.5	χ/χ_o for building 303
	66-75	E10.5	χ/χ_o for building 304

Figure 3.4-5. Format for concentration data tabulation.

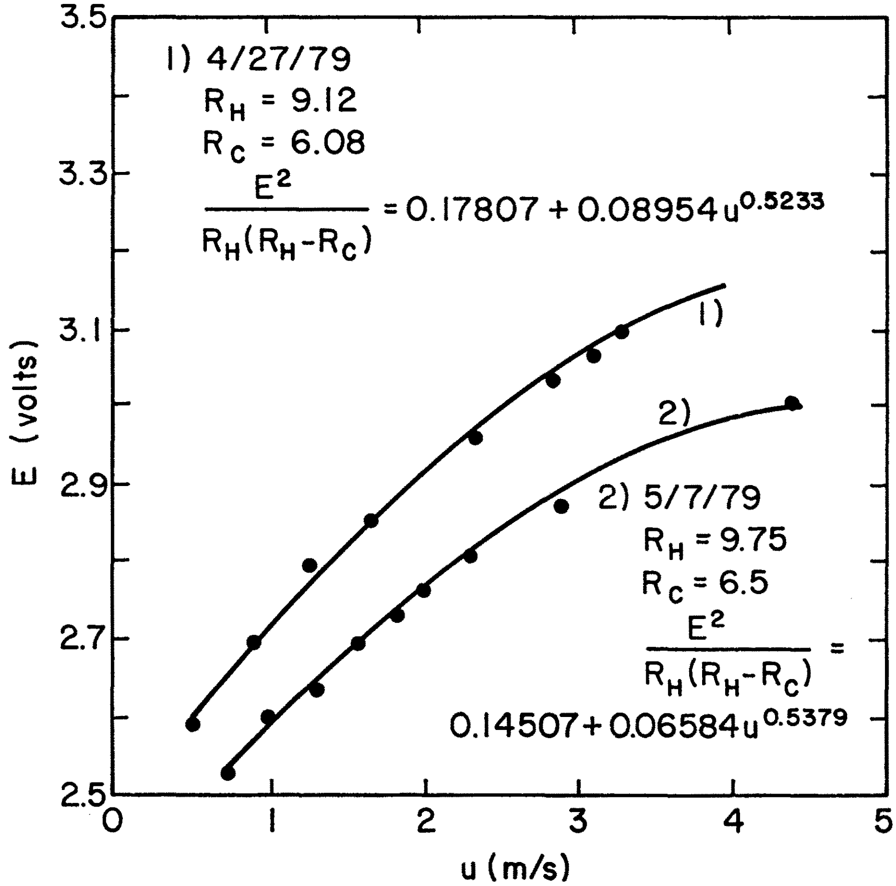

Figure 3.5-1. Typical hot-film calibration curves.

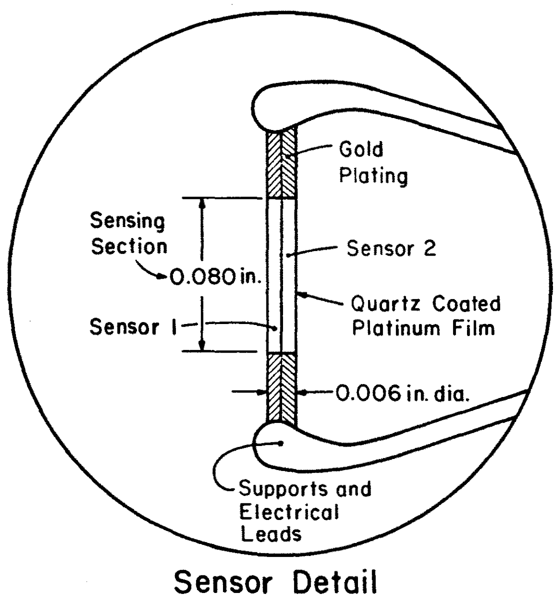

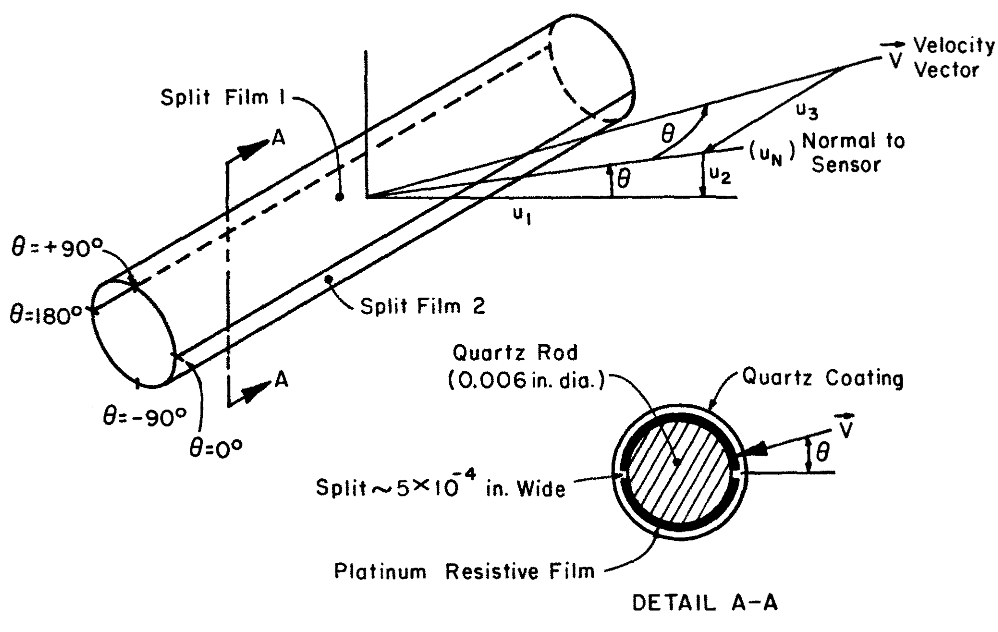

Figure 3.6-1. Description of split film sensor.

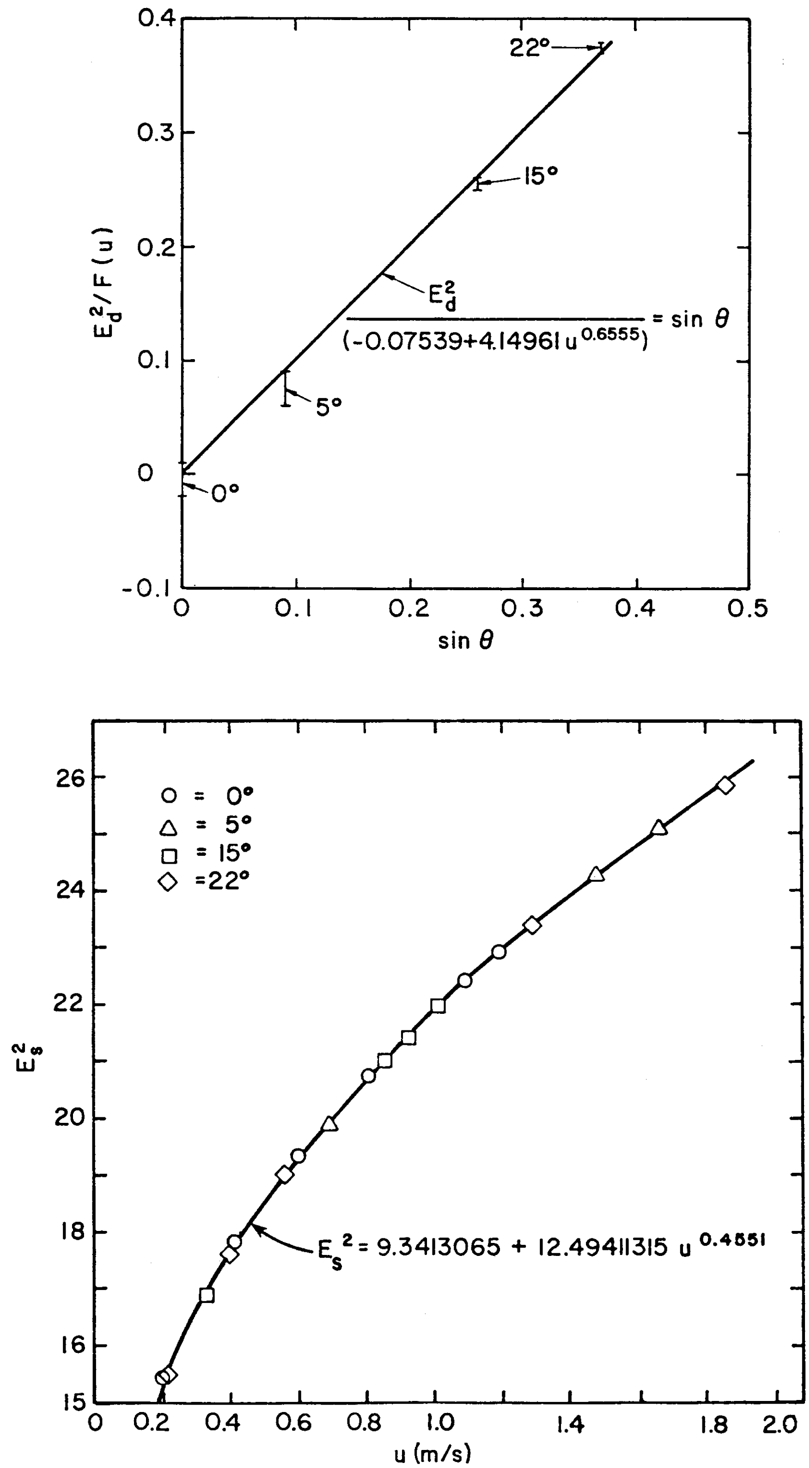

Figure 3.6-2. Calibration curve of a) $\frac{E_d^{\ 2}}{F(u)}$ versus $\sin\theta$, and b) $E_s^{\ 2}$ versus u for split-film velocity profile measurements.

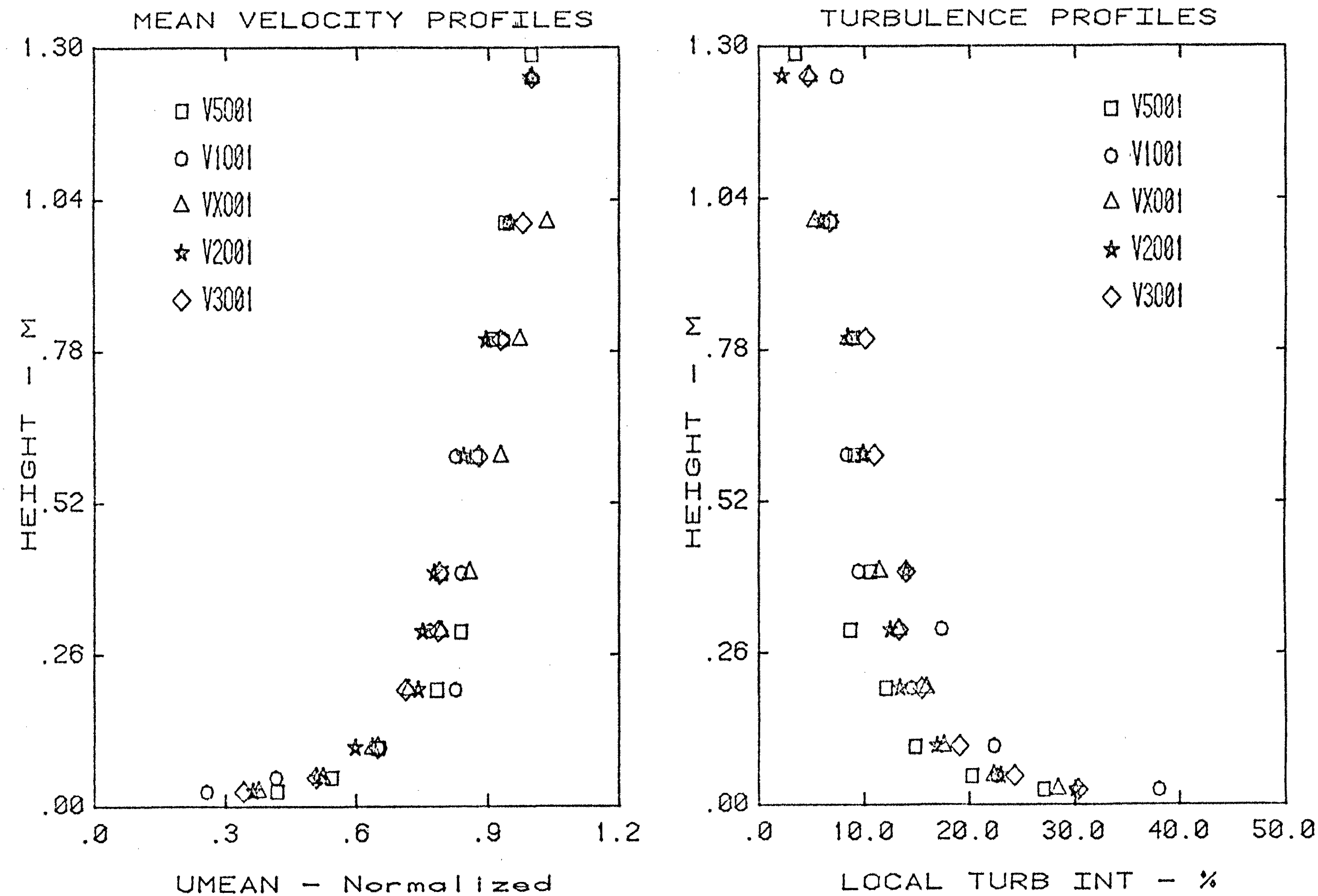

Figure 4.1-1. Mean velocity and turbulence intensity profiles for velocities of 1 (○), 1.5 (△), 2 (☆), 3 (□) and 5 (◇) m/s taken at location D.

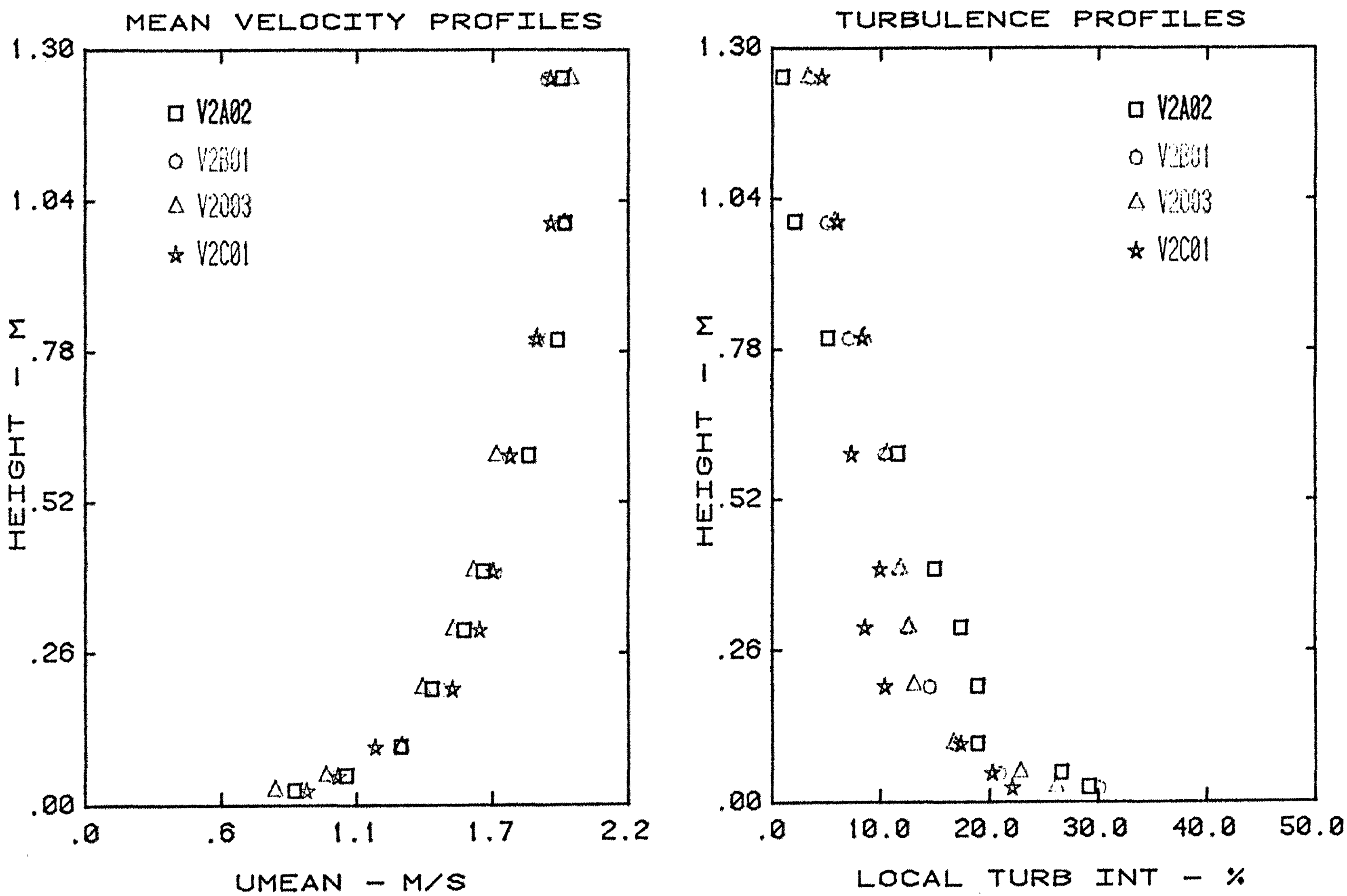

Figure 4.1-2. Mean velocity and turbulence intensity profiles down the center of the tunnel at locations A (□), B (○), C (☆) and D (△) for $\bar{u}_\infty$ = 2 m/s.

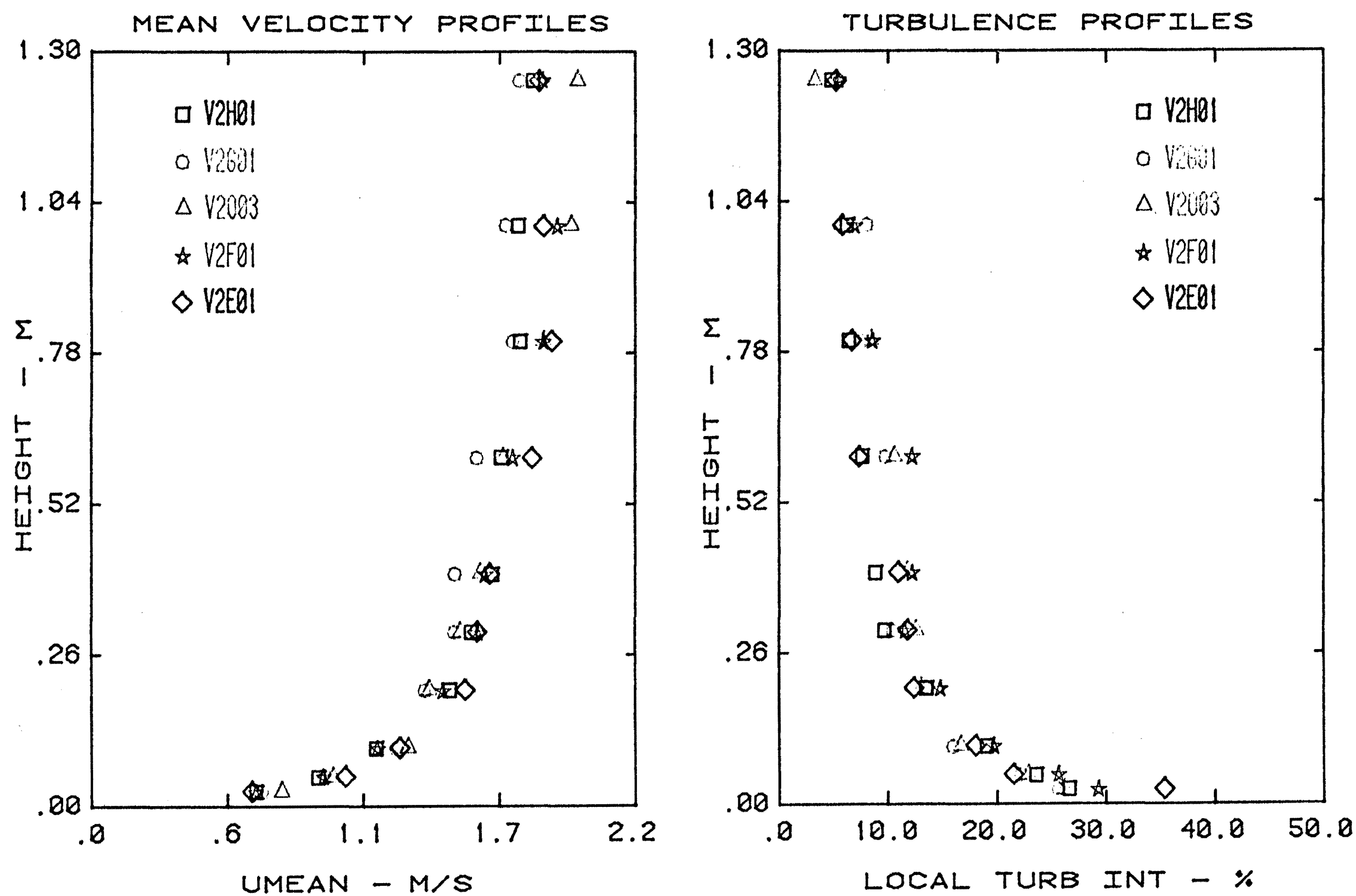

Figure 4.1-3. Mean velocity and turbulence intensity profiles lateral to the tunnel at locations H (□), G (○), D (△), F (★) and E (◇) for $\bar{u}_\infty = 2$ m/s.

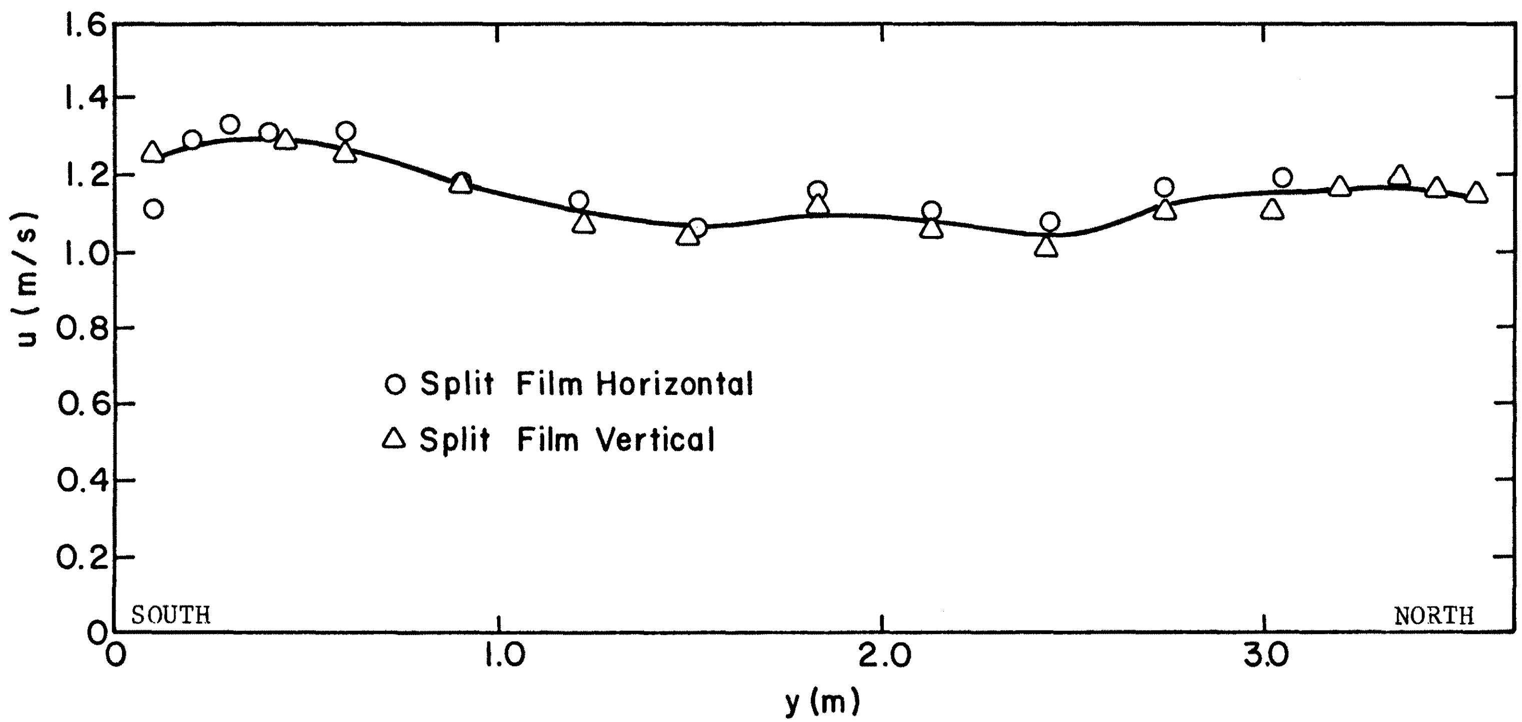

Figure 4.1-4. Split film velocity profile across tunnel at z = 10 cm for $\overline{u}_{\infty}$ = 1.94 m/s.

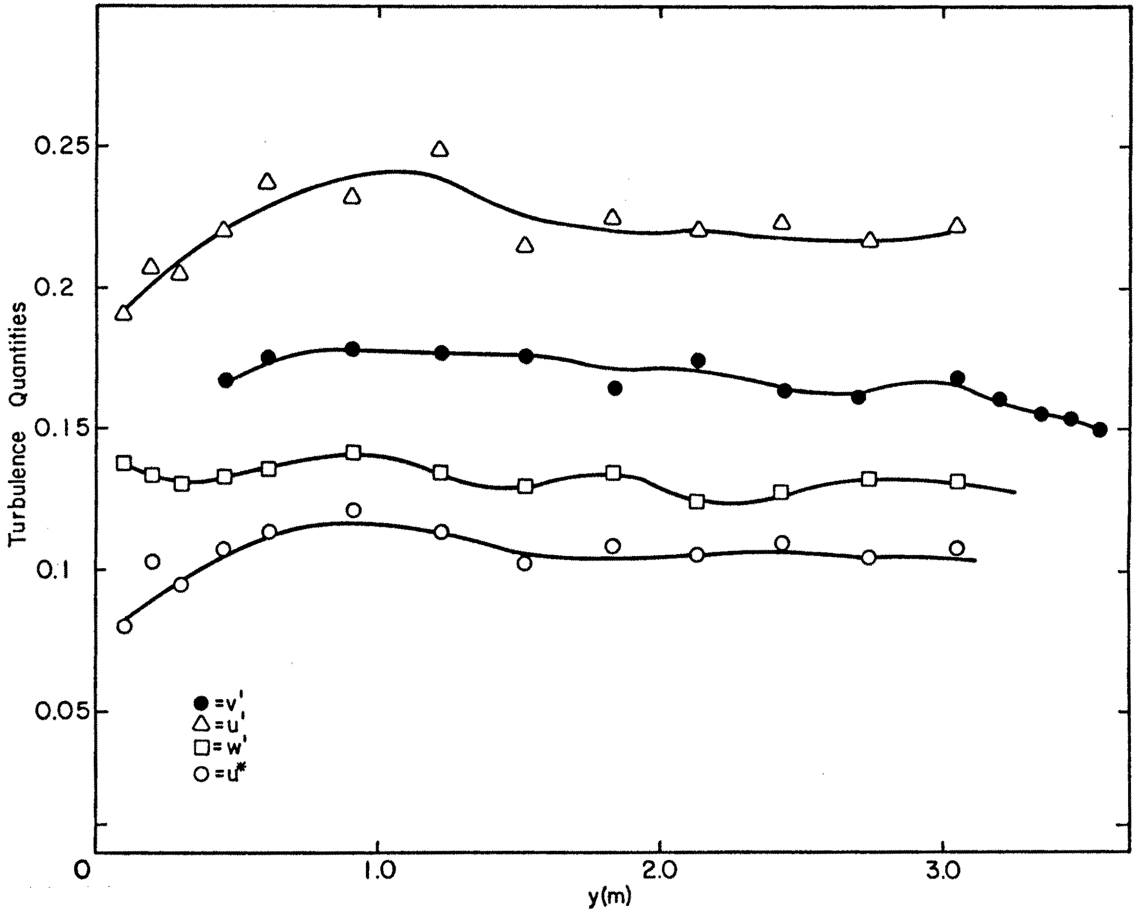

Figure 4.1-5. Split film profile across tunnel of u', v', w' and u* at z = 10 cm for $\overline{u}_{\infty}$ = 1.94 m/s.

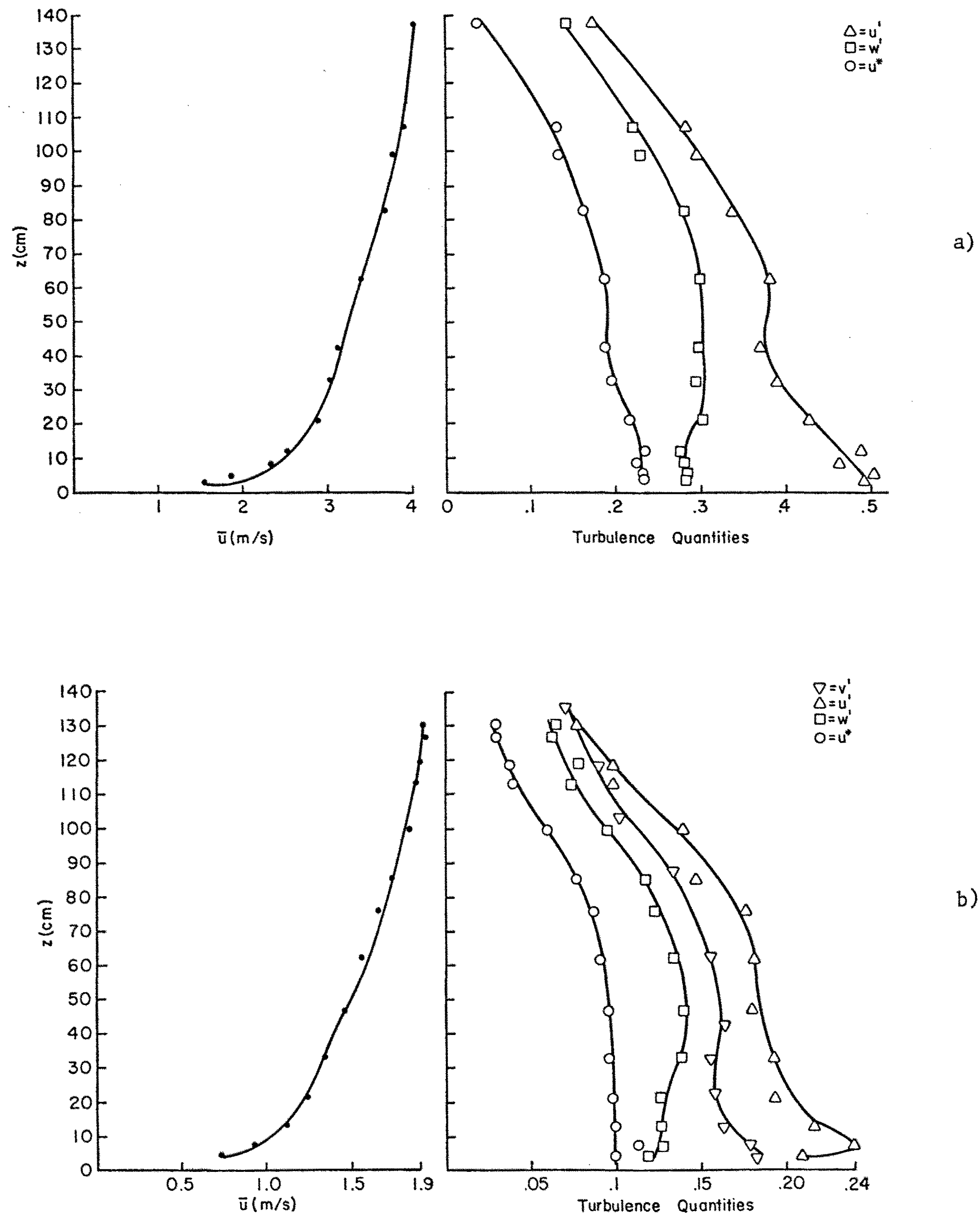

Figure 4.1-6. Split film mean velocity and turbulence quantities profiles for a) $\bar{u}_\infty$ = 4 m/s and b) $\bar{u}_\infty$ = 1.94 m/s.

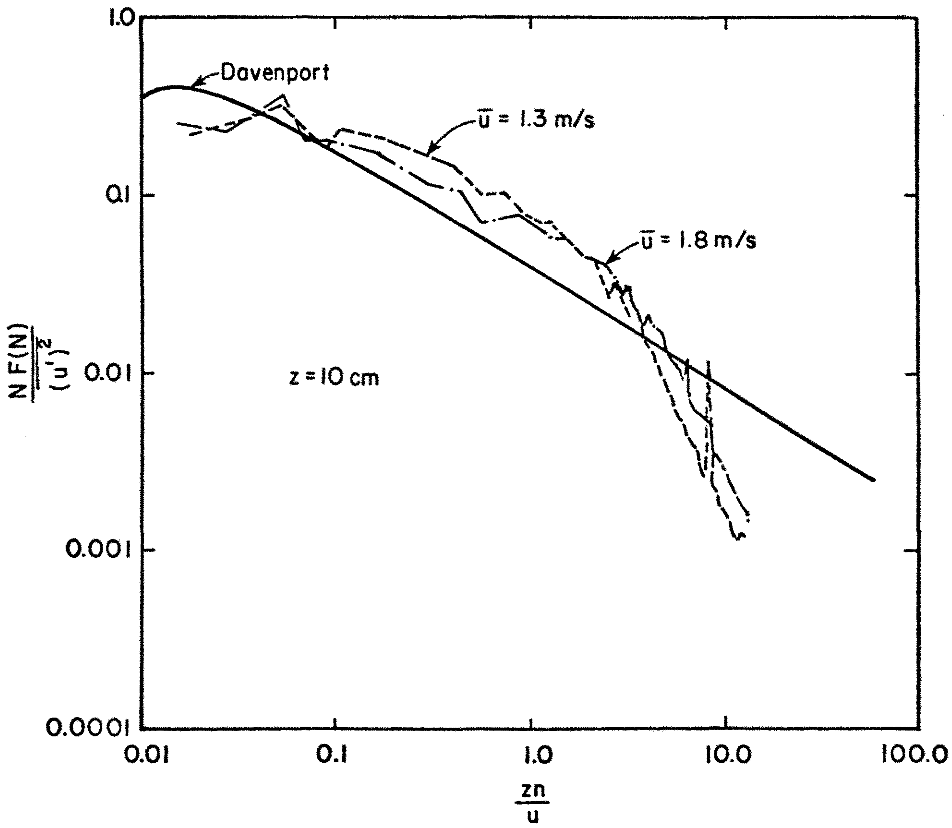

Figure 4.1-7. Wind-tunnel and Davenport velocity spectra at 10 cm for free stream velocities of 2 and 3 m/s.

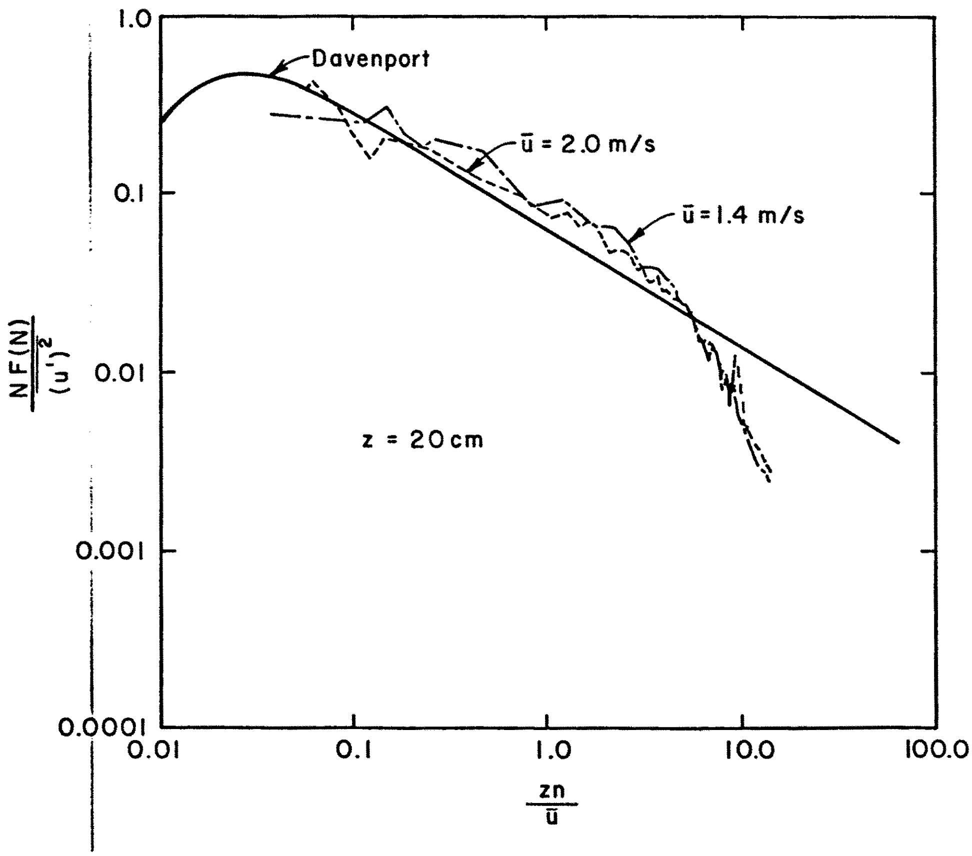

Figure 4.1-8. Wind-tunnel and Davenport velocity spectra at 2.0 cm for free stream velocities of 2 and 3 m/s.

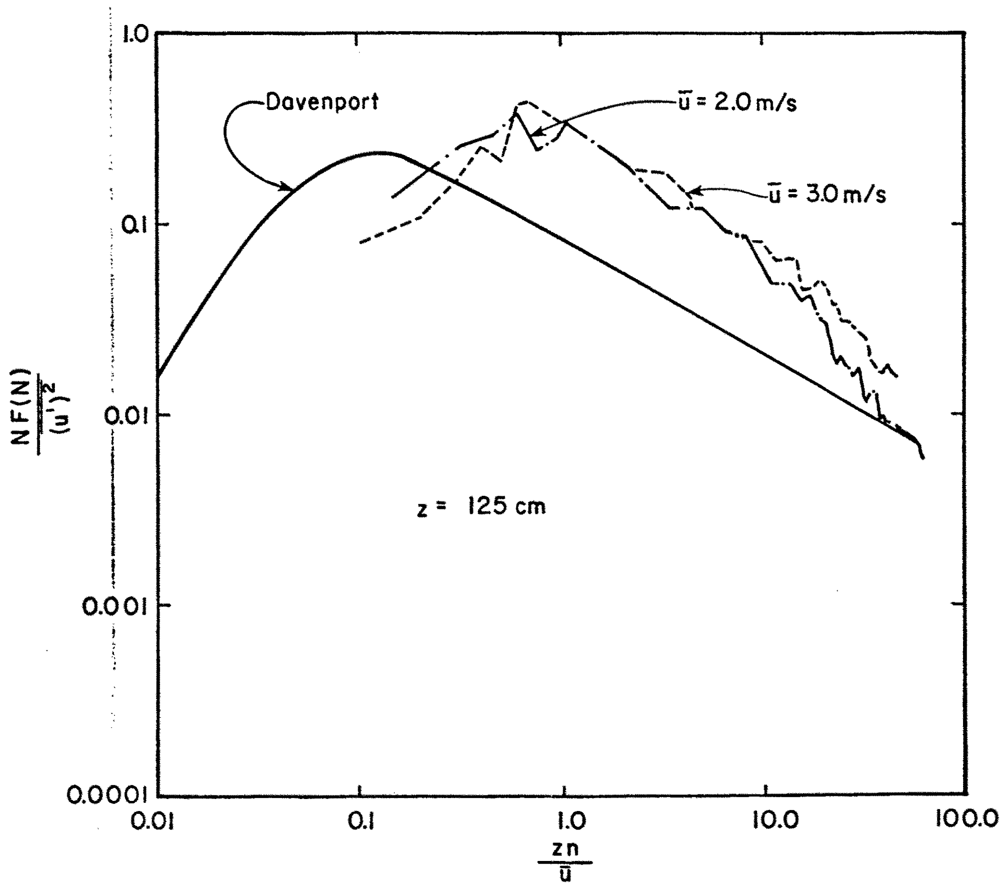

Figure 4.1-9. Wind-tunnel and Davenport velocity spectra at 125 cm for free stream velocities of 2 and 3 m/s.

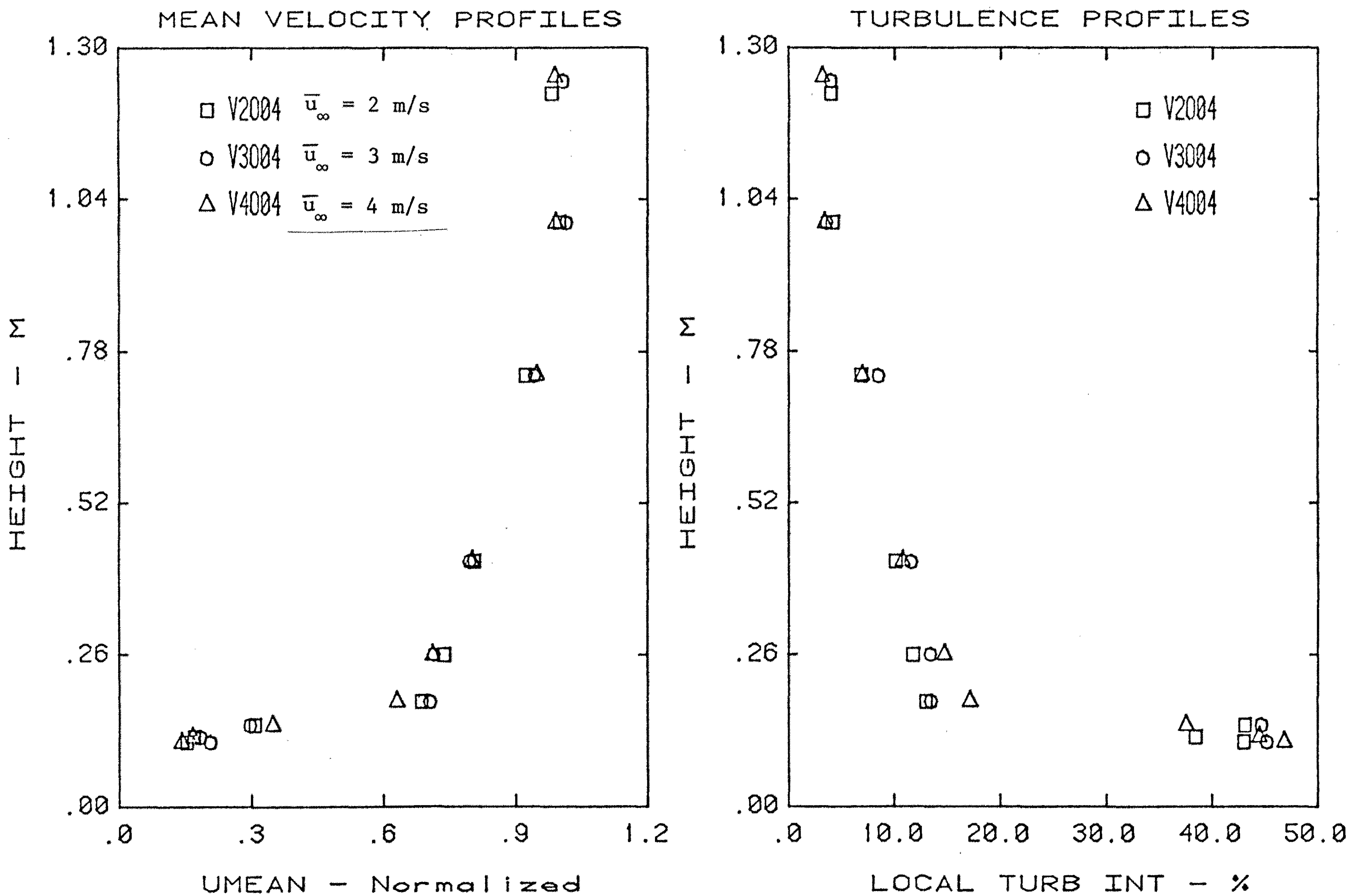

Figure 4.2-1. Mean velocity and turbulence intensity profiles for the SW - Phase I wind direction at location 0 and free stream velocities of 2, 3 and 4 m/s.

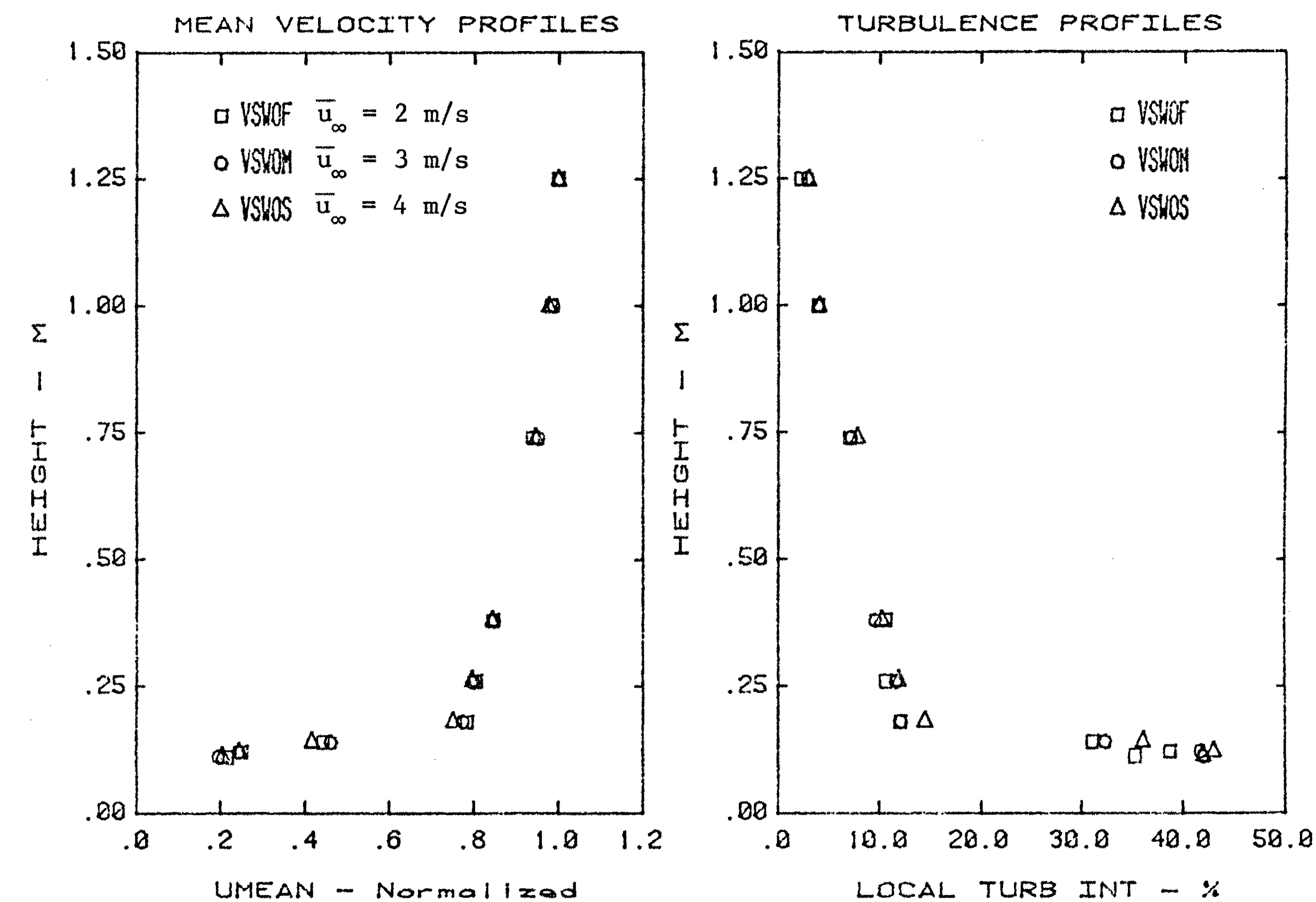

Figure 4.2-2. Mean velocity and turbulence intensity profiles for the SW - Phase II wind direction at location 0 and free stream velocities of 2, 3 and 4 m/s.

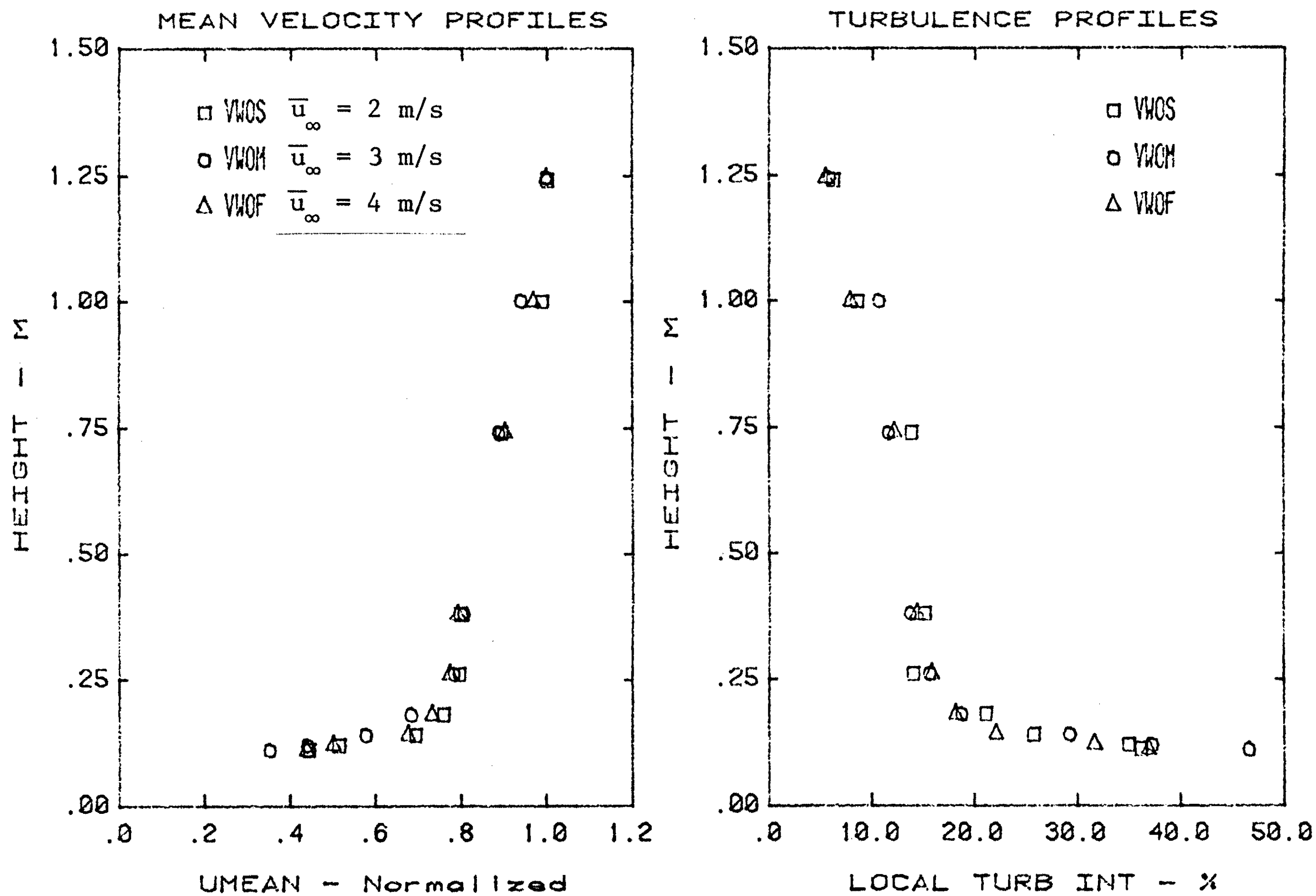

Figure 4.2-3. Mean velocity and turbulence intensity profiles for the west wind direction at location 0 and free stream velocities of 2, 3 and 4 m/s.

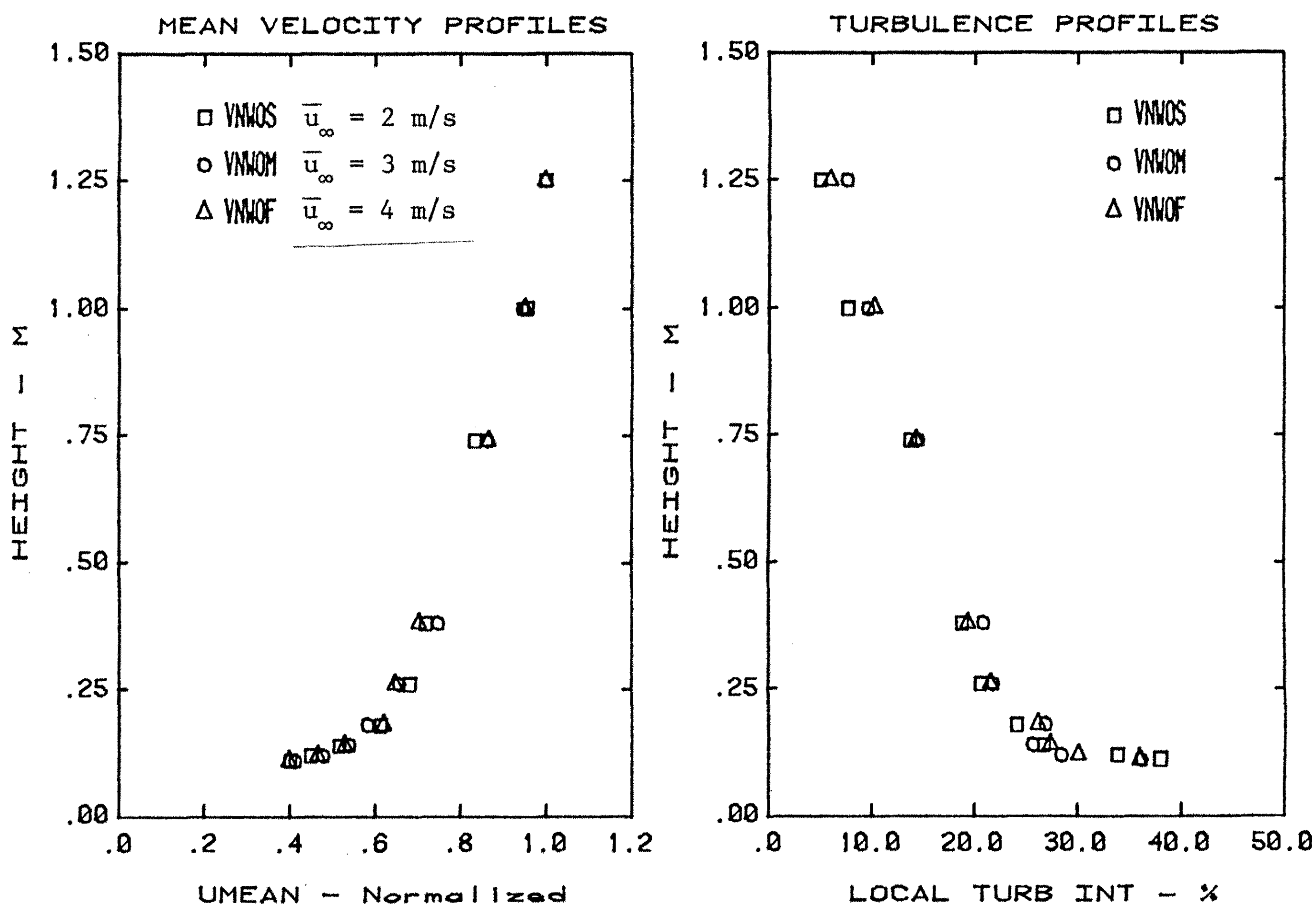

Figure 4.2-4. Mean velocity and turbulence intensity profiles for the northwest wind direction at location 0 and free stream velocities of 2, 3 and 4 m/s.

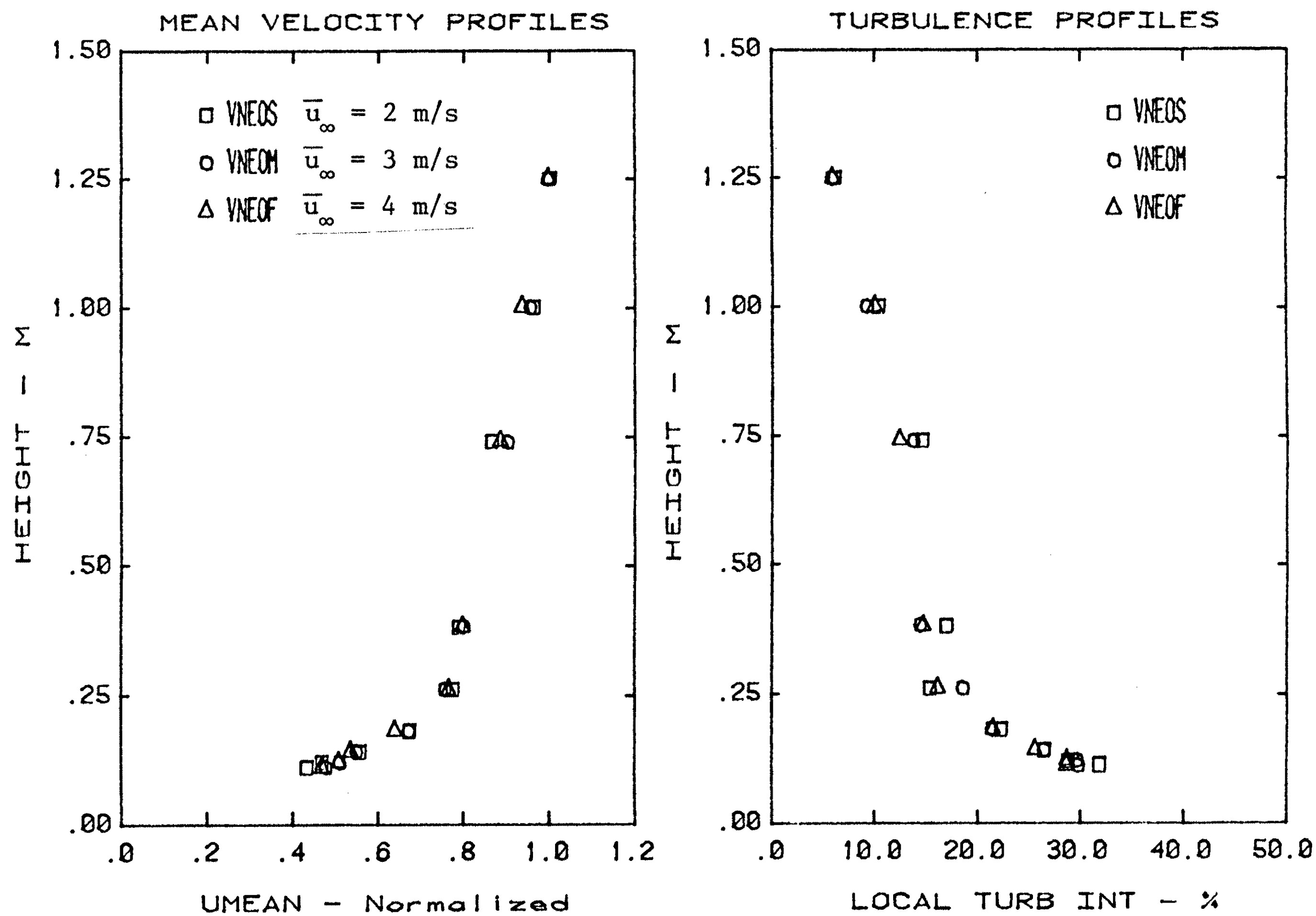

Figure 4.2-5. Mean velocity and turbulence intensity profiles for the northeast wind direction at location 0 and free stream velocities of 2, 3 and 4 m/s.

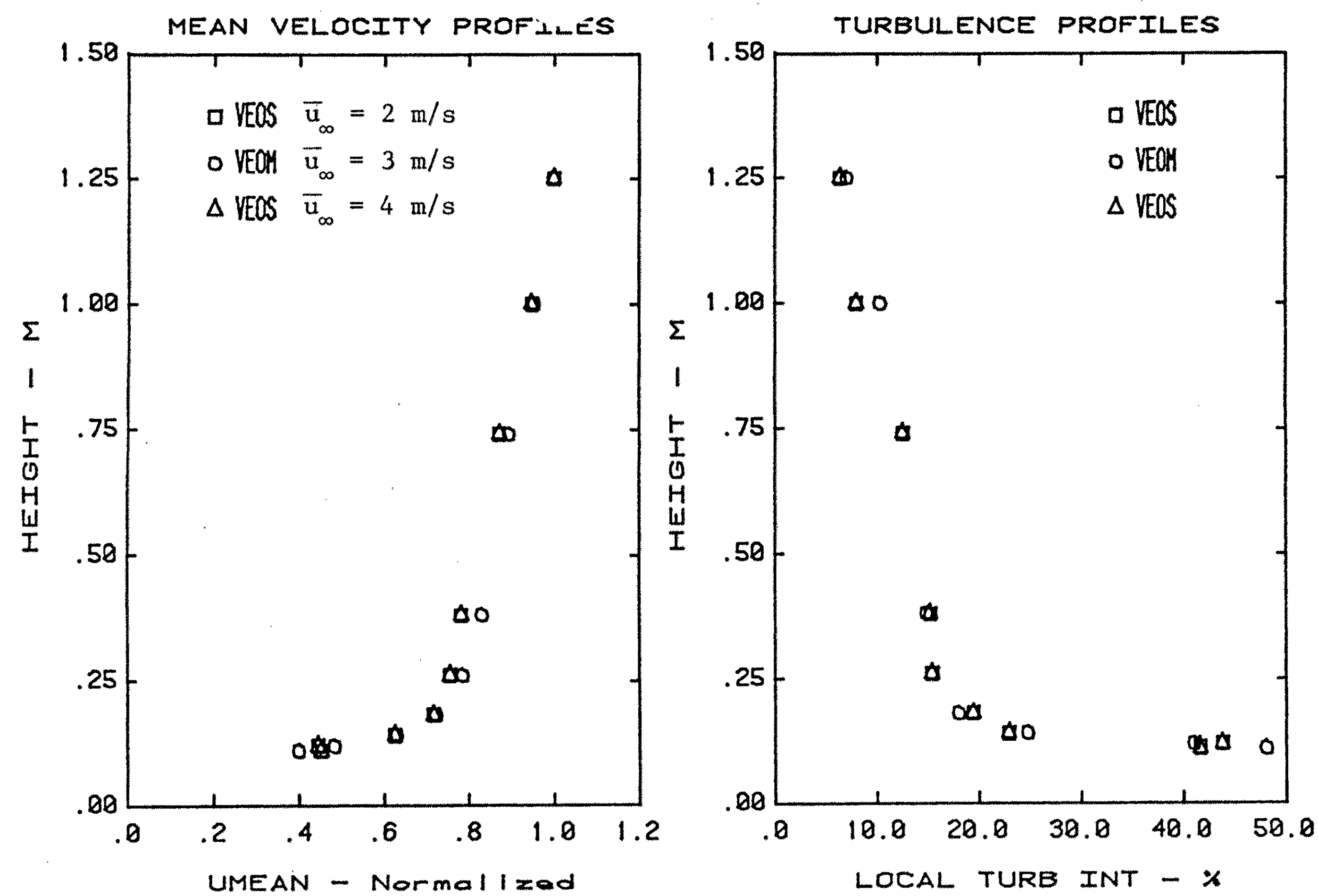

Figure 4.2-6. Mean velocity and turbulence intensity profiles for the east wind direction at location 0 and free stream velocities of 2, 3 and 4 m/s.

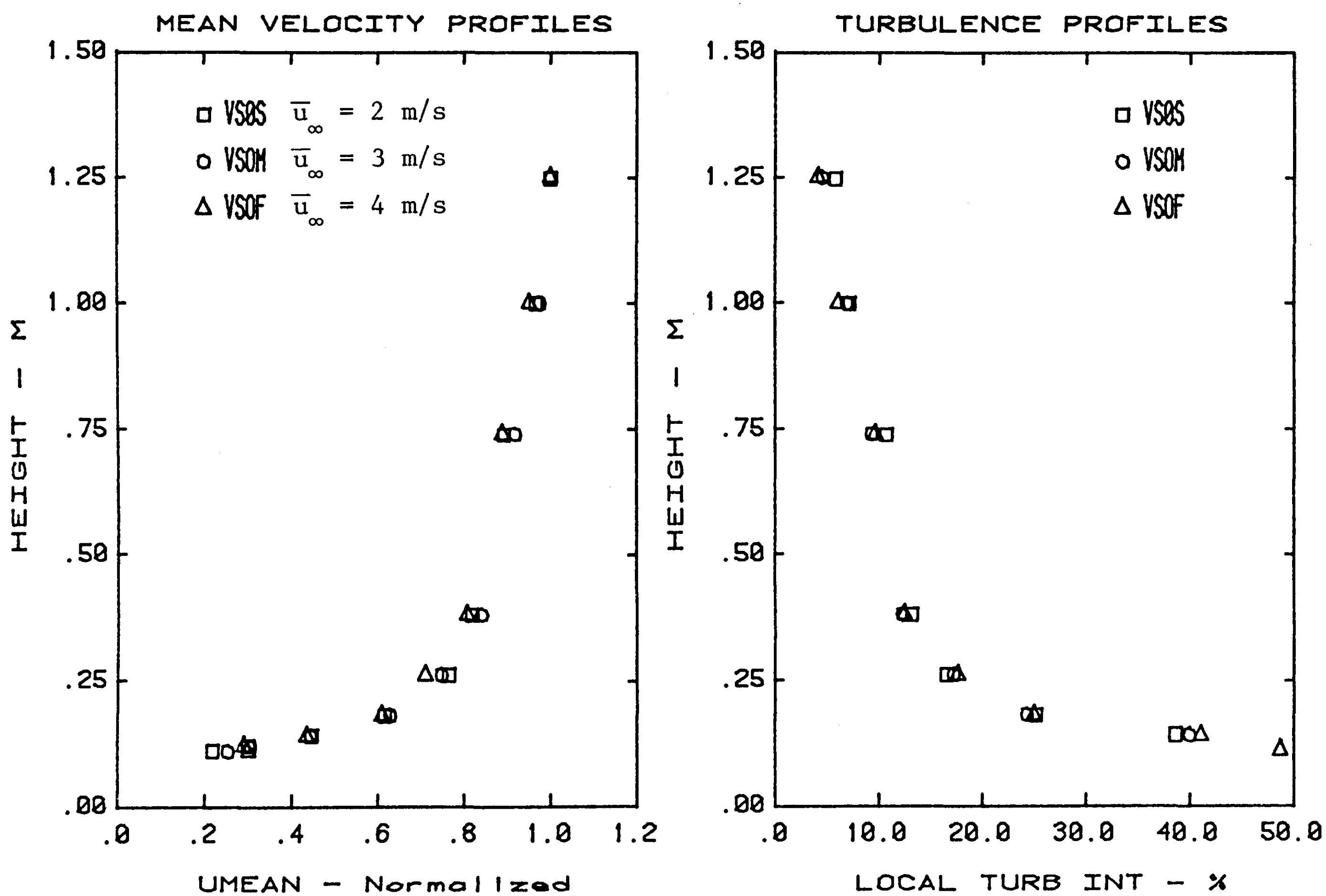

Figure 4.2-7. Mean velocity and turbulence intensity profiles for the south wind direction at location 0 and free stream velocities of 2, 3 and 4 m/s.

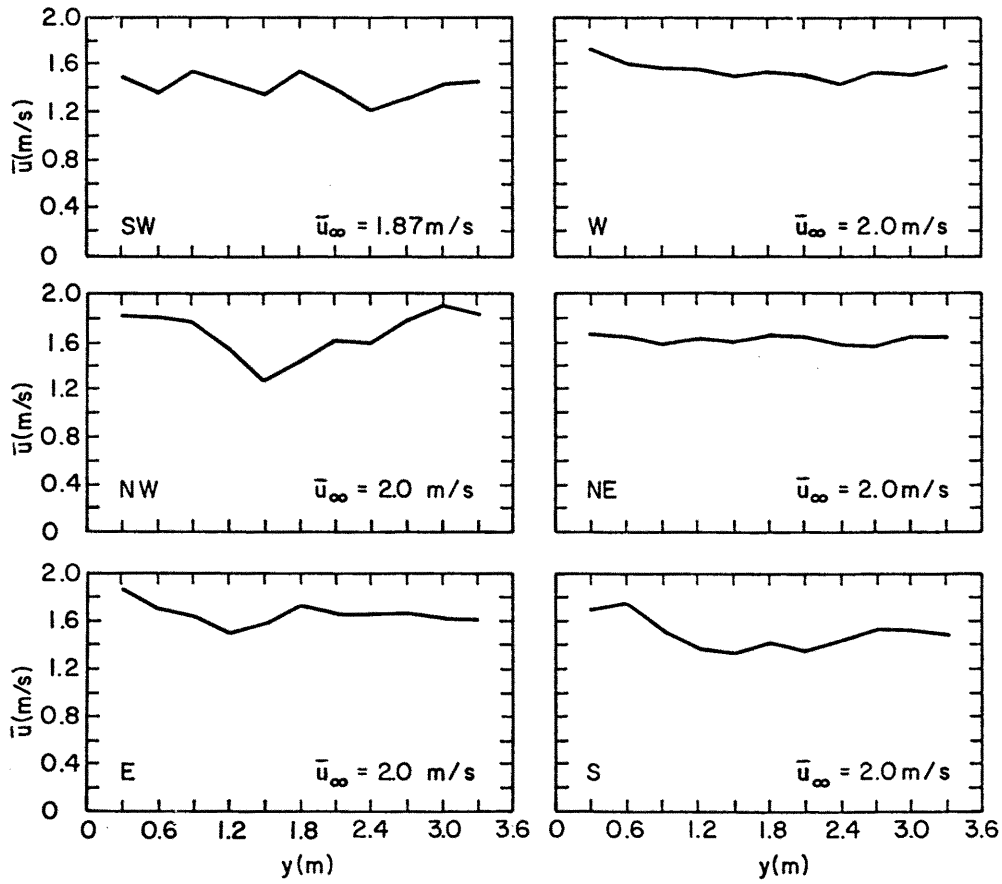

Figure 4.2-8. Lateral variation of mean velocity over point 0 at a height of 0.3 m for all wind directions (except SW - Phase I).

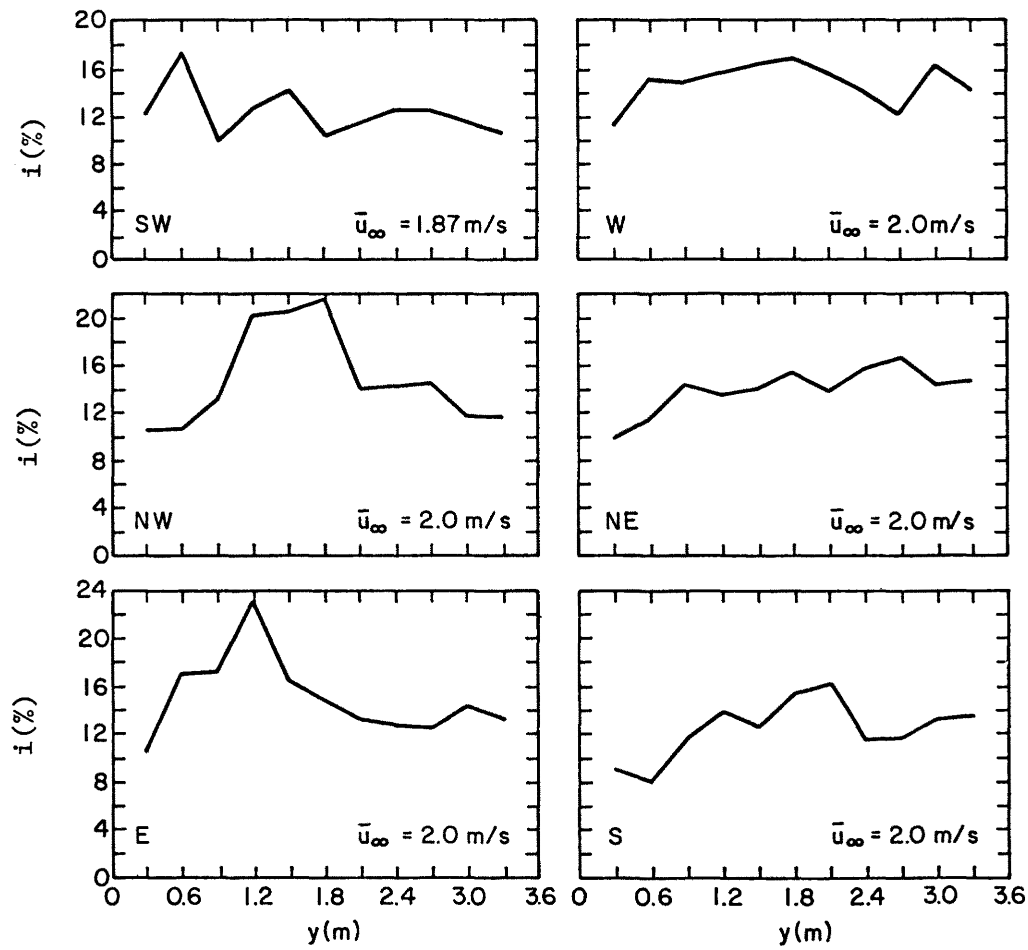

Figure 4.2-9. Lateral variation of turbulence intensity over point 0 at a height of 0.3 m for all wind directions (except SW - Phase I).

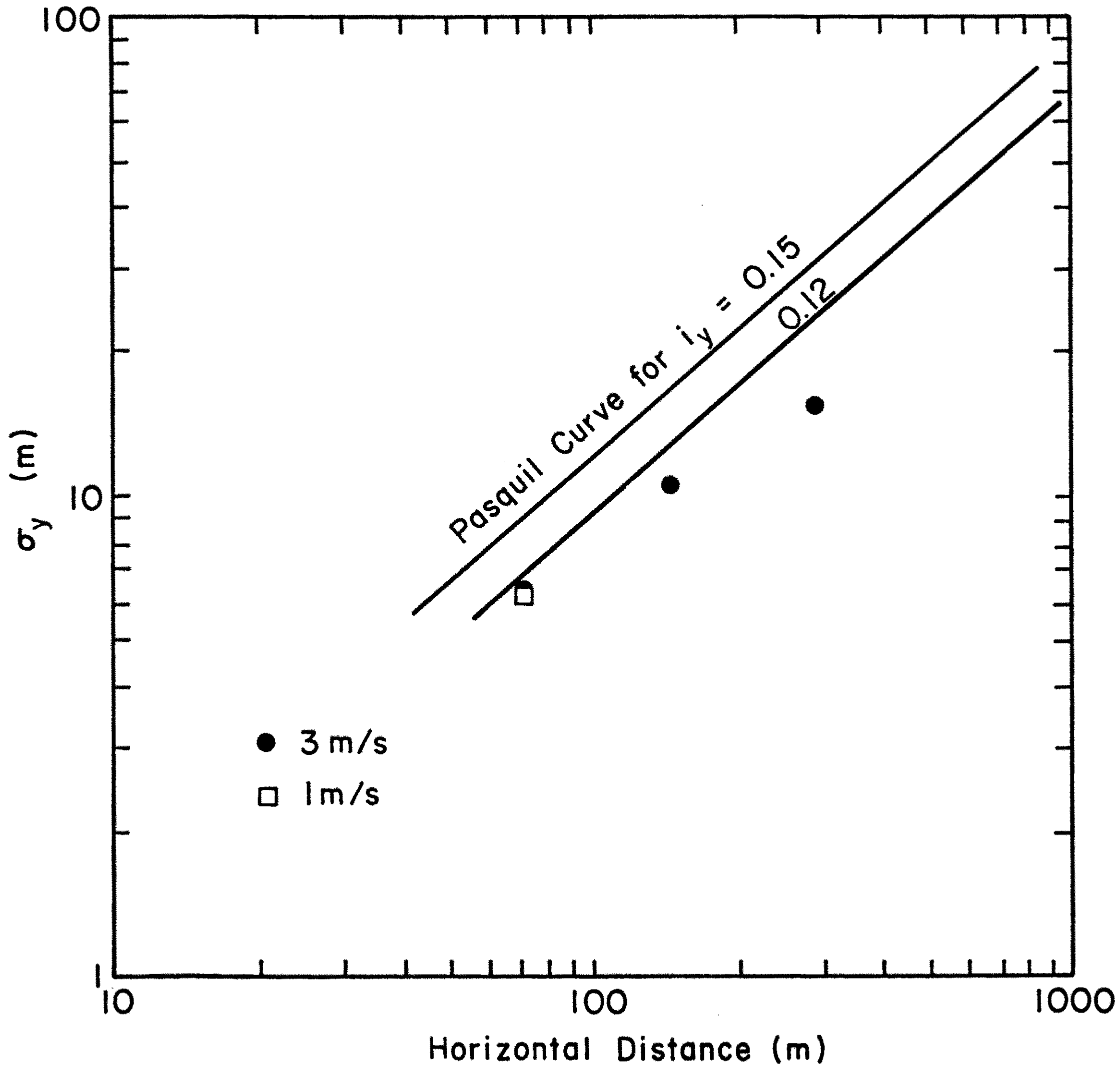

Figure 5.1-1. Comparison of σ_y values observed in the wind tunnel and those calculated using Pasquill (1976).

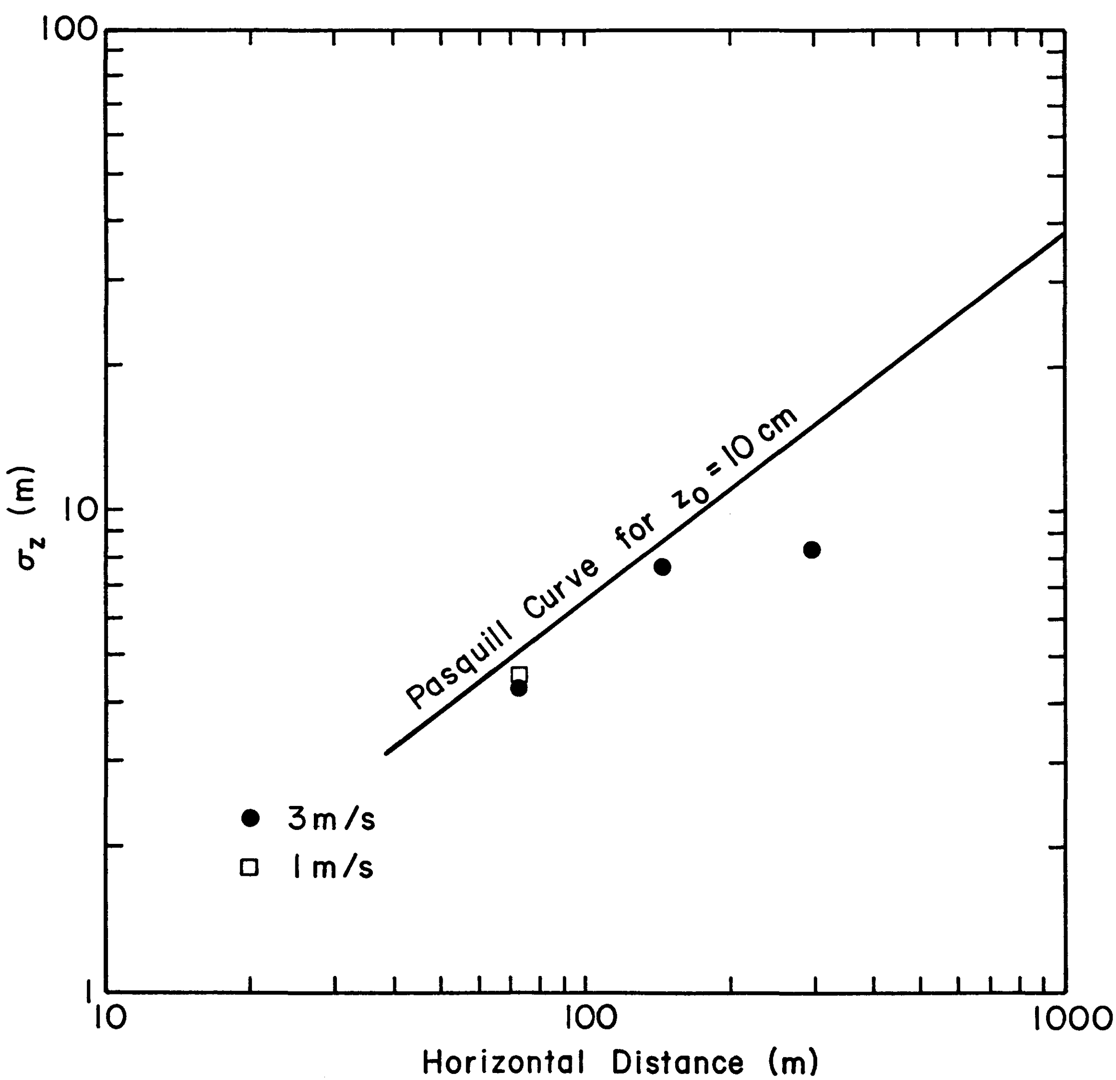

Figure 5.1-2. Comparison of σ_z values observed in the wind tunnel and those calculated using Pasquill (1976).

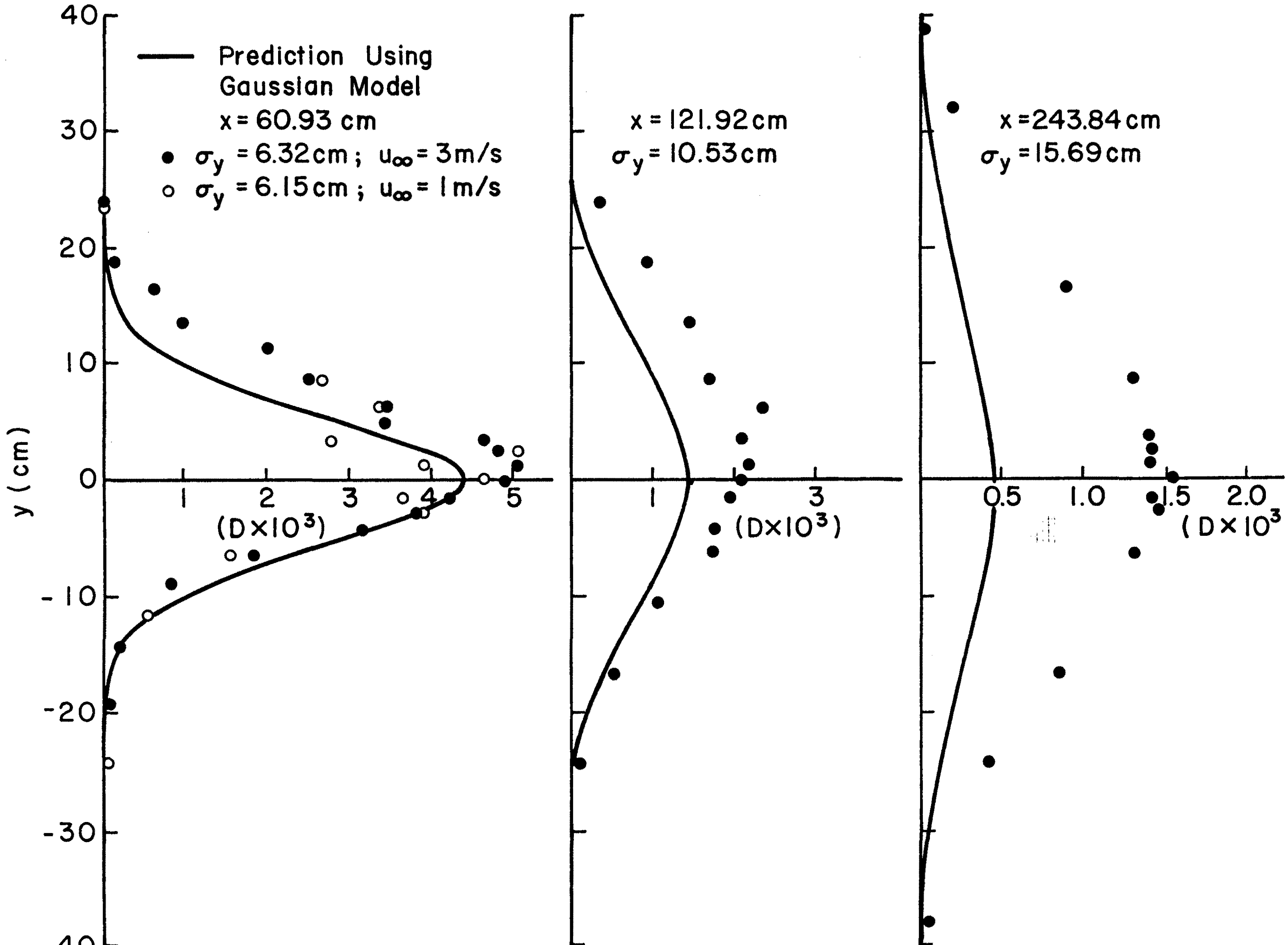

Figure 5.1-3. Horizontal concentration distributions from a 'point' source as observed in the wind tunnel and predicted using the Gaussian diffusion equations (see Tables 5.1 through 5.4 for data coordinates).

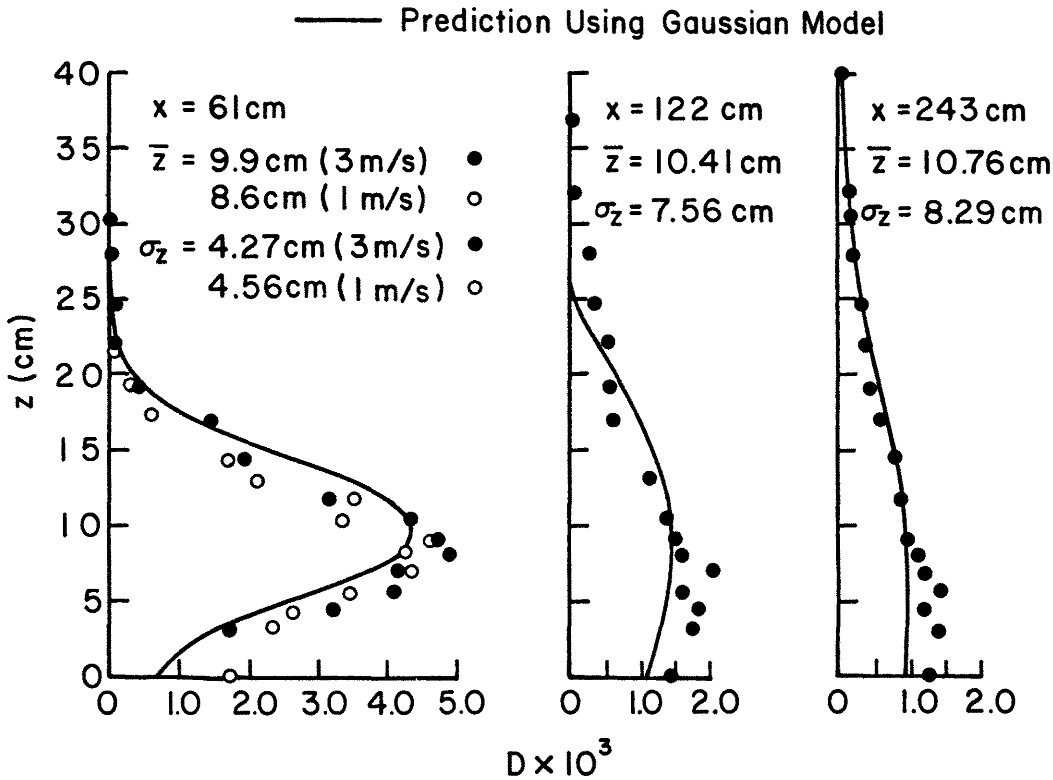

Figure 5.1-4. Vertical concentration distributions from 'point' source as observed in the wind tunnel and predicted using Gaussian diffusion equations (see Tables 5.1 through 5.4 for data coordinates).

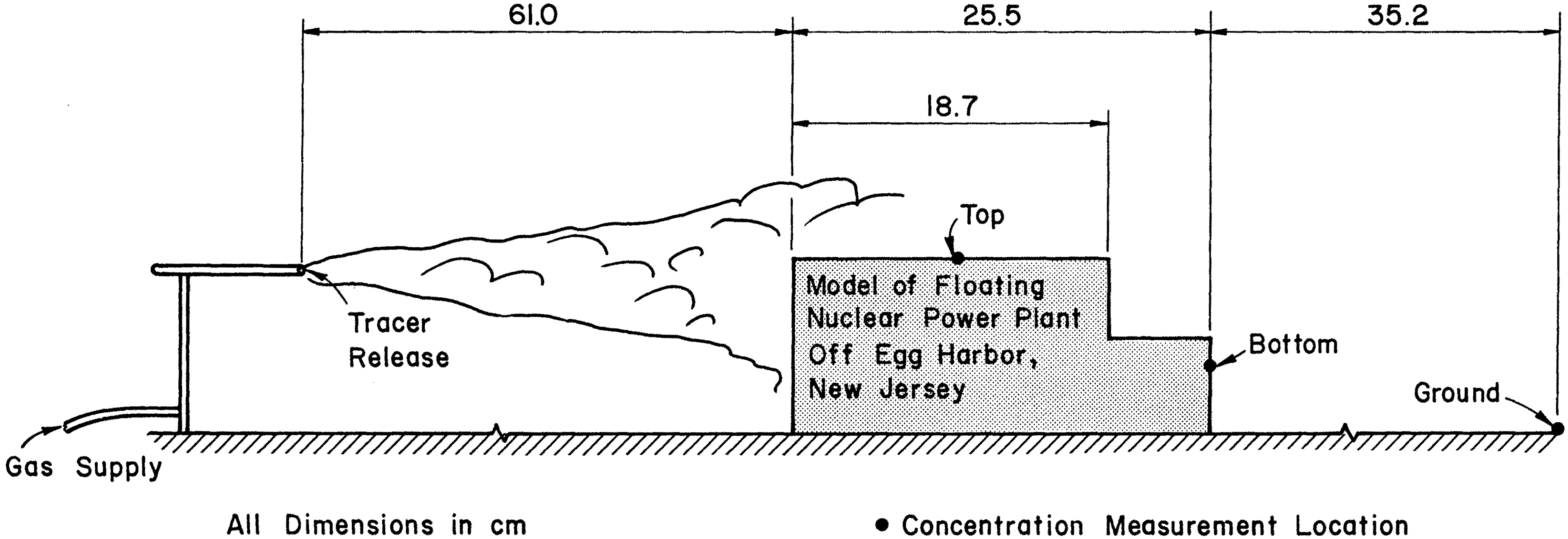

Figure 5.2-1. Test set-up for Reynolds number independence tests